International Institute for Applied Systems Analysis
IIASA www.iiasa.ac.at

Releases of Radionuclides to Surface Waters at Krasnoyarsk-26 and Tomsk-7

Waters, R., Compton, K.L., Novikov, V. and Parker, F.

IIASA Research Report
May 1999

Releases of Radionuclides to Surface Waters at Krasnoyarsk-26 and Tomsk-7

Robert D. Waters
Keith L. Compton
Vladimir Novikov
Frank L. Parker

RR-99-3
May 1999

International Institute for Applied Systems Analysis, Laxenburg, Austria
Tel: +43 2236 807 Fax: +43 2236 71313 E-mail: publications@iiasa.ac.at
Web: www.iiasa.ac.at

International Standard Book Number 3-7045-0133-6

Cover design by Anka James.

Printed by **Rema***print*, Vienna.

Contents

Acknowledgments

This work could not have been accomplished without the help and cooperation of Minatom, including the Mining and Chemical Combine (MCC), the Siberian Chemical Combine (SCC), the regional administrations of the Tomsk Oblast and the Krasnoyarsk Krai, the Kurchatov Institute, and the Russian Academy of Sciences, including the Institute of Geology of Ore Deposits, Petrography, Mineralogy, and Geochemistry (IGEM). Among those participating were Nicolai Egorov, deputy minister of Minatom; Vasili Zhidkov and Alexei Shishlov of the MCC; Georgii Zubkov of the SCC; Leonid Rikhvanov and Yuri Zubkov of the Tomsk regional administration; Nicolai Abramov and Yuri Maltsev of the regional administration of the Krasnoyarsk Krai; Yuri Gorlinskii and Vladimir Georgievskii of the Kurchatov Institute and Yuri Lapschin and Alla Dvorzhak of the Ukranian Academy of Sciences; and Vasili Velitchkin of IGEM.

The joint study with our Russian colleagues, primarily the team led by Vladimir Georgievskii, was undertaken with the intention of using common input data and different mathematical models to determine likely future radioactive material deposition and resultant doses. All Western mathematical models were made available to our Russian colleagues. Although we were able to reach agreement on the substance and text of the conclusions and recommendations of the study, different models, philosophic points of view, and methods of handling experimental data prevented us from reaching complete agreement on the final text.

We would like to thank the US Department of Energy for funding this study under Grant No. DE-FG 02-96 EW 13112 and Mr. David Huizenga, acting deputy assistant secretary, Office of Nuclear Material and Facility Stabilization, for his sponsorship of the work. We would also like to thank Gordon MacDonald, director of the International Institute for Applied Systems Analysis (IIASA), for his interest in the work and Academician Nicolai Laverov, vice president of the Russian Academy of Sciences, Academician Eugeny Velikhov, president of the Kurchatov Institute, and Deputy Minister Nicolai Egorov of Minatom for their help in improving access to data.

Abstract

During the Cold War, production and testing of nuclear weapons in the United States and the Soviet Union led to major releases of radioactive materials to the environment. Although large studies have begun to clarify the magnitude and impact of releases in the United States, only since Perestroika has information become available to begin an evaluation of the significance of releases to the environment in the former Soviet Union (FSU). The Radiation Safety of the Biosphere (RAD) Project at the International Institute for Applied Systems Analysis (IIASA), begun in 1995, is currently evaluating the radiation legacy of the nuclear weapons complex in the FSU. Because the three sites of Chelyabinsk-65 (Mayak Production Association – MPA), Tomsk-7 (Siberian Chemical Combine – SCC), and Krasnoyarsk-26 (Mining and Chemical Combine – MCC) account for the vast majority of the radioactive materials released to the environment in the FSU, these sites are the focus of RAD's studies. Contamination of such sites has resulted from normal and emergency atmospheric releases (such as the 1993 tank explosion at Tomsk-7), discharge of radioactively contaminated waste and cooling waters into rivers, spills and leaks, and deep-well injection disposal of liquid radioactive waste. This study is limited to the impact of past discharges of radioactive materials to the Yenisei River at the MCC and the Tom River at the SCC. Future studies are planned to assess the significance of deep-well injection of wastes at the MCC.

This report draws on data ranging from published reports by Western scientists to unpublished data from the sites and affected regions to compile an initial picture of the currently most contaminated portions of these two rivers and to make a preliminary estimate of the potential doses. The report also considers two hypothetical scenarios. The first scenario examines the potential for redistribution of existing contamination by a major flood and the significance of the dose resulting from such an event. The second scenario considers a release of radioactively contaminated sediments from the surface storage basins into the adjacent river with an estimate of the resultant doses. This movement of the contaminated particles is based on an original, unvalidated model. Thus the results, based on incomplete data, provide insight into the magnitude of the problems that might occur but should not be used to determine regulatory compliance or degree of cleanup required.

The results of the study indicate that some areas of the Yenisei River floodplain and island system are significantly contaminated. Conservative estimates of the maximum potential annual dose along the Yenisei are in the range of 5–15 millisieverts (mSv) per year. However, conservative estimates of the potential

doses along much of the river are near or below the commonly accepted annual dose limit of 1 mSv per year. Contamination is mainly limited to relatively small areas, particularly in deposition zones around islands and depressions in floodplains that trap contaminated sediments during floods. Contamination is lower in the Tom River; only within the first few kilometers of the discharge point is there a significant potential for exceeding the 1 mSv annual dose limit. Doses along most of the river are substantially below this level. In addition, data on contamination of fish were available for the Tom River: based on conservative estimates, annual doses from fish consumption of up to 3 mSv are possible. This dose is primarily due to short-lived activity released from the control systems of the reactor at the SCC. At both sites, the discharge of radioactive material into the adjacent river has been significantly reduced by the shutdown of the single-pass reactors; at the MCC, additional reductions have resulted from reduced processing rates at the site's reprocessing plant.

Based on the results of the hypothetical scenarios, there is no significant potential for extensive contamination downstream from the plants from existing contamination along the floodplains and islands. The resulting contamination would be well below background levels and would be essentially undetectable. The increase in the annual dose resulting from such an event is likely to be less than 100 microsieverts in the Yenisei River, and substantially less in the Tom River. During a flood, the majority of contaminated sediments resuspended by the higher flows would remain in suspension for long distances, resulting in a more uniform distribution of radioactive material farther downstream. However, release of highly contaminated sediments from the surface storage basins could result in high contamination levels, particularly near the release point. Because accurate data on the characterization of a hypothetical release were not available, the authors assumed unit releases of a relatively small fraction of the contamination in these ponds. However, even these relatively limited releases resulted in high levels of contamination. Higher releases would likely result in higher levels of contamination, and a large-scale pulse release could result in annual doses exceeding 1 sievert for tens of kilometers along the river if emergency responses were not carried out.

It is important to note that discharges into the rivers are not the only pathways for radiological contamination at these sites. Contamination has resulted from routine and emergency atmospheric releases of radioactivity (most notably from a 1993 high-level waste tank explosion at Tomsk), wastes have been injected underground at both sites, and there are likely to be significant areas of contaminated soil within the territory of each site. These releases are not evaluated in the current report. This report is therefore an initial step in evaluating the legacy of nuclear weapons production in the FSU.

1
Introduction

It is now well-known that early nuclear weapons development led to large releases of radioactive material to the environment. The United States and the Soviet Union were responsible for the majority of these releases. The effects of releases of these radioactive materials to the environment have been studied extensively in the United States, including major dose reconstruction studies at several sites of the nuclear weapons production complex. In the Soviet Union all such matters were classified as state secrets. Only since Perestroika has this veil begun to be lifted. Despite increased interaction between Russian scientists and engineers and their Western counterparts, and the publication of vast amounts of information, a great deal of data needed to determine the present and potential risks at the sites is currently unavailable. This lack of information has many causes. In the early days of operation of nuclear sites, alpha and gamma spectrometers did not exist. The military mission was paramount, and much was still unknown about the human and environmental consequences of exposure to ionizing radiation. Everything associated with the Russian nuclear complex was classified as secret, even the existence of such facilities.

Since the end of the Cold War, this situation has changed somewhat. However, although Article 42 of the Russian Federation's Constitution mandates the right to a favorable environment and to reliable information about its condition, a great deal of this information is still not available. The reasons for this may include security issues, lack of money to declassify documents, and bureaucratic inertia, among others. In particular, site-specific data on the installations, their contents, and their safety are lacking. This lack of information has strongly influenced our decision about how to proceed, affecting everything from model choice to the end points of the analysis.

The Radiation Safety of the Biosphere (RAD) Project at the International Institute for Applied Systems Analysis (IIASA) was initiated to study these large releases of radioactive material to the environment. RAD has already released its draft final "Mayak Case Study" (IIASA, 1996). The Mayak site was studied first because of its large release of radioactive material to the accessible environment and the resulting health consequences. Sites with plutonium production reactors and reprocessing plants have the largest potential for impacts to the environment. This hypothesis has been validated by Bradley (1997, p. 11), who synthesized a number of reports and estimated that, as of the mid-1990s, Tomsk, Mayak, and Krasnoyarsk

had released 6.3×10^{19} becquerels (Bq), equivalent to 1.7 billion curies (Ci), to the environment (including deep-well injection). In comparison, all other Russian releases, including those from Chernobyl, were only 1.1×10^{17} Bq (3 million Ci). The releases from Tomsk, Krasnoyarsk, and Mayak were 4.2×10^{19}, 1.7×10^{19}, and 4.4×10^{18} Bq (1.13, 0.45, and 0.12 billion Ci), respectively. While releases of radioactivity cannot be directly translated into health effects, they are the best surrogates for impacts in the absence of much more extensive information and risk assessment.

Much less was initially known about conditions at Tomsk and Krasnoyarsk than conditions at Mayak. This remains true. Cochran *et al*. (1995), for example, devote 47 pages to Mayak but only 12 and 13 pages to Tomsk and Krasnoyarsk, respectively. Bradley (1997) confirms this disparity of information and devotes 22, 28, and 80 pages to Tomsk, Krasnoyarsk, and Mayak, respectively. This combination of large releases and less available information prompted the current RAD Project study of these two sites.

The prospect of this study was discussed with the Russian member of the International Advisory Committee of the RAD Project, Deputy Minister N.N. Egorov of Minatom, and with Academician N. Laverov of the Russian Academy of Sciences. Both agreed it would be a useful study. The project named three in-country managers, representing the three major centers of Russian scientific activity in the nuclear field: Yuri Gorlinskii of the Kurchatov Institute, Anatoli Iskra of Minatom, and Vasili Velichkin of the Russian Academy of Sciences.

Field visits were organized to the two sites and meetings were held with the site authorities, regional authorities, local experts, and concerned citizens. Protocols were signed with the site and local authorities to cooperate on the studies. Because of the sensitive and/or classified nature of some of the data, it was agreed that the study would begin with off-site effects and that source terms on the sites would be aggregated. Thus, individual on-site sources of radioactive material and the safety of their storage were not identified. The results reported in this study only reflect the information that was available at the time of the study, and the conclusions are therefore valid only within that limited context.

Liaison people were designated for each region (Nikolai Abramov for Krasnoyarsk and Leonid Rikhvanov for Tomsk), and a scientific supervisor for the Russian studies was appointed (Vladimir Georgievskii of the Kurchatov Institute). The first topic to be studied was the impact of releases to the Tom and Yenisei Rivers on the inhabitants. Further studies at the sites will include, at a minimum, an analysis of deep-well injection of wastes into geological formations.

It was also agreed that the Yenisei River would only be studied up to its confluence with the Angara River, 245 kilometers (km) downstream from the site, and the Tom River, up to its confluence with the much larger Ob River, 44 km downstream

from the site. Although evidence of the releases from both sites can be found all the way to the Kara Sea, the majority of the waste is deposited closer to the plant sites. This distribution of contamination is presented in papers by Bradley and Jenquin (1995) and Robinson and Volosov (1996). They note that the ^{90}Sr content in floodplain soils is practically at global background levels 600–800 km downstream from Krasnoyarsk-26; for ^{137}Cs the distance is even less.[1] The results from Tomsk-7 are similar: contamination of riverbed sediments is fairly low at long distances from the release points. The combined ^{90}Sr and ^{137}Cs content in sediment at the junction of the Tom and Ob Rivers, approximately 44 km downstream from the discharge site, is 1.6–15 becquerels per kilogram (Bq/kg). The situation on the Yenisei is similar. Robinson and Volosov (1996) report sediment concentrations of 8–27 Bq/kg of ^{137}Cs downstream from the junction of the Angara and Yenisei Rivers, 255 km downstream from the discharge site.

Further evidence of low potential doses in more distant locations is given in a report by the International Arctic Seas Assessment Project (1997). According to their best-estimate scenario, the maximum annual dose to the critical population group was less than 0.1 microsieverts (μSv) per year; according to their plausible worst-case scenario, the maximum annual dose was less than 1 μSv per year. This population group lives in the Ob and Yenisei estuaries at the Kara Sea. The people primarily eat locally obtained fish, marine mammals, seabirds, and their eggs, and spend 250 hours per year on the seashore. The decision to limit the modeling to the nearest major waterway was based on these low concentrations and estimated doses.

In addition to evaluating existing contamination, two other scenarios were evaluated: redistribution of existing contamination by flooding and a hypothetical release of radionuclides from each site into the adjacent river system. It was agreed that IIASA would provide the hydrodynamic models and that IIASA would use a Western, public domain transport and dose assessment model while the Russians would use their own transport and dose assessment model. The results of each would then be compared.

Background material on Tomsk-7 and Krasnoyarsk-26, including meteorological, plant operation, contamination, and radionuclide discharge data, are provided in Chapter 2. The methodology used in this analysis is described in Chapter 3. Site-specific data and results for Krasnoyarsk-26 and Tomsk-7 are presented in Chapters 4 and 5, respectively. Conclusions are presented in Chapter 6.

[1] The Northern Hemisphere background levels of ^{137}Cs due to fallout from atmospheric testing are approximately 2–2.5 kilobecquerels per square meter (kBq/m^2). The values for ^{90}Sr are approximately 1.5 times less at 1–2 kBq/m^2.

2
Background

In the former Soviet Union (FSU), the production of weapons-grade plutonium was concentrated at three enterprises:

- Production Association (PA) "Mayak" in Ozersk, Chelyabinsk Oblast.
- Siberian Chemical Combine (SCC) in Seversk, Tomsk Oblast.
- Mining and Chemical Combine (MCC) in Zheleznogorsk, Krasnoyarsk Krai.

All three enterprises are located within the territory of the Russian Federation.

The process of extracting plutonium from irradiated uranium fuel includes the separation of the two metals and the removal of fission products. Metallic plutonium articles are the final products of the plutonium purification process. Production of nuclear materials generates radioactive wastes, which undergo processing and are then stored, discharged, or disposed of. Radioactive wastes are differentiated by their physical form, specific (volume) activity level, and origin.

Radioactive wastes are divided into liquid, solid, and gaseous wastes. Waste processing solutions, various suspensions, and sludges are considered liquid wastes. According to public health regulations (NRB-76/87, 1988; OSP-72/87, 1988; SPORO-85, 1985), liquid radioactive wastes are classified as low level [$<10^{-5}$ curies per liter (Ci/L)], intermediate level (from 10^{-5} to 1 Ci/L), or high level ($>$ 1 Ci/L). Solid radioactive wastes include metals, concrete, wood, organic films, work clothes, etc. Gaseous wastes may be provisionally subdivided into two groups: gases containing induced activity, and fission product gases resulting from irradiated uranium reprocessing and further chemical and metallurgical treatment of radioactive materials. High-, medium-, and low-level wastes are currently stored and disposed of at all three of these nuclear enterprises.

2.1 Krasnoyarsk Region

Construction of a plant to produce plutonium was authorized in 1950. The resulting complex is known variously as the Mining and Chemical Combine (MCC),

Much of the material for this chapter is taken from Egorov *et al*. (forthcoming), Bradley (1997), and Cochran *et al.* (1995). Information on environmental conditions at the sites is primarily from Velichkin *et al.* (1996); data on waste management are primarily drawn from Egorov *et al.* (forthcoming).

Krasnoyarsk-26, and, most recently, Zheleznogorsk. It is located on the Yenisei River, one of the great Siberian rivers, approximately 60 kilometers (km) northeast of the city of Krasnoyarsk (see Color Plates for a map of Krasnoyarsk Krai).

2.1.1 Geology

The MCC covers about 360 square kilometers (km^2) and occupies 15 km along the right bank of the Yenisei River. The region is characterized by complex relief and is divided into a mountainous region and a plains region. The MCC and its associated disposal areas lie partially in a mountainous area belonging to the joint zone of the West Siberian platform and the Sayan–Altay–Yenisei folded area.

The West Siberian platform (an artesian basin) corresponds in geomorphology to the West Siberian plain, one of the largest plains on earth. In the north it opens to the Arctic Ocean, in the northeast its boundary is the Yenisei River, and in the southeast it borders the Kustanay bank. The plain has a gradual inclination to the north only along the Ob and Yenisei River valleys; other parts are characterized by complex relief with a combination of low plains and heights. Consequently, the Ob and Yenisei Rivers can be considered the main pathways for possible migration of radionuclides from the Combines into the Arctic Ocean.

The West Siberian artesian basin is one of the largest groundwater reservoirs on earth. In terms of tectonics it is a two-staged structural depression. The lower stage represents a Paleozoic folded rock basement composed of dislocated metamorphic, sedimentary, and igneous rocks. The upper tectonic stage is a gently sloping Mesozoic–Cenozoic sedimentary formation. The depression has an asymmetric morphology with gentle western and steeper eastern slopes. The surface of the Paleozoic basement dips to the central and northern parts of the depression to a depth of 5–6 km. The artesian basin is generally open toward the Arctic Ocean, but the surface of its Paleozoic basement is not a plain; rather, there are sequences of basins and heights that create the complicated forms of the present relief. Its relative elevation is about 300 meters (m); the minimum true elevation is 20 m in the area of the Irtysh and Ob junction. Taking into account these structures, a number of researchers have identified artesian basins of the second order on the territory of the West Siberian artesian basin. However, the regular distribution of heads in the water-bearing horizons, which correlate to the areas of groundwater recharge and flow, characterize the West Siberian artesian basin as a unified watershed.

The Sayan–Altay–Yenisei hydrogeologic folded area is characterized by a combination of mountains, plateaus, folded zones, and intermountain depressions formed as a result of Baikalian, Caledonian, and Hercynian orogeny. The middle and high mountain systems are located in the southern part of the area. General lowering of ridges is noted to the west, northwest, and north up to 500–1,000 m. The southern part of the Yenisei ridge, where the MCC is located, is representative

of typical lowlands, with heights up to 600–710 m above sea level and depth of river valley cuts up to 300–350 m.

Neotectonic movements have been the main factor in the formation of the present relief. In accordance with different ages of folded formations, there are three complex hydrogeologic regions of the first order consisting of artesian and subartesian basins and basins of crevice waters. These are the Yeniseisky (the oldest), Sayano–Altaysky (old, mainly Caledonian, the most widespread in the folded area), and Zharmino–Rudno–Altaysky (the youngest, Hercynian) hydrogeologic regions. The Yeniseisky hydrogeologic region is located at the Yenisei ridge and is drained by the Yenisei River.

The Yenisei ridge and northeastern slope of the Baikal Sayan surround the MCC and are related to Baikal folded formations. The Yenisei ridge is a complex meganticlinorium built with highly metamorphosed and dislocated crystal shales and Archean gneisses. Metamorphosed terrigenous and carbonate rocks are also present. Archean and late Proterozoic rocks are broken by granitoids. The direct prolongation of the Yenisei meganticlinorium is the northeastern slope of Eastern Sayan, called the chief anticlinorium of Eastern Sayan or Protero–Sayan. It has dislocated Archean and Proterozoic gneisses, crystal shales, phyllites, migmatites, amphibolites, quartzites, marbles, and dolomites. Small intermountain depressions occur on the Baikal basement.

Deep faults with lengths of more than 500–1,000 km and large amplitude occurred during formation of the structures of the Sayan–Altay–Yenisei folded area. Crush zones with widths up to 15–125 km have connections with deep faults. Most faults have a northwestern direction. The meridional zone of faults is a border between the West Siberian artesian basin and the Yenisei ridge and coincides with the bed of the Yenisei. Most of the deep faults are old and stable. Displacements occurred throughout the Paleozoic and Cenozoic eras. Faults and crush zones coincide with intrusive and effusive rocks, ore deposits, and specific conditions forming underground waters. The natural seismicity at the MCC and SCC areas and at testing areas of deep disposal of radioactive waste is estimated to be about 6.

Plains with heights of 124–185 m are located on the right bank of the Yenisei and are occupied by forest, meadows, plowed fields, swamps, and a shelving slope from the south–southeast. The absolute height of this slope is 185–225 m. The plain is called a “Jurassic cavity.”

The mountain part forms the banks of the Yenisei. The Atamanovskii ridge is one of the distant spurs of the Yenisei ridge. The ridge represents a plateau stretching to the southeast with an absolute height of 370–420 m. The ridge is deeply cut with stream valleys and large and small ravines. On the left bank of the Yenisei, the Atamanovskii ridge becomes narrow and low, and gradually merges with the plain.

Table 2.1. Average and extreme monthly temperatures (°C).

	Jan	Feb	Mar	Apr	May	June	July	Aug	Sep	Oct	Nov	Dec	Annual
Average	–18	–16	–8	2	9	16	19	16	10	2	–9	–17	0.5
Average minimum	–38	–34	–28	13	–6	3	7	3	–4	–14	–28	–37	–42
Average maximum	–2	2	9	18	28	32	32	31	23	18	6	1	34
Absolute minimum	–55	–44	–39	24	–17	–3	0.3	–2	–12	–33	–47	–48	–55
Absolute maximum	6	10	17	32	35	38	40	36	33	25	14	10	40

Table 2.2. Average monthly precipitation (mm).

Jan	Feb	Mar	Apr	May	June	July	Aug	Sep	Oct	Nov	Dec	Annual
15	12	15	27	43	57	84	76	51	41	34	24	479

2.1.2 Meteorology

The climate is strongly continental, with a long cold winter, a late spring, a short dry summer, and a rainy autumn. The average air temperature of the coldest month (January) is –18.3 degrees Celsius (°C); that of the warmest (July) is 19.4°C. The daily amplitude of air temperature ranges between 12°C and 14°C. The average annual air temperature is approximately 0.5–0.6°C. The highest temperature ever recorded was measured in July (40°C), and the lowest, in January (–55°C). The average monthly and extreme temperatures are shown in *Table 2.1*.

The average air humidity of the coldest month is 83% and that of the warmest month is 76%. Average precipitation is 479 millimeters per year (mm/yr), with the majority (379 mm, or 86%) occurring between April and October. Monthly precipitation distribution is given in *Table 2.2*.

The highest level of precipitation in a single day (67 mm) was observed 10 July 1912, corresponding to 1% of the annual precipitation. Precipitation intensity equaling 2.1 millimeters per minute (mm/min) occurs once every five years (20%); 3.2 mm/min, once every 10 years (10%); and 4.15 mm/min, once every 20 years (5%).

Snow cover typically occurs in Krasnoyarsk in the middle of October, with the earliest recorded date being 4 September and the latest being 9 November. The formation of a stable snow cover occurs mainly in the first 10 days of November. Maximum height of snow cover occurs during the first 20 days of March and begins to decrease during the last 10 days of March. Data on snow cover height for different probabilities are given in *Table 2.3*.

Table 2.3. Maximum height of snow cover (cm) for different probabilities.

	Probability (%)							
	95	90	75	50	25	10	5	Average
Open area	10	12	15	19	24	28	32	21
Protected area	22	25	31	40	49	60	67	48

Stable snow cover reduction occurs in the first 10 days of April. Snow cover typically ends at the end of April. Snow density ranges between 0.15 grams per cubic centimeter (g/cm^3) in the beginning of winter and 0.24 g/cm^3 in the first 10 days of February.

Storms are mainly observed during the warm period of the year, accompanied by cumulus and nimbus clouds, squalls, strong showers, and hail. Winter storms are rare. The average number of days with storms in Krasnoyarsk is 21. The highest probability of storms occurs in July (37%), when storms may occur every fourth day.

Hail is observed mainly during the warm period of the year. During the summer Krasnoyarsk experiences 1–2 days with hail on average, and in years with higher storm activity up to 5 days with hail can be registered. The maximum amount of hail was registered 19 July 1966 (20–40 mm).

Snowstorms are normally observed from September to May. On average, up to 29 snowstorms occur during the year, but in the winter of 1959–1960, 50 snowstorms occurred in the town. Snowstorms occur most frequently in November and December. In 80% of the cases snowstorms are accompanied by winds with speeds of 6–13 meters per second (m/sec), predominantly from the southwest (72%).

Prevailing winds (occurring 55% of the time) are from the southwest and west. Winds from the southeast and north (2–4%) are the least frequent. Wind speed is minimal in July and August (2.5–2.7 m/sec). In these months, winds with speeds of 0–1 m/sec are the most frequent (10–11%). Data on wind speed are given in *Table 2.4*.

In Krasnoyarsk, strong winds (exceeding 15 m/sec) can be observed throughout the year. On average, such winds occur 33 days per year, most often in the winter period and in transitional seasons, and only rarely in July and August. In individual years, the number of days with such wind speeds can be 60% higher (62 days in 1961). The average number of days with strong winds is given by month in *Table 2.5*.

Equally dangerous are squalls, unexpected short increases in wind speeds exceeding 15 m/sec. Squalls are accompanied by storm clouds, storms, and sometimes hail. The values of maximum wind velocity probability are given in *Table 2.6*.

Wind velocities during gusts may significantly exceed the average wind velocity. For example, with prevailing low wind speeds, there is the possibility of gusts

Table 2.4. Wind speed (m/sec) and direction.

Wind	Winter				Spring				Summer				Autumn				Year			
direction	V_A	P	V_M	P	V_A	P	V_M	P	V_A	P	V_M	P	V_A	P	V_M	P	V_A	P	V_M	P
N	2	3	9	6	3	4	12	9	3	5	10	9	2	3	9	7	2	4	12	7
NW	3	7	12	8	3	6	12	9	3	11	12	10	2	6	10	8	3	8	12	7
W	3	5	15	9	4	6	12	9	3	12	10	9	3	8	10	8	3	7	15	9
SW	3	1	17	11	3	2	10	7	3	3	9	8	3	2	12	10	3	2	17	10
S	6	4	24	15	5	6	17	12	3	5	16	13	4	6	18	15	5	5	24	15
SE	7	37	34	21	6	31	22	16	4	22	20	17	5	34	24	20	6	32	34	20
E	5	35	28	18	6	35	28	20	4	30	24	20	5	33	21	18	5	33	28	17
NE	3	8	20	12	5	10	24	18	3	12	17	14	4	8	17	14	4	9	24	15
Windless	–	28	–	–	–	13	–	–	–	22	–	–	–	21	–	–	–	23	–	–
Average period without wind per season																				
Hours	56				10				18				14				98			
%	57				10				19				14				100			

Abbreviations: V_A = Average wind speed; V_M = Maximum wind speed; P = Probability (%).

Table 2.5. Days with winds exceeding 15 m/sec by month.

Jan	Feb	Mar	Apr	May	June	July	Aug	Sep	Oct	Nov	Dec	Annual
3.8	1.9	3.5	3.1	5.0	2.3	0.7	0.8	1.7	3.7	3.5	3.1	33

Table 2.6. Probability of maximum wind speeds.

Return period (years)	1	5	10	15	20
Wind speed (m/sec)	25	31	33	34	35

up to 36 m/sec. Maximum wind speeds are highest for southwestern and western winds and lowest for northern and northeastern winds.

The probability of surface inversions and above-surface inversions (with the lower border in the 0.01–0.5 km layer) with wind speeds of 0–1 m/sec near the earth's surface is given in *Table 2.7*.

Fogs in Krasnoyarsk are observed mainly during cold periods. Depending on the weather conditions, fogs in the town can be one of three types: irradiation (with strong frost); advective; or advective-irradiation. Ice fogs develop with low temperatures and high humidity. The maximum number of fogs occurs in winter and at the end of the summer. The average yearly number of days with fog is 32, of which 21 occur between October and March, and 11 occur between April and September. The minimum number of days with fog (1–2 days per month) occurs in April and May, and the maximum number (up to 18 days per month) occurs from December to February. The average total duration of fog during the year is 114 hours. The maximum fog duration (781 hours) was registered in 1970 and the minimum (32 hours), in 1958. The duration of fogs during cold periods is two

Table 2.7. The probability of surface inversions and above-surface inversions (%).

	Time of day				
Month	3:00	9:00	15:00	21:00	Day
Surface inversions					
January	55	49	60	62	57
February	68	48	55	71	60
March	68	23	32	68	48
April	56	6	6	43	28
May	56	2	2	69	32
June	59	3	3	75	35
July	77	1	6	80	41
August	75	2	5	78	40
September	66	2	16	71	39
October	50	8	37	52	37
November	45	23	47	39	38
December	54	49	55	57	54
Above-surface inversions					
January	8	10	7	7	6
February	4	10	4	5	4
March	4	9	4	5	4
April	2	3	2	2	2
May	4	2	2	2	2
June	6	2	3	2	2
July	4	3	2	2	2
August	2	3	2	3	1
September	3	7	2	2	2
October	4	7	2	3	2
November	5	9	5	7	5
December	8	14	10	7	6

to three times longer than during warm periods. The majority of fogs do not last longer than 3 hours.

The average annual temperature of soil at the surface in the region is 2°C. The absolute maximum of surface soil temperature is over 61°C and the absolute minimum is –55°C. The annual distribution for soil temperatures is similar to the annual distribution of air temperature. Soil at the surface is usually frozen from November to March, with temperatures above 0°C from April to October. Average temperatures of soil at the surface are given in *Table 2.8*.

The average annual temperature of soil deeper than 20 cm is almost constant at about 3°C, with temperature increasing with depth. Stable freezing of soil occurs at the end of October, and the maximum depth of soil freezing can exceed 175 cm.

Table 2.8. Average temperature of soil at the surface (°C).

	Jan	Feb	Mar	Apr	May	June	July	Aug	Sep	Oct	Nov	Dec	Annual
Average	–18	–16	–9	2	12	21	24	19	10	0	–10	–17	2
Average minimum	–24	–22	–17	–6	1	9	12	10	3	–4	–16	–23	–6
Average maximum	–14	–10	0	13	27	38	41	34	22	8	–6	–13	12
Absolute minimum	–55	–48	–42	–31	–19	–4	1	–2	–13	–36	–47	–52	–55
Absolute maximum	4	9	22	44	52	59	61	54	44	30	11	7	61

In winters with low snow cover, the depth of freezing can be up to 253 cm. The minimum freezing depth is 126 cm.

2.1.3 Hydrology

The Yenisei River is regulated by the Krasnoyarskaya Hydroelectric Power Plant (HPP), which began operation in 1967. The HPP is located approximately 85 km upstream from the MCC, and thus reduces the annual fluctuations in river flow in the areas affected by discharges from the MCC. At the city of Krasnoyarsk, approximately 38 km upstream from the MCC, the river is open, not frozen, throughout the year. The average water temperature is 7°C, the speed of the current is 1.7 m/sec, the average depth is 2 m, the average width is 1,000 m, and the average annual discharge is 2,760 m^3/sec (Kosmakov, 1996).

The average water discharges before and after the regulation of the river are shown in *Table 2.9*. Typical variations in discharge before and after the dam began operation (*Figure 2.1*) indicate the dampening of fluctuations in discharge provided by the dam.

The Yenisei and its tributaries (the Shumikha and Ledyanoy Rivers) represent the hydrographic network within the MCC area. Islets often divide the Yenisei into a number of channels.

2.1.4 Operations at the Mining and Chemical Combine

The MCC is unique in that the majority of the facility is located underground, with the reactors and reprocessing plant in tunnels about 250–300 m below the earth's surface. The MCC consists of 22 different divisions. The main plants are the three plutonium production reactors, the radiochemical reprocessing plant, and the boiler house. The three reactors and the radiochemical plant are located at depths of 250–300 m and, in contrast to the SCC and Production Association (PA) Mayak,

Table 2.9. Average discharge of the Yenisei River near Bazaicha, 7 km upstream from Krasnoyarsk (m^3/sec).

	1902–1966			1967–1986		
Month	Mean	Maximum	Minimum	Mean	Maximum	Minimum
January	597	852	382	2,356	2,950	1,140
February	523	713	355	2,557	3,550	1,140
March	491	635	322	2,486	4,200	1,210
April	1,580	3,540	597	2,606	4,350	1,430
May	6,300	10,000	2,690	3,228	5,240	2,510
June	8,930	17,300	3,730	3,239	5,460	2,640
July	5,270	9,400	2,510	3,285	5,480	2,630
August	4,060	6,290	1,850	3,442	5,400	2,560
September	3,460	5,430	1,500	3,004	4,930	2,470
October	2,290	4,450	1,060	2,454	3,290	1,910
November	967	1,740	492	2,057	2,810	1,340
December	646	990	429	2,331	3,090	1,140
Annual	2,920	3,980	1,980	2,754	4,229	1,843

Source: Kosmakov (1996).

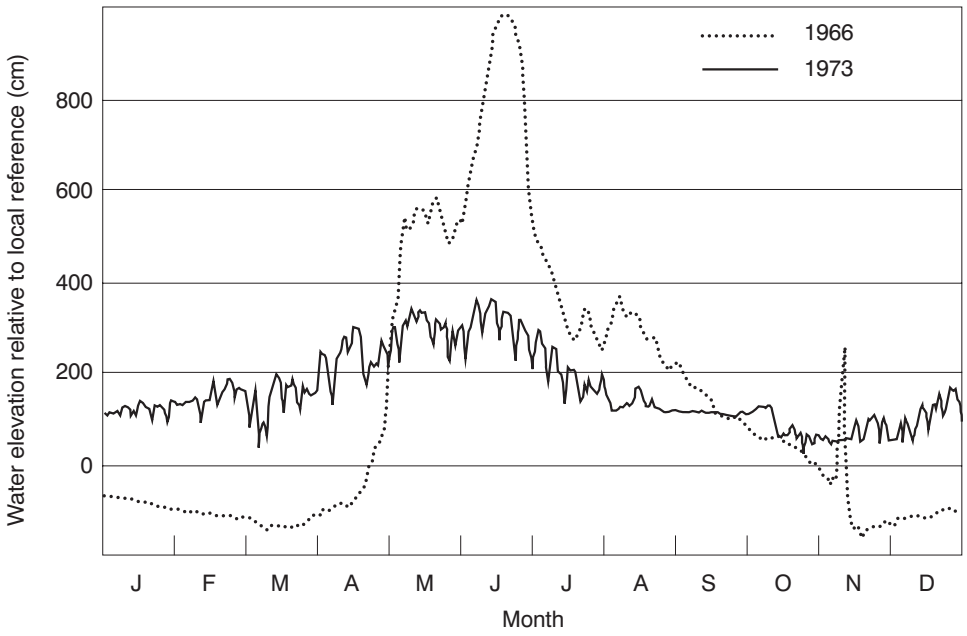

Figure 2.1. Daily variation of water level of the Yenisei River near Atamanovo, 84 km downstream from Krasnoyarsk (Kosmakov, 1996).

are reliably isolated from the biosphere. The MCC is equipped with a ventilation system with filters that serve as barriers to release of radioactive materials to the atmosphere.

The first reactor (AD) was activated in 1959; the second (ADE-1), in 1961; and the third (ADE-2), in 1964. All are uranium-graphite reactors similar to civil RBMK-type reactors. The first two reactors are likely identical to reactors for plutonium production at PA Mayak (AV-1, AV-2, and AV-3).

AD was decommissioned 30 June 1992; ADE-1 was decommissioned 29 September 1992. ADE-2 is still operating and supplies the MCC and Zheleznogorsk with electric power and heat, although the power level has been decreased by 20% since 1990. This reactor will be used until a fossil fuel (coal) electric plant is constructed in Sosnovoborsk, 10 km south of Zheleznogorsk.

The first two reactors used open-loop core cooling. Coolant entered into the reactors from the Yenisei River and was discharged back into the river. Therefore, cooling-water activation products, corrosion products from the fuel cladding and structural members of the reactor, and fission products from "tramp" uranium and leakage from faulty fuel rods entered the river with the cooling water. These past releases have resulted in radioactive contamination of river water and sediments north of the complex. The third reactor, which is still in use, has a closed primary cooling cycle. However, the control rods are cooled in a once-through coolant loop and thus represent a potential source of continuing discharge of radioactivity to the Yenisei.

The radiochemical reprocessing complex for plutonium and uranium was commissioned in 1964. Plutonium dioxide and uranium nitrate were produced on-site and then shipped to chemical, metallurgical, and sublimate plants located at other combines for further reprocessing. With a reduction in plutonium production resulting from the end of the Cold War, operations at the reprocessing plant have been scaled back considerably.

In 1976, a decision was made to construct a new reprocessing complex (RT-2) in Zheleznogorsk for spent nuclear fuel from nuclear power plants. Construction began in 1984. RT-2 was designed for reprocessing spent nuclear fuel from VVER-1000–type reactors. The first phase of the complex, a facility designed for wet storage of up to 6,000 tons of spent nuclear fuel, was put into operation in 1985 and is now 30% full. The complex is 30–40% complete. Although the facility was to be completed by 1998, construction was halted in 1991 due to financial problems and strong local opposition. In 1995, the Russian president approved completion of RT-2, and Minatom is seeking financial assistance to complete the construction. Plans are being made to set up an international company to provide funding. The MCC's administration is conducting talks with representatives of

Table 2.10. Total amount of radionuclides in waters discharged into the Yenisei River, 1993–1994 (GBq/yr).

	Actual discharge		Permissible	Ratio	Ratio
Radionuclide	1993	1994	discharge (PD)	1994/1993	1994/PD
^{56}Mn	90,095	<865.8	7,400	<0.01	<0.11
^{24}Na	465,645	68,894	185,000	0.2	0.37
^{239}Np	6,364	4,366	7,400	0.7	0.59
^{76}As	3,034	1,110	5,550	0.4	0.20
^{32}P	14,800	18,093	18,500	1.2	0.98
^{64}Cu	10,915	1,036	5,550	0.1	0.17
^{51}Cr	7,104	4,181	14,800	0.6	0.28
^{59}Fe	51.8	29.6	185	0.6	0.16
^{54}Mn	16.28	11.1	148	0.7	0.07
^{58}Co	78.81	74	370	0.9	0.20
^{60}Co	103.6	77.7	370	0.8	0.21
^{46}Sc	59.2	29.6	370	0.5	0.08
^{65}Zn	70.3	48.1	370	0.7	0.13
^{140}Ba	51.8	44.4	370	0.8	0.11
^{131}I	61.05	51.8	555	0.9	0.09
^{144}Ce	111	<25.9	370	<0.2	<0.07
^{141}Ce	15.91	<5.18	185	<0.4	<0.03
^{103}Ru	10.36	<8.88	185	<0.80	<0.04
^{106}Ru	<40.7	<13.69	370	–	<0.04
^{137}Cs	54.39	44.4	111	0.8	0.38
^{134}Cs	<2.59	<2.59	29.6	–	<0.1
^{95}Zr	54.76	25.9	370	0.4	0.07
^{95}Nb	57.35	22.2	370	0.4	0.06
^{90}Sr	51.8	22.2	74	0.4	0.30
^{152}Eu	<18.5	<5.92	185	–	<0.03
^{154}Eu	<8.88	<2.96	37	–	<0.08
^{124}Sb	136.9	55.5	370	0.4	0.15
Total β–γ activity	62,160	99,160	251,600	0.16	0.39

the atomic industry from South Korea, China, Japan, Taiwan, and some European companies to allow processing of spent nuclear fuel from these countries.

2.1.5 Discharges to surface waters

Operation of the three reactors and radiochemical plant resulted in large amounts of radioactive waste. Solid radioactive wastes are stored within the confines of the MCC. Liquid radioactive wastes generated as a result of operations have been collected in reservoirs, treated, and discharged into the river or pumped into deep wells.

Table 2.11. Annual concentrations of radionuclides in Yenisei River surface waters in 1994 in MCC zone of impact (Bq/L).[a]

	At Dodonovo (17 km upstream from discharge point 2a)[b]		250 m downstream from discharge point 2a[b]		1 km upstream from Bolshoi Balchug (∼10 km downstream from discharge point 2a)	
	Average	Maximum	Average	Maximum	Average	Maximum
^{56}Mn			<3.0	<3.0	<1.9	<1.9
^{24}Na			19	33	2.3	3.7
^{32}P			1.9	4.6	0.44	2.5
^{51}Cr			0.52	0.96	0.010	0.20
^{54}Mn			<0.002	0.0041	<0.00074	<0.00074
^{58}Co			<0.0044	0.012	<0.0015	<0.0015
^{60}Co			0.011	0.017	0.0030	0.0074
^{46}Sc			0.0052	0.0074	<0.0019	<0.0019
^{65}Zn			0.0078	0.016	<0.0037	<0.0037
^{137}Cs	0.0015	0.0037	0.014	0.018	0.0048	0.0081
^{95}Zr			<0.0037	0.0081	<0.0037	<0.0037
^{95}Nb			<0.0037	0.0037	<0.0074	<0.0074
^{90}Sr	0.0044	0.0052	0.0078	0.0085	0.0044	0.0056
MED from water surface (μR/hr)[c]	9		15		10	

[a] Differences in detection limits may be due to a variety of causes including different laboratories, different instruments, different days, and different levels of contamination.
[b] The main discharge point, 2a, is located 85 km downstream from the dam.
[c] MED = Mean exposure dose, in microroentgens per hour (μR/hr).

Table 2.12. Radionuclide concentration in Yenisei River surface waters in 1994 (Bq/L).

Distance downstream from discharge point 2a (km)	^{137}Cs	^{90}Sr
99	0.0019	0.0052
177	0.0014	0.0048
245	0.0017	0.0059
278	0.0011	0.0041
803	0.0022	0.0044
1,365	0.0019	0.0059

All waste releases now have spray clean-up equipment so that fixed norms are not exceeded. Releases of all radionuclides now range between 4% and 98% of the maximum tolerated releases (MTRs). The releases for two recent years are shown in *Table 2.10*. These releases resulted in the radionuclide concentrations in river water shown in *Table 2.11*. The concentrations of ^{137}Cs and ^{90}Sr in the river water are given in *Table 2.12*.

Since the AD and ADE-1 single-pass reactors were shut down, the release of radionuclides into the Yenisei River has been mainly limited to short-lived isotopes (e.g., ^{24}Na, ^{32}P) in the cooling water of the control and protection system of the dual-purpose ADE-2 reactor. Velichkin *et al*. (1996) have reported data on effluent activities from the MCC. The activity of the water discharged into the Yenisei River is in the range of 1.2–7.0 times the allowable dose concentration for the general population outside the site (the "B category" of the population; DC_B) for ^{24}Na and in the range of 0.05–1.5 of DC_B for ^{32}P. In recent years the summed release of all radionuclides generally has not exceeded permissible levels and has typically been within 0.3–6.0% of the maximum permissible release. The volume activity of radionuclides in the river water is below 0.3 of DC_B at the discharge location, 0.08 of DC_B 500 m upstream from the discharge location, and 0.015 of DC_B 15 km downstream from the discharge location (1 km upstream from Bolshoi Balchug, the first settlement on the right bank of the Yenisei River). The summed values for ^{239}Pu and ^{240}Pu volume activity are lower than the sensitivity limit of the measurement method, and they do not exceed 8.0×10^{-5} of DC_B. The maximum values of ^{90}Sr and ^{137}Cs volume activity are 1.2×10^{-3} and 6.0×10^{-3} of DC_B, respectively. The annual effective dose due to the consumption of water from the centralized water supply (which draws water from the Yenisei) is estimated to be 5 microsieverts (μSv) per year (0.5 millirem per year) at Bolshoi Balchug. Since the decommissioning of the single-pass reactors, the water surface exposure rate and activity of all radionuclides (summed) in the water generally have not exceeded the limits set by NRB-76/87 (1988) at the discharge location.

The radioecological conditions in the floodplain of the Yenisei River are mainly due to past reactor coolant discharges from the (now decommissioned) single-pass AD and ADE-1 reactors. The exposure rate in most of the inhabited areas of the river bank 15–500 km downstream from the MCC discharge location does not exceed 10–15 microroentgens per hour (μR/hr). However, on particular islands and in some local sections of the floodplain 15–250 km downstream from the MCC discharge location, there are limited areas with exposure rates of 30–200 μR/hr (Khizhnyak, 1995). In the 300-km zone downstream from the MCC, the radioactive contamination of the Yenisei River floodplain is thought to be primarily due to two intense floodings in 1966 and in 1988. The river water discharges were up to 21,000 m^3/sec, leading to deposition of suspended bottom sediments containing radionuclides on islands and floodplains (Kosmakov, 1996).

As of 1 January 1996 the area of contaminated lands was 779 hectares. The lands are contaminated primarily with ^{137}Cs and ^{90}Sr radionuclides. The data on the contaminated lands are presented in *Table 2.13*. More than 5.7 km^2 of the total contaminated land area are at the underground liquid radioactive waste disposal site and at basins 354, 354a, 365, and 366.

Table 2.13. Contaminated land at the MCC (ha).

Distribution of contaminated land by exposure rate level (μR/hr)[a]	Production zone	Sanitary and protective zone	Observation zone	Total
Up to 60	0.5	66.6	10.6	77.7
61–120	–	14.9	–	14.9
121–240	329.7	6.0	339.4	675.1
241–1,000		5.0		5.0
More than 1,000		6.2		6.2
Total	330.2	98.7	350	778.9

[a] Dose rates as measured in the field.
Source: Egorov (forthcoming).

The bottom sediments of the Yenisei downstream from discharge sites are contaminated mainly with long-lived radionuclides – ^{60}Co, half-life (t_h) = 5.3 years; ^{137}Cs, t_h = 30 years; and ^{152}Eu, t_h = 13.3 years – due to discharges from previous years. Specific activities of radionuclides in bottom deposits of the Yenisei are discussed in more detail in the modeling section.

2.1.6 Atmospheric releases

Releases to the atmosphere from the MCC for 1994 are given in *Table 2.14*.

The MCC monitors atmospheric radioactivity in the production zone, in the sanitary and protective zone, and in the observation zone. Fallout of ^{137}Cs from the atmosphere in the MCC area in 1993 and 1994, respectively, was as follows:

- Production zone: 4.8 and 8.1 Bq/m^2/yr (1 km north of source of release).
- Sanitary and protective zone: 6.9 and 3.9 Bq/m^2/yr.
- Observation zone: 4.2 and 5.0 Bq/m^2/yr (8 km north of source of release).

Since the AD and ADE-1 single-pass reactors were decommissioned, the activity level in the near-surface layer of the atmosphere has fallen eightfold. At the nearest settlements (Bolshoi Balchug and Zheleznogorsk), in the near-surface layer of the atmosphere mainly only ^{137}Cs is detected at levels under 0.13 of DC_B. On the whole, the effect of gaseous and aerosol effluents of the MCC's active production works on the contamination of the sanitary and protective zone and the observation zone is practically indistinguishable from global background levels.

2.1.7 Solid radioactive waste disposal

Operations at the MCC have generated large amounts of liquid and solid high-, medium-, and low-level radioactive wastes. The solid and liquid radioactive wastes

Table 2.14. Radionuclide releases to the atmosphere from the MCC, 1994 (GBq/yr).

Radionuclides	Actual releases (total)	Norms without cleanup	Permissible releases	Maximum tolerated releases
^{41}Ar	261,220	18,3520	1.48E+06	4.56E+08
Other inactive gases	55,130	–	5.92E+05	2.46E+08
Σ, α	0.0555	0.037	7.4	2,029
^{131}I	4.97	–	185	1,175
^{90}Sr	0.718	0.555	14.8	2,274
^{137}Cs	1.71	1.52	18.5	2,224
^{95}Zr	5.88	5.37	74	1,563
^{95}Nb	9.51	8.44	148	208,717
^{103}Ru	5.49	5.22	48.1	192,770
^{106}Ru	12.0	11.1	81.4	396,492
^{141}Ce	0.37	0.296	3.7	27,210
^{144}Ce	8.07	6.92	111	326,710
^{51}Cr	5.55	5.55	137	886,150
^{59}Fe	0.37	0.333	3.7	5,032
^{58}Co	0.37	0.111	3.7	7,067
^{60}Co	0.37	0.185	3.7	94
^{140}Ba	0.37	0.333	3.7	17,131
^{134}Cs	0.0074	–	1.85	11,100
^{65}Zn	0.851	0.814	7.4	60,310
^{46}Sc	0.17	0.148	3.7	5,032
^{54}Mn	0.181	0.148	3.7	6,031
^{32}P	65.2	39.1	555	89,540

Source: Velichkin *et al.* (1996).

are kept in storage facilities within the confines of the MCC. The solid waste storage facilities are described in *Table 2.15*.

2.1.8 Liquid radioactive waste disposal

Depending on their activity level, liquid radioactive wastes resulting from the production operations are sent to cleaning facilities or are collected in special tanks or in open storage reservoirs. After treatment and cleaning, wastes are sent to underground disposal (at the Severny site) and decontaminated waters are discharged into the Yenisei River.

Basin 365 is an open water storage reservoir located on the first super-floodplain terrace of the Yenisei River, approximately 100 m from the river and 50 m above river level. It is designated for reception and interim storage of reactor emergency

Table 2.15. Solid radioactive wastes (RW) at the MCC.

Description	Time period of operation		Volume (1,000 m^3)		Area (1,000 m^2)	Amount of RW (tons)	Notes
	Start	End	Design	Actual			
Solid RW storage facilities (4). Reinforced-concrete reservoirs in the ground: bottom is a layer of compacted crushed rock 70 mm thick impregnated with bitumen and covered by asphalt layer 35 mm thick.	1963		27.4	24.2	5.0		Fine granular solid RW of Groups II and III in shielded containers. Large-sized solid RW of Groups II and III.
Solid RW storage facilities (7). Filled earthen trenches in compacted loam. Once filled, trenches are covered by 1 m of soil.	1963–1983		111.6	109.6	38.3		Burial of Group I solid RW.
Solid RW storage facilities (4). Reinforced-concrete shafts lined with stainless steel.							Groups II and III solid RW reactor.
Total solid RW						105,170	Solid RW containing ^{90}Co, ^{90}Sr, ^{95}Zr, ^{95}Nb, ^{103}Ru, ^{106}Ru, ^{137}Cs, ^{141}Ce, ^{144}Ce, ^{238}U, ^{239}Pu, etc.
Group I with exposure rates in the range of 0.015–5.5 μR/sec						52,170	
Groups II and III with exposure rates in the range of 5.5–250+ μR/sec						53,000	

Notes: The solid RW groups include the following: *Group I*: Household rubbish, deteriorated work clothes and footwear, breathing apparati, package materials, cleaning cloth, wooden containers, wastes from repair shops, dismounted washed-out equipment, tubing scrap, building refuse, etc.; *Group II*: Graphite bushing, fuel channel briquets, deteriorated metallic components, radiochemical laboratory glassware, building refuse, filters, etc.; *Group III*: Instrument sensors, wastes from repair and construction work at radioactively contaminated sites, radioactive materials spreads and places, radiochemical production works' solid RW containing alpha-emitting nuclides, etc. The solid RW gamma-exposure rate measurements are made at the surface of the source.

waters and off-grade non-process wastewaters from the radiochemical plant before they are sent to cleaning facilities. Isolation from groundwater is provided by an anti-filtration shield of clay, two asphalt layers on the bottom and slopes, and bottom and bank drainage systems for interception and leak detection in case of damage to the liners.

Basin 366 is an open water storage reservoir on the first super-floodplain terrace of the Yenisei River. It is located near basin 365, approximately 100 m from the river and 50 m above river level. It was built by hydraulic deposition of soil and is designated for reception of decontaminated (in accordance with the set standards) waters from the Combine's cleaning facilities to provide for their holding, settling, and filtration before their discharge into a stream and eventually into the Yenisei River. The water filters through the bottom and the dam body; in the event of excessive filling, it discharges over the spillway.

Basin 354a is an open pit water storage reservoir built in essentially impermeable rocks. It is designated for reception, composition balancing, and interim storage of regeneration solutions and sludges from cleaning facilities and low-level wastes and condensate after evaporation of the radiochemical plant process wastes before they are sent to underground disposal. The wastes are isolated from contact with groundwater by a two-layer anti-filtration shield on the bottom and slopes and a drainage system between the shield's layers. In addition to the engineered geological and hydrogeological structure of the area, the presence of a thick covering of uniform and essentially impermeable clays provides protection.

Basin 354 is situated 100 m from basin 354a on a site with similar engineered geological and hydrogeological conditions. Its designation and design are similar to those of basin 354a. At present, the basin is completely empty and is being taken out of service.

The liquid radioactive waste storage facilities are described in *Table 2.16*. The majority of the wastes are injected underground. The injection area is located east of the MCC at the border between the South Yenisian crystalline massif and the southeastern part of the Chulym artesian basin. The radioactive waste disposal site is located within an old subsurface erosional cavity, which is overlain by a thick layer of sand-clay Jurassic deposits. The maximum depth of the erosional cavity is 550 m from the surface.

The sand-clay layer is thinner to the west, south, and southeast, where hard rocks are exposed at the surface. From the west the cavity is bounded by tectonic faults that strike north–south. The fault plane is composed of clay, which divides the down-dip blocks from the up-dip blocks. The bottom and edges of the hollow are formed by gneisses and many-colored overlapping clays. Jurassic formations are represented by interbedding of permeable sand formations and

Table 2.16. Liquid radioactive wastes (RW) at the MCC.

Description	Beginning of operation	Volume (1,000 m^3) Design	Volume (1,000 m^3) Actual	Area (1,000 m^2)	Amount of RW (tons)	RW activity Specific (Ci/L)	RW activity Total (Ci)	Notes
High-level liquid RW storehouse. Complex includes 24 stainless steel 300 m^3 tanks placed in canyons. Canyon walls are lined with stainless steel. Each canyon is covered by a concrete plate 1-m thick. Tanks are provided with coil coolers.	1963–1973	6.84	2.02	4.4	2,020	Up to 500	83×10^6	High-level solutions received for storage and processing from the radiochemical plant contain ^{238}U, ^{239}Pu, ^{95}Zr, ^{95}Nb, ^{103}Ru, ^{106}Ru, ^{144}Ce, ^{137}Cs, ^{90}Sr, etc.
Medium-level liquid RW storehouse. Complex includes reinforced-concrete tanks, 9 with 3,000 m^3 capacity, 8 with 8,500 m^3 capacity. Tanks are lined with stainless steel or with carbon steel with epoxy coating and are equipped with systems for blowing air in upper part and for cooling solutions.	1964–1965	94.55	53.1	4.0	53,000		22.8×10^6	Liquid medium-level RW received from radiochemical plant contain ^{238}U, ^{239}Pu, ^{95}Zr, ^{95}Nb, ^{103}Ru, ^{106}Ru, ^{144}Ce, ^{137}Cs, ^{90}Sr, etc.
Medium-level pearlite sludge-storage facility. Stainless steel tank placed in a compartment with reinforced-concrete walls lined with stainless steel.	1986	0.5	0.17	0.078	170			Sludge contains 50 m^3 of solid RW from process solutions.
Storage basins	1958–1966	794	520	130	566,800		38,000	Contains ^{137}Cs, ^{144}Ce, ^{152}Eu, ^{154}Eu, ^{60}Co, ^{106}Ru.
Underground liquid RW disposal site	1967	11,000	5,000	6,300	5×10^6	5.0×10^{-6} to 4.0	290×10^6	Contains ^{90}Sr, ^{95}Zr, ^{95}Nb, ^{103}Ru, ^{106}Ru, ^{137}Cs, ^{144}Ce, ^{235}U, ^{238}U, ^{239}Pu.
Total liquid RW		11,895.9	5,575.3	6,438.5	5,622,000	396×10^6		

Table 2.17. Stratigraphic scheme of Paleozoic and Mesosoic–Cenozoic formations in the MCC area.

System	Epoch	Suite	Index	Horizon thickness (m)	Rock description
Jurassic	Middle	Itats-	E	20–50	Aleurolite clays
		kaya	IIIa	20–50	Aleurolite sands
			E	20–50	Aleurolite argillic clays
			III	0–30	Arkosic sands
			D	30–50	Argillic coal clays
			II	50–95	Aleurites and aleurolites with interbeds of sands and clays
			II	50–95	Carbonaceous clays
			II	50–95	Arkosic sands, sometimes highly carbonaceous with interbeds of clays
			C	45–75	Argillic clays with interbeds of clayey sandstones
			F	0–24	Green argillic clays
			B	30–75	Arkosic sands
	Early	Makarov-	B	30–75	Gray argillic clays
		skaya	I	0–100	Gravel sands, breccias
			I	0–100	Unsorted wreckage of rocks with limestone cement
Triassic	Late		A	0–43	Many-colored kaoline clays and breccia
Pre-cambrian					Crystalline shales, gneisses

low-permeability clay formations. Thin Quaternary formations slightly filled with water are deposited in the upper part of the section.

The stratigraphic scheme of pre-Quaternary deposits in the MCC area is shown in *Table 2.17*. Hydrologic parameters of the Severny site's disposal strata are given in *Table 2.18*.

The formation is divided into sandy permeable horizons (labeled I, II, and III) separated by clay horizons (labeled B, C, D, E, and F). Low-permeability deposits of weathered crust (horizon A) underlie horizon I. Horizons I and II occur in the center of the site at depths of 355–500 m and 180–280 m, respectively, and are recommended for use as waste disposal strata.

Disposal strata are characterized by medium-grained sands and poorly cemented sandstones with the following composition: 70–80% quartz, 5–15% potassium or sodium feldspars (orthoclase, microcline, plagioclase), 10% mica and hydromica minerals, and 3–5% clayey minerals.

Table 2.18. Hydrologic parameters of disposal strata at the Severny disposal site (MCC).

Parameters	Horizon I	Horizon II (lower part)
Depth (m)	355–500	180–280
Thickness (m)	55–85	25–45
Effective thickness (m)	25–35	23–45
Total porosity	0.2–0.25	0.3
Effective porosity	0.07	0.08–0.12
Transmissivity (m^2/day)	5–40	20–80
Hydraulic conductivity (m/day)	0.3–1.6	0.1–2.2
Coefficient of pressure conductivity (m^2/day)	1.6×10^5	2.2×10^5
Pressure head above roof (m)	360–370	62–147

Low-permeability layers are composed of various clays: argillites and "fat" clays (horizon B), aleurites, carbonaceous clays (in upper part of section), interbedding of different clays and sands, and, sometimes, limestone. Clay horizons overlie the area of possible impact of radioactive waste disposal. They wedge out on the edges of the hollow in the east and the south.

The MCC site area is a small artesian basin in a downthrust block opened to the Chulym artesian basin from the north. There are aquifer complexes of Quaternary and Jurassic formations and complexes of metamorphic and igneous Cambrian rocks. Quaternary formations and hard rocks of the basement are only slightly water-bearing and are not suitable for groundwater exploitation.

The main water-bearing horizons of Jurassic deposits are horizon I of the early Makarovskaya subsuite and horizon II of the middle Itatskaya subsuite formed with sands and clays. Horizon III is saturated to a lesser extent and does not occur everywhere.

The recharge area of horizon I is believed to be located 7 km south of the Severny site, with the main discharge area located in the Kan River valley (12–14 km from the site). Groundwater in horizon I travels northward at 5–6 meters per year (m/yr) under the influence of a hydraulic gradient of 0.003.

The recharge area of horizon II is believed to be located 4–5 km south of the Severny site, with the discharge area located partially in the Kan and partially in the Tel River valleys beyond the area of predicted waste migration. Disposal strata contain waters with low salinity [up to 0.3 grams per liter (g/L)]; piezometric pressure heads above the tops of the water-bearing strata are 360–370 m and 62–147 m for horizons I and II, respectively.

Geophysical research shows that horizons I and II exhibit inhomogeneity in horizontal flow. Selected intervals of maximum flow are not correlated between

different wells, thus one can expect steady contribution of waste in the disposal strata.

The geological features that make the MCC site suitable for radioactive waste disposal are the limited extent of the sedimentary formations with disposal strata, the synclinal character of these formations, and the existence of a tectonic screen in the west. The tectonic screen isolates the disposal strata from horizons in hydraulic contact with the Yenisei River valley.

More-detailed data characterizing geologic–hydrogeologic features of the MCC and SCC areas are given in articles published by the Severny site. The site is used for disposal of low-level radioactive wastes (up to 800 m^3/day) in the second sandy stratum and of medium-level radioactive wastes (up to 500 m^3/day) in the first sandy stratum.

The Severny site is situated 12 km from the MCC's main production works, within the limits of the sanitary and protection zone. The disposed wastes contain fission products, including strontium, cesium, zirconium, niobium, ruthenium, and cerium; trace amounts of unrecoverable uranium; and transuranium elements. Before underground disposal, treatment is carried out at the MCC's cleaning facilities and at the radiochemical plant in order to make the wastes compatible with the geological medium and to recover additional long-lived transuranium elements.

The wastes are transferred to the disposal site by pipeline. They are placed in the site via a system of 16 injection wells. The injection pressure is about 2 megapascals (MPa). Within and outside the disposal site there are 70 observation wells used for monitoring the geological medium and waste migration.

The first and second sandy strata used for the disposal occur at depths of 300–500 m and 180–280 m, respectively. The strata are underlain, separated, and covered by loamy floors, isolating the strata containing radioactive wastes from the surface and from shallow groundwater. The natural speed of water movement is 5–6 m/yr in the first stratum, and 10–15 m/yr in the second stratum. Radionuclides are strongly sorbed to the rocks.

Special geological prospecting works and explorations preceded the creation of the Severny underground disposal site. These studies substantiated the feasibility of radioactive waste injection and the disposal safety. At present, the site holds a mining license that permits disposal of the wastes.

2.2 Tomsk Region

The plant known variously as the Siberian Chemical Combine (SCC), Tomsk-7, and most recently Seversk was built to produce plutonium. The site is located on the Tom River approximately 15 km north of the city of Tomsk (see Color Plates for a map of the Tomsk Region).

Table 2.19. Average monthly ambient temperatures (°C).

Jan	Feb	Mar	Apr	May	June	July	Aug	Sep	Oct	Nov	Dec	Annual
–19.2	–16.6	–10.2	–0.6	8.4	15.3	18.1	15.3	9.2	0.6	–10.1	–17.3	–0.6

Table 2.20. Average monthly precipitation (mm).

Jan	Feb	Mar	Apr	May	June	July	Aug	Sep	Oct	Nov	Dec
18	19	23	27	45	65	78	71	48	48	49	34

2.2.1 Geology

The SCC territory is located at the boundary of the West Siberian platform, in the southeastern part of the Ob artesian basin. Here, hard rocks dip under the formation of sandy-clayey Mesozoic–Cenozoic rocks represented by interbedding of water-collecting sandy layers and horizons of low-permeability clays. Hard rocks outcrop near Tomsk (25–30 km south of the disposal site) and dip to the west, northwest, and north to depths of 350–450 m in the area.

2.2.2 Meteorology

The climate of the Tomsk Region is strongly continental, with an average annual air temperature of –0.6°C. The lowest monthly temperature is observed in January (–19.2°C) and the highest, in July (18.1°C). The average monthly ambient temperatures are given in *Table 2.19*. The absolute minimum is –55°C and the absolute maximum is 39.6°C.

Average annual precipitation is 525 mm, with 420 mm occurring as rain. In winter, precipitation is observed 60% of the days. During the rest of the year, precipitation is observed 11–14% of the days. Up to 30% of the total annual precipitation is snow. The average monthly precipitation is shown in *Table 2.20*.

Snow remains on the ground 187 days of the year on average. The maximum thickness of the snow layer occurs in March, with up to 57 cm in open areas and 69 cm in the forest. The average maximum snow cover in winter is 60 cm.

The primary direction of the wind is north–northeast, occurring 57% of the time, particularly in winter.

Evaluation of atmospheric stability category classifications was made on the basis of three years of observations consisting of standard eight times daily cycle monitoring of meteorological measurements and wind data gathered by the base meteorological station nearest to the SCC. The stability category classifications were arranged on the Smith algorithm, which corresponds to the analytical representation of vertical dispersion of a discharge jet according to Khoskek-Smith. It was based on standard monitoring measurements of wind velocity and direction at

Table 2.21. Distribution of atmospheric stability categories and wind velocity (%).

Wind velocity	Atmospheric stability category								Average wind
range (m/sec)	A	B	C	D	E	F	G	Sum	velocity (m/sec)
Calms	0.21	0.60	1.03	2.53	0.61	0.28	3.74	9.00	–
0.5–1.0	0.46	0.61	0.86	3.19	0.68	0.41	2.40	8.61	0.9
1.0–2.0	1.09	1.89	2.03	6.79	1.53	0.58	3.77	17.68	1.6
2.0–4.0	1.54	5.02	4.84	16.20	2.47	1.05	3.36	34.48	3.0
4.0–8.0	0.00	1.52	4.20	20.31	0.90	0.18	0.20	27.31	5.4
8.0–15.0	0.00	0.00	0.00	2.92	0.00	0.00	0.00	2.92	9.1
15.0–50.0	0.00	0.00	0.00	0.00	0.00	0.00	0.00	0.00	15.5
Category total	3.09	9.04	11.92	49.42	5.58	2.22	9.73	91.00	
Average wind velocity (m/sec)	1.98	2.79	3.35	3.99	2.43	2.08	1.55	3.25	
Total events	3,024	7,991	10,800	45,984	6,028	3,473	10,291	87,591	

Note: General wind frequency is 91%; calm frequency is 9%.

Table 2.22. Frequency of water flow for the Tom River near Tomsk.

Cumulative frequency (%)	Annual maximum (m^3/sec)	Cumulative frequency (%)	Summer maximum (m^3/sec)	Winter maximum (m^3/sec)
1	14,600	50	275	310
2	13,900	75	220	215
5	12,500	90	183	148
10	11,400	95	162	110
25	9,700	97	150	87
50	8,300	99	120	46
Maximum observed	13,600	Minimum observed	117	52.6
Date of observation	14.05.37	Date of observation	14.08.74	22.11.34

Sources: Novosibirsk (1985, 1986, 1987).

the standard meteomast height, night cloudiness, and day summary solar radiation. The data are shown in *Table 2.21*.

2.2.3 Hydrology

Flow in the Tom River is primarily due to runoff. The local relief is sloped to the west toward the river. There are many small rivers and streams flowing to the west on the terrain. The riverside area is swampy and falls to the main river behind the

embankment. The left (west) bank of the river is low. Water flow characteristics are given in *Table 2.22*.

Discharge records at Tomsk exist for the period 1918–1994. The average annual maximum discharge is 8,500 m^3/sec. The average monthly minimum is 280 m^3/sec during the summer; the autumn and winter low discharge is 110 m^3/sec. The average discharge is 1,120 m^3/sec.

The river flow is quite variable, with a maximum flow of 13,600 m^3/sec observed in both 1930 and 1937 and a minimum of 52.6 m^3/sec observed in 1934. The river is frozen from early November (average date 8 November) until the end of April (average date 24 April).

The total flow of suspended solids in the Tom River is about 3 million metric tons per year. Most (80–99%) of this flow occurs during floods, when water turbidity (defined by quantity of suspended solids) is at a maximum, with average monthly values of 77–220 g/m^3. During summer it is 4.7–60 g/m^3; in autumn, 4.3–32 g/m^3; and in winter, 1–1.5 g/m^3 (Novosibirsk, 1985, 1986, 1987; State Hydrological Institute, 1985; Hydrometizdat, 1984).

2.2.4 Operations at the Siberian Chemical Combine

The production site of the SCC is situated on the second super-floodplain terrace on the right (east) bank of the Tom River 12–15 km north of Tomsk. Construction began on the plant in March 1949. The SCC was designed to produce plutonium and enriched uranium and contains the following production facilities:

- Reactors – plutonium production, electric and heat power generation.
- Radiochemical plant – reprocessing of irradiated materials to separate and purify uranium and plutonium salts.
- Chemical and metallurgical plant – production of metallic uranium and plutonium.
- Sublimate plant – U_3O_8 and UF_6 production.
- Isotope enrichment plant – production of enriched uranium.
- Nuclear fissile materials storehouses – facilities for storage of uranium oxides, uranium hexafluoride, metallic uranium of various enrichments, standard uranium slugs irradiated in production reactors, plutonium oxides, articles of metallic plutonium.
- Facilities for radioactive waste processing, storage, and disposal.
- Thermal electric plant – electric and heat power generation.

Construction of the uranium enrichment plant began in 1951. The first stage of the plant began operation 26 July 1953. Until 1973, gaseous diffusion technology

was used for uranium isotope separation. Later, the plant adopted the highly efficient centrifuge technology. At present, because of the reduction of state orders for enriched uranium, separation capacities are not fully utilized at the plant. This allows the SCC to render commercial services to foreign firms interested in uranium enrichment.

Construction of the first uranium-graphite production reactor began in 1952. The resulting I-1 reactor began operation 20 November 1955. It went through several stages of modernization over its 35-year life and was shut down 21 August 1990 in connection with the reduction of weapons-grade plutonium production.

In 1954 a conceptual design for a new type of power and plutonium production reactor known as the Siberian Nuclear Plant was carried out. In September 1958, the first stage of the NPP-1, based on the 100 megawatt (MW) EI-2 uranium-graphite reactor, began operation. The third reactor, AD-3, was started up 14 July 1961. The second and the third reactors were shut down 31 December 1990 and 14 August 1992, respectively. In 1959, construction began on the dual-purpose uranium-graphite reactors ADE-4 and ADE-5. These reactors began operation in 1965 and 1967, respectively, and are still operating. The I-1 reactor had a single-pass core coolant system; the cooling water was discharged into the Tom River after dilution. The other four reactors have closed-loop primary coolant systems, although some still use a single-pass system for control rod cooling.

The uranium hexafluoride production (sublimate) plant was constructed in 1951. The anhydrous hydrogen fluoride production department was put into operation in April 1954, followed a year later by the uranium tetrafluoride production department. The plant has been modernized, allowing it to increase its production capacity by several times and to decrease releases of radionuclides and toxic chemical substances by a hundredfold.

The radiochemical plant design was carried out between 1953 and 1961. The first stage of the plant was put into operation in August 1961, the second, in October 1962. Irradiated uranium slugs were reprocessed using the acetate precipitation process. In 1983 the plant switched to high-capacity extraction technology, which allowed the similar production works at the PA Mayak to cease operations. The new technology also significantly decreased the volumes of radioactive wastes. In 1958 the decision was made to build a chemical and metallurgical plant at the SCC, and in August 1961 the plant began production.

2.2.5 Discharges to surface waters

Industrial waters of the SCC are discharged into the Romashka River and flow into the water system of the Tom River near the village of Chernilschikovo. From there, they flow into the Ob River, the Ob Bay, and then to the Kara Sea. Discharged waters at the SCC are contaminated with various radionuclides, with a total annual

Table 2.23. Distribution of radionuclides in waters discharged from the SCC.

Half-life period	Radionuclide	Total activity Bq/yr	%
0–1 day	^{24}Na, ^{56}Mn	8.62×10^{14}	75.1
1 day–1 month	^{239}Np, ^{32}P, ^{51}Cr	2.45×10^{14}	21.3
1 month–1 year	^{58}Co, ^{46}Sc, ^{59}Fe, ^{65}Zn, ^{144}Ce, ^{54}Mn	3.64×10^{13}	3.2
>1 year	^{239}Pu, ^{137}Cs, ^{90}Sr, ^{106}Ru, ^{60}Co	4.37×10^{12}	0.4

activity release of about 7.58×10^{14} Bq (20,500 Ci; data as of 1992). In 1995, total activity of radionuclides in the discharged waters was 1.15×10^{15} Bq (31,000 Ci). The content of radionuclides with half-lives of more than one year is 0.4%, with a total activity of 4.37×10^{12} Bq/yr (119 Ci), as shown in *Table 2.23*.

Permissible levels of individual radionuclides have been exceeded in discharged waters. Before the once-through reactors were decommissioned, the radioactive contamination of the Tom River by SCC discharges had resulted in increased gamma radiation above the water surface. In 1989 and at the beginning of 1990, the exposure dose rate of gamma radiation near the mouth of the Romashka River and inside the sanitary and protective zone exceeded 600 μR/hr. Samples of contaminated water near the discharge point revealed the presence of radionuclides of induced activity: ^{24}Na, t_h = 15 hours; ^{143}Ce, t_h = 33 hours; and ^{140}La, t_h = 40.2 hours. Concentrations of these radionuclides equaled or exceeded the allowable dose concentrations in drinking water for the general population (the "B category" of the population; DC_B). Concentrations of ^{32}P were not measured in 1990, and concentrations of other radionuclides were 0.001–0.1 of DC_B.

Following the decommissioning of two reactors, the exposure dose above the Tom decreased by a factor of six. Water samples from the Chernilschikovskii channel near the mouth of the Romashka showed the presence of ^{46}Sc, ^{51}Cr, ^{60}Co, and ^{65}Zn with concentrations at 0.0001–1 of DC_B.

After the third reactor was decommissioned exposure dose rates decreased compared with 1991 levels, reaching 75 μR/hr near the mouth of the Romashka in 1992. In September 1992, concentration of total beta activity of radionuclides in the Tom near the discharge area was 23 Bq/L, and in the mouth of the Tom near the village of Kozjilino the beta activity concentration was 8.5 Bq/L. In 1992, in the control range of the river and at the water supply closest to the discharge point the concentration of ^{32}P was 2.9 times higher than its tolerable concentration for some population groups (2.9 of DC_B; 703 Bq/L or 1.9×10^{-8} Ci/L) due to exceedances of the permissible discharge. In the first quarter of 1993, installation of equipment

Table 2.24. Specific activity of radionuclides in bottom deposits of Romashka and Chernilschikovskii channels in 1994 (Bq/kg of air-dry paste).

Point of data collection	MED at height (μR/hr)		Radionuclide									
	3–4 cm	1 m	^{106}Ru	^{137}Cs	^{65}Zn	^{60}Co	^{226}Ra	^{232}Th	^{152}Eu	^{134}Cs	^{54}Mn	^{46}Sc
1	95	85	5.5	33	200	64	38					
2	60	53			50	17	32	46				
3	40	35	1,300	240	1,240	750			360	67	42	
4	22	20		39	77	57	43	47				
5	18	17		50	445	120	46					72
6	14	13		60	270	105						24

Note: ^{90}Sr and Pu content in bottom deposits was not examined. MED = Median exposure dose.

for salt removal from the control rod cooling water resulted in a decrease of the ^{32}P discharge.

Measures to improve environmental protection at the SCC in 1993–1994 resulted in radionuclide concentrations below the permissible concentration levels. In 1994, concentrations for most of the technogenic radionuclides were below the detection limit. Concentrations of ^{32}P exceeded DC_B only near the river ranges, but did not exceed DC_B near where water is used.

Long-lived radionuclides were detected in bottom deposits in 1994 (*Table 2.24*). Maximum concentrations of radionuclides observed in bottom deposits of the Tom near the mouth of the Romashka are as follows: ^{106}Ru, 1,336 Bq/kg; ^{65}Zn, 1,240 Bq/kg; ^{60}Co, 748 Bq/kg; ^{152}Eu, 363 Bq/kg; ^{137}Cs, 239 Bq/kg; ^{134}Cs, 67 Bq/kg; and ^{54}Mn, 42 Bq/kg.

Many years of discharges of industrial waters containing radionuclides to the Tom River have resulted in contamination of floodplain soils and vegetation. In 1991, local contaminated areas with ^{51}Cr and ^{65}Zn concentrations of 2.2×10^5 Bq/m^2 and ^{60}Co concentrations of 3.7×10^4 Bq/m^2 were detected on the floodplain of the Tom. Much lower concentrations of ^{58}Co, ^{46}Sc, ^{144}Ce, and ^{59}Fe were also detected. The global radioactive soil background does not contain these radionuclides, so their origin is connected with SCC discharges. The level of ^{137}Cs contamination on the floodplain of the Romashka and in the Chernilschikovskii channel was 7×10^4 Bq/m^2 in 1994.

In drinking water samples collected at the settlements the content of technogenic radionuclides with gamma radiation was below levels detectable by the equipment in place. In 1992 the total beta activity of drinking water at Samus was 7.4 Bq/L, at Chernilschikovo it was 37 Bq/L, and at Orlovka it was 14.8 Bq/L. In water samples collected from 76-m and 159-m wells near the village of Naumovka

Table 2.25. Contaminated land at the SCC (km^2).

Distribution of contaminated land by exposure rate level (μR/hr)	Production zone	Sanitary and protective zone	Observation zone	Total
Up to 60	3.8	–	–	3.8
61–120	1.6	–	–	1.6
121–240	1.0	0.3	–	1.3
241–1,000	1.7	–	–	1.7
More than 1,000	2.0	–	–	2.0
Total	10.1	0.3	–	10.4

Table 2.26. Radionuclide releases to the atmosphere from the SCC in 1993–1994 (% of tolerance dose level).

Substance	1993	1994 (8 months)
Integrated α-active nuclides	0.3	0.3
Integrated β-active nuclides	0.1	0.2
Integrated inert radioactive gases	0.3	0.2
^{131}I	0.2	0.4
^{90}Sr	0.6	0.6

(the Kantessky site) in 1992, ^{90}Sr concentrations of 0.03–0.04 Bq/L and ^{137}Cs concentrations of 16–29 Bq/L were detected.

In 1993, GPP Berezovgeologia detected the presence of ^{137}Cs in underground waters collected from wells (90 m and 140 m deep) near the village of Georgievka. This concentration was less than DC_B – for ^{90}Sr, DC_B = 15 Bq/L (4×10^{-10} Ci/L); for ^{137}Cs, DC_B = 550 Bq/L (1.5×10^{-8} Ci/L) – but the ^{137}Cs concentration equaled or exceeded the temporary permissible levels of 18 Bq/L (5×10^{-10} Ci/L). The presence of technogenic radionuclides in underground waters gives evidence of their penetration into the water-bearing horizons.

2.2.6 Surface contamination

The total amount of land contaminated by releases from the SCC is shown in *Table 2.25*.

2.2.7 Atmospheric releases

Data on atmospheric releases in 1993 (excluding the accidental release of 6 April 1993) and for eight months of 1994 are presented in *Table 2.26*. Releases were 0.1–0.6% of the permissible dose (tolerance dose level, or TDL).

The radionuclide content in the ground layer of air in 1993 (from SCC data) is presented in *Table 2.27*.

Table 2.27. Radionuclide content in ground layer of air in 1993 (% of atmospheric DC_B).

Point of observation	Observed substance									
	Sum of α-active nuclides[a]	Sum of β-active nuclides[b]	^{90}Sr	^{137}Cs	^{103}Ru	^{106}Ru	^{144}Ce	^{95}Zr	^{95}Nb	^{131}I
Sanitary and protective zone	33	240	5.0	6.5	2.7	51.2	3.6	14.9	38.5	30
Observation zone										
Seversk	45	119	0.5	4.9	0.2	3.0	0.8	0.8	1.7	30
Naumovka	34	87	0.8	1.4	0.4	6.4	1.4	4.0	3.6	30
Tomsk region	21	40	0.3	1.3	0.5	2.2	1.8	0.6	0.6	30
Background (Pobeda)	12	41	1.2	0.9	0.4	3.2	1.8	0.6	0.4	30

[a] Percentage based on DC_B for ^{239}Pu.
[b] Percentage based on DC_B for ^{90}Sr.

Table 2.28. Long-lived integrated beta activity of atmospheric radionuclide fallout within the 100-km SCC zone (Bq/m^2/yr).

Point of observation	1990	1991	1992
Tomsk	285	365	212
Tomsk Oblast			
Kozhevnokovo	226	402	272
Bogashevo	359	475	285
Krasnii Yar	173	146	252
Rervomayskoe	319	365	279
Baturino	–	402	238
Average for western Siberia	386	411	207

Air basin radiation conditions in the SCC sanitary and protective zone were characterized as satisfactory according to SCC and Rosgidromet data. At the same time, as a result of SCC activity the zone of Combine influence was formed, extending tens of kilometers north–northeast of the SCC.

Monitoring of radioactive pollution of the atmosphere is carried out by Rosgidromet with daily sampling and analysis of atmospheric particulates at eight meteorological stations within in the 100-km Combine zone. Monthly average summary beta activity of fallout at these stations in 1900–1992 ranged between 0.04 and 2.9 Bq/m^2/day. Annual beta-active radionuclide fallout is presented in *Table 2.28*.

2.2.8 Solid radioactive waste disposal

In its more than 40 years of operation, the SCC has generated more than 130,000 metric tons of solid radioactive wastes. Data on accumulated solid radioactive wastes and characterization of the waste storage and disposal facilities are presented in *Table 2.29*.

The methods used to manage solid waste depend on the waste type. Depending on the specific activity level, it is either disposed of in earthen or concrete trenches, or piled up in special compartments at regular storage sites. Solid wastes from production reactors and enrichment and uranium production plants are stored and disposed of at the production sites. Since 1961, a specially equipped facility has been used for burial of solid radioactive wastes from the radiochemical, chemical, and metallurgical plants. Low-level solid wastes are buried in trenches. Medium- and high-level wastes are buried in concrete structures.

2.2.9 Liquid radioactive waste treatment and disposal

Significant amounts of high-, medium-, and low-level radioactive wastes have accumulated as a result of reprocessing of irradiated uranium at the SCC. Solutions and sludges are treated as liquid radioactive wastes. The majority of liquid process waste (more than 95%) is generated at the radiochemical plant.

Open storage facilities and underground disposal sites are used in the liquid radioactive waste management scheme. To process liquid radioactive wastes at the SCC there is a system of open storage facilities, two deep-well injection sites, a low-level waste processing ground, and a station for treating medium- and high-level waste.

The SCC has adopted waste disposal in deep underground strata as the main way to manage liquid radioactive waste. High-level wastes are stored in stainless steel reservoirs; after treatment, they are sent to underground disposal. Medium-level wastes are also sent to underground disposal after appropriate treatment. Both open surface-level facilities and special closed facilities are used for intermediate storage of liquid radioactive wastes. Medium-level process wastes from the chemical and metallurgical production works are stored in an open pool. Process wastes from the enrichment plant are added to the wastes sent for underground disposal. Liquid radioactive wastes from the sublimate plant are sent to two sludge-storage facilities.

Low-level non-process wastes from all plants are sent to two water reservoirs and from there to treatment facilities for processing. Up to 50% of the treated wastewaters are disposed of underground. Another part, after being treated to standard levels (utilizing coagulation, mechanical cleaning, and ion exchange), is

Table 2.29. Solid radioactive wastes (RW) at the SCC.

Description	Time period of operation		Volume (1,000 m^3)		Area (1,000 m^2)	Amount of RW activity			Notes
	Start	End	Design	Actual		RW (tons)	Specific (Ci/L)	Total (Ci)	
Earthen trench-type burials, no waterproofing of bottom and slopes. Once trench is full, vertical leveling with soil on waste top is carried out; total of 17 burials.	1955–1987	1970–present	166.8	146.7	53.66	84,410			Solid RW of the uranium enrichment plant; UF_6 production; chemical, metallurgical, and radiochemical plants; production reactors; containing ^{234}U, ^{235}U, ^{238}U, ^{60}Co, ^{65}Zn, ^{137}Cs, ^{90}Sr, ^{103}Ru, ^{106}Ru, ^{239}Pu radionuclides.
Solid RW storage facilities. Underground reinforced-concrete structures with reinforced-concrete cover. External and internal isolation with bitumen, concrete (or asphalt) on bottom. Some structures lined with stainless steel.	1955–1992		129.2	95.35	18.04	46,743		29,912	Solid RW containing ^{60}Co, ^{65}Zn, ^{14}C, ^{137}Cs, ^{90}Sr, ^{95}Zr, ^{95}Nb, ^{103}Ru, ^{106}Ru, ^{234}U, ^{235}U, ^{239}Pu radionuclides.
Total solid RW						131,153		$>3\times10^4$	

discharged into the river through an intermediate water reservoir settling basin. The liquid radioactive wastes that are not subjected to processing are sent to open sludge-storage facilities. Sludges, filtering materials, and regenerates from treatment facilities fall mainly into this category.

During the early operations of the radiochemical plant, medium-level liquid radioactive wastes were discharged into the B-1 basin and from there into the B-2 basin. Afterward, as the underground liquid radioactive waste disposal site was put into operation, the basins were used as reservoirs for intermediate storage of solutions before these solutions were pumped into the underground strata. These basins have been removed from service. The total activity of long-lived nuclides collected there is estimated to be 4.6×10^{18} Bq (126 megacuries, or MCi). The reservoirs are not large in volume, and in dry summers partial evaporation of the water is possible.

The B-1 basin is a surface storage facility with a 1-m-thick loamy wall on the bottom and slopes. The wall is covered with a 1-m-thick soil layer. The basin area is 60,300 m^2, with a volumetric capacity of 150,000 m^3, of which 110,000 m^3 are currently used. The total activity of the radionuclides collected in the basin is estimated to be 2.7×10^{18} Bq (73 MCi). At present, the basin is being decommissioned.

The B-2 basin is a surface storage facility with a 1-m-thick loamy wall on the bottom and slopes. The wall is covered with a 1-m-thick soil layer. The basin area is 51,400 m^2, with a volumetric capacity of 135,000 m^3, of which 63,700 m^3 are currently used. The total activity of the collected radionuclides is 1.9×10^{18} Bq (50.5 MCi). At present, the basin is being decommissioned. Since 1991, work has begun filling the B-2 basin with soil.

The B-25 basin is a surface storage facility with a 1-m-thick loamy wall on the bottom and slopes. The wall is covered with a 1-m-thick soil layer. Its area is 10,000 m^2 and it has a volumetric capacity of 20,000 m^3, of which 13,000 m^3 are currently used. Radionuclides with a total activity of 5.2×10^{13} Bq (1,400 Ci) are collected in the basin. Annual discharges to the basin from the chemical and metallurgical plant total 1,300 m^3 of liquid radioactive wastes. The same volume of liquid radioactive wastes is sent to the RKh-1 sludge-storage facility after retention. The RKh-1 is a surface storage facility for liquid radioactive waste with a 0.45-m-thick loamy wall on the bottom and slopes. The wall is covered with a 0.5-m-thick soil layer. Its area is 20,000 m^2 and it has a volumetric capacity of 100,000 m^3, of which 70,000 m^3 are currently used. The total radionuclide activity is 6.7×10^{13} Bq (1,800 Ci). Each year, the enrichment and UF_6 production plants and clean-up facilities send up to 100,000 m^3 of liquid radioactive waste to the sludge-storage facility, which is used as an intermediate settling basin.

The same volume of solution is sent to the RKh-2 sludge-storage facility. The RKh-2 is a surface storage facility with a 0.45-m-thick loamy wall on its bottom

and slopes. The wall is covered with a 0.5-m-thick soil layer. The sludge-storage area is 46,000 m^2 and it has a design capacity of 210,000 m^3, of which 84,500 m^3 are currently used. Annual receipt to the sludge-storage facility from the RKh-1 is 100,000 m^3; after settling, the same volume is sent to underground disposal. The radionuclide activity in the sludge-storage facility is estimated to be 3.3×10^{13} Bq (900 Ci).

VKh-1 is an engineered flowing water storage reservoir used for settling and intermediate holding of wastewaters. Its bottom has no waterproofing. It has an area of 300,000 m^2 and a volume of 500,000 m^3, 375,000 m^3 of which are actually filled. The collected radionuclide activity is 3.0×10^{12} Bq (80 Ci).

VKh-3 is an engineered flowing water storage reservoir used for balancing, settling, and intermediate holding of special canalization waters before cleaning. The reservoir's bottom is made of natural soil with an area of 1,362,000 m^2 and a volume of 2,470,000 m^3, of which 2,336,000 m^3 are actually filled. The total radionuclide activity is 2.2×10^{14} Bq (6,000 Ci).

Annually, about 1,800,000 m^3 of liquid radioactive wastes enter the water reservoir from production works. The same volume of wastewaters is sent to VKh-4, a water storage reservoir located at the cascade after the VKh-3 and before the clean-up facilities. Its bottom has no waterproofing. It has an area of 1,350,000 m^2 and a volume of 4,350,000 m^3, of which 2,880,000 m^3 are currently used. The total radionuclide activity is is 4.4×10^{12} Bq (120 Ci). Details of liquid waste storage facilities at the SCC are given in *Table 2.30*.

The majority of wastes are injected underground. The Paleozoic and Mesozoic–Cenozoic stratigraphic column in the SCC area is described in *Table 2.31*. Paleozoic beds are mainly composed of shales with a clayey weathering crust in the upper part. A thick sandy-clay layer of Mesozoic–Cenozoic mantle consists of Cretaceous and Quaternary sedimentary formations. The Cretaceous formations are represented by sandy horizons I, II, III, and IV, and clay horizons A, B, C, and D; the Quaternary formations consist of sandy horizons IVa, V, and VI, and clay horizons E, F, and G. The boundary between Cretaceous and Quaternary sediments is horizon E, which divides sandy horizons IV and IVa.

Horizons II and III are used as disposal strata and overlie low-permeability A and B clayey horizons and clays of weathering crust with interbedding of D low-permeability formations. Horizon I, which divides the A and B horizons, is not widespread. Horizons II and III are formed from middle-granular sands of various degrees of clayiness. The main minerals are quartz (70–80%), feldspar (orthoclase, microcline, plagioclase), and minerals of the micas and hydromicas group. Carbonate minerals and organic matter also occur. Low-permeability horizons consist of clay rocks: many-colored, dense clays, including sandy-aleurite or siderose clays. Jointing occurs in places but it is not a characteristic feature in general.

Table 2.30. Liquid radioactive wastes (RW) at the SCC.

Description	Time period of operation		Volume (1,000 m^3)		Area	Amount of RW activity			Notes
	Start	End	Design	Actual	(1,000 m^2)	RW (tons)	Specific (Ci/L)	Total (Ci)	
Basins B-1, -2, -25. Surface storage facilities. Loamy isolation layer on bottom and slopes; 1-m-thick soil layer above loamy shield.	1961–1965	1982–present	305	187	122	186,750		1.23×10^{8}	Medium-level wastes containing ^{90}Sr, ^{137}Cs, ^{144}Ce, ^{60}Co, ^{106}Ru, ^{235}U, ^{238}U, ^{239}Pu radionuclides.
Surface sludge-storage facilities PKh-1, -2. Loamy isolation layer on bottom and slopes; soil layer above loamy shield.	1961–1971		310	155	66	155,000		27×10^{3}	Medium-level wastes containing ^{90}Sr, ^{137}Cs, ^{144}Ce, ^{103}Ru, ^{238}U, etc., radionuclides.
Water storage reservoirs VKh-1, -2, -3, flowing, used for settling and intermediate holding of wastewaters. Bottom sediments accumulated in water reservoirs.	1955–1960		7,320	5,580	3,012	55.8×10^{5}		6.21×10^{3}	Low-level wastes containing ^{90}Sr, ^{90}Y, ^{95}Zr, ^{95}Nb, ^{137}Cs, ^{144}Ce, ^{103}Ru, ^{106}Ru radionuclides.
Underground liquid RW disposal sites (18 and 18a)	1963		86,000	40,000	12,000	40,000	5.0×10^{-8} to 7	4.8×10^{8}	Low- and medium-level wastes containing ^{90}Sr, ^{95}Zr, ^{95}Nb, ^{137}Cs, ^{144}Ce, ^{106}Ru, ^{238}U, ^{239}Pu radionuclides.
Total liquid RW								6.03×10^{8}	

Table 2.31. Stratigraphic scheme of Paleozoic and Mesosoic–Cenozoic formations in the SCC area.

Group	System	Epoch	Suite	Index	Horizon thickness (m)	Rock description
Ceno-zoic	Quaternary	Holocene Pleistocene		VI	50–60	Sands with pebble and gravel lens with interbeds of loam, sandy loam, and clays
	Neogene	Pliocene	Kochkovskaya	G	10–55	Clays with sandy lens; sands with pebbles and gravel
	Paleogene	Oligocene	Azharminskaya		1–32	Clays with interbeds of sand
			Novomikhailovs-kaya		0.5–80	Clays with sand lens and interbeds; lignite
			Altymskaya	V	35–74	Sands with pebble and gravel with interbeds of clay; lignite
		Eocene	Yurkovskaya	F	2–18	Kaolinized clays
			Lyulivorskaya	IVa	0.5–26	Clayey sands
			Kuskovskaya	E	8–10	Finely dispersed clays
Meso-zoic	Creta-ceous	Late	Symskaya	IV	40–60	Sands with interbeds of clays
				D	20–47	Clays with interbeds of sands
			Simonovskaya	III	37–94	Sands with interbeds of clays
				C	10–20	Heavy clays
				II	25–40	Sands with interbeds of clays
		Early	Kiyskaya	B	20–35	Kaolinized clays
				I	18–48	Sands with interbeds of clays
			Kiyalinskaya	A2	Up to 74	Many-colored clays with stratum of sandstones
	Triassic Jurassic			A1	Up to 64	Weathering crusts, white kaolinized clays
Paleo-zoic	Carboni-ferrous	Early	Basandayskaya Lagernosidskaya Yarskaya		160	Aleurolite-clayey shales with interbeds of sandstones, with diabases and lamprophyres

There are two water-bearing rock complexes: a lower complex consisting of horizons I, II, and III, and an upper one consisting of horizons IV, IVa, V, and VI. The complexes are divided by a horizon of low-permeability clay layers D with waterproof features. Hydrologic parameters of the disposal strata and horizon D

Table 2.32. Hydrologic parameters of disposal strata and horizon D in the area of sites 18 and 18a.

Parameters	Site 18		Site 18a
	Horizon I	Horizon III (lower part)	Horizon II
Depth (m)	349–386	270–320	314–341
Thickness (m)	30–50	50–90	30–50
Effective thickness (m)	13–24	22–75	13–30
Total porosity	0.35	0.4	0.35
Effective porosity	0.1	0.15	0.05–0.14
Transmissivity (m^2/day)	224	34	17–24
Hydraulic conductivity (m/day)	0.5–3.0	0.2–2.2	0.7–0.9
Coefficient of pressure conductivity (m^2/day)	1.2×10^5	2×10^5	10^5
Pressure head above roof (m)	325–350	25–280	300–320
Thickness of horizon D (m)	58–62	58–62	28–29
Hydraulic conductivity of horizon D (m/day)	1.2×10^{-4}	1.2×10^{-4}	1.2×10^{-4}

are given in *Table 2.32*. The upper part of the section differs significantly from the lower part in terms of hydrologic characteristics. Tectonic structures which could lead to abnormal vertical migration of waste have not been identified in the SCC area.

Site 18 is used for low-level waste disposal (up to 6,300 m^3/day) and site 18a is used for medium-level waste disposal (up to 550 m^3/day). The latter was also used for experimental disposal of limited amounts of high-level wastes, but such wastes are no longer disposed of at this location. The underground storage sites are situated close to the main production complexes of the SCC, within the limits of its sanitary and protective zone. The waste contains uranium fission products, including isotopes of strontium, zirconium, niobium, ruthenium, cesium, and cerium, as well as non-recoverable microconcentrations of uranium and transuranium elements, salts, detergents, acids, alkalines, and finely dispersed solid materials.

Before disposal, waste processing is carried out at the treatment facilities and at the radiochemical plant to make the wastes compatible with the geological medium. Additional extraction of long-lived transuranium elements also takes place. The wastes are then transferred to the disposal site by pipeline. Pumping is carried out through a system of 37 injection wells. The injection pressure is up to 2 MPa at site 18 and up to 1.2 MPa at site 18a. Within and outside the limits of the disposal sites there are 244 observation wells used to monitor the geological medium and to control waste migration.

The medium-level waste disposal at site 18a is carried out in the second sandy stratum located in the depth interval of 315–340 m. The strata used for liquid radioactive waste disposal are separated, underlain, and covered by weakly

permeable loamy floors, isolating the strata containing the liquid radioactive waste from shallow groundwaters. The natural velocity of water movement in the strata is 3–5 m/yr. Radionuclides are strongly sorbed to the rocks.

Special geological prospecting studies and investigations preceded creation of the underground disposal sites. In principle, these studies substantiated the feasibility and safety of disposal operations. The site has received a temporary license that permits underground disposal of radioactive wastes.

3

Sediment Transport and Dose Calculation Methodology

This chapter describes the general methodology for analysis of doses to the population. Three general scenarios are presented here; site-specific aspects are presented in Chapters 4 and 5. This chapter also provides an overview of the mathematical basis of the modeling of contaminated sediment transport and the dose assessments based on existing and redistributed radionuclides.

3.1 General Scenarios

Three general scenarios of exposure are analyzed in this report. The first scenario involves a dose assessment for current contamination levels along the rivers. The other scenarios involve the modeling of radionuclide transport due to redistribution by flooding (Scenario 2) and failure of a holding pond (Scenario 3), and dose assessments for the resulting contamination.

3.1.1 Scenario 1: Existing contamination levels and locations

The baseline scenario was based on exposure to radionuclides at present levels and locations in the contaminated river valleys. The locations and levels of radionuclide contamination were based on a variety of sources, including published and unpublished site data and analysis of data in the literature. The doses resulting from this scenario were estimated using two computer codes: RESRAD (Yu *et al.*, 1993), developed by Argonne National Laboratory, and a beta version of a Russian code, SAMAD, based on the methodology outlined by Georgievskii (1994). Available Russian data pertaining to village populations and typical food consumption rates, and estimates of various exposure-generating activities were used as inputs to these models.

3.1.2 Scenario 2: Redistribution of existing contamination by flooding

The second scenario was based on a redistribution of radionuclides in the river sediments and floodplain soils due to flooding. The redistribution was calculated for

floods with discharges varying throughout the range of historically observed discharges. The redistribution of radionuclides was estimated by post-processing the hydraulic output from the River Analysis System (HEC-RAS), a river hydraulics computer code developed by the Hydrologic Engineering Center of the US Army Corps of Engineers (USACE, 1997). The post-processing routines were developed by the Radiation Safety of the Biosphere (RAD) Project staff to estimate contaminated sediment transport. Redistribution of contaminated sediments was estimated by assuming that the radionuclides were irreversibly sorbed to the sediments and soils in the contaminated reaches. As with the first scenario, the increase in annual dose resulting from this scenario was estimated using the computer codes RESRAD and SAMAD.

3.1.3 Scenario 3: Release of stored radionuclides into the river system

The third scenario was based on a hypothetical release of radionuclides in the liquids and sediments of a holding pond at the site into the adjacent river and its sediments. The redistribution of the contaminated sediments was calculated for river discharges of various magnitudes throughout the range of reasonable discharges. The radionuclide inventories associated with these hypothetical releases were based on scenarios considered feasible by the engineers at both the Mining and Chemical Combine (MCC) and the Siberian Chemical Combine (SCC). The releases were assumed to enter the rivers primarily as contaminated sediments via runoff channeled through streams used by the sites to discharge process water. The release and redistribution of radionuclides in the river were modeled using river hydraulic computations from HEC-RAS and sediment transport estimates from in-house post-processing routines. The resulting doses were estimated using RESRAD and SAMAD.

3.2 Radionuclides for Evaluation

The radionuclides in sediments and soils evaluated in this study are listed in *Table 3.1*. In addition to the nuclides listed in *Table 3.1*, several shorter-lived radionuclides are evaluated in Chapter 5 to estimate doses from consumption of contaminated fish. In general, levels for the gamma-emitting radionuclides were determined using results of gamma spectrometry analyses of sediment and soil samples performed by previous investigators. To estimate contamination levels where no direct sampling took place, exposure rate data were used in conjunction with the relative ratios of radionuclides based on nearby samples and published external

Table 3.1. Radionuclides evaluated in the present study.

Radionuclide	Half-life in years
^{60}Co	5.3
^{106}Ru[a]	1.0
^{137}Cs	30.2
^{90}Sr	29.1
^{152}Eu	13.5
^{154}Eu	8.6
^{232}Th[a]	1.4×10^{10}
^{238}U[a]	4.47×10^{9}
^{239}Pu[a]	24,100

[a] Evaluated only for the contaminated fish pathway.

exposure dose conversion factors. In addition, contamination levels were estimated from exposure dose rate data using the radionuclide distribution of nearby samples and dose conversion factors from external exposure to nuclides. Data on ^{90}Sr contamination, which is a pure beta emitter, were practically nonexistent for Krasnoyarsk. Therefore the environmental concentrations for this radionuclide were assumed to be the same as those for ^{137}Cs (see discussion in Section 4.2.2). Adequate data on alpha-emitting nuclides were also generally lacking for the Yenisei River, and therefore these nuclides were not included in the current analysis.

The primary release pathway for ^{137}Cs and ^{90}Sr was probably accidental releases of reprocessing waste from the radiochemical plants. This same pathway is likely the cause of releases of ruthenium, uranium, plutonium, and other transuranic radionuclides. The radionuclides ^{60}Co, ^{152}Eu, and ^{154}Eu are activated corrosion products that were probably discharged with water used to cool the once-through reactors at these two sites. Contamination levels for other activation products, including ^{22}Na, ^{24}Na, ^{51}Cr, ^{54}Mn, ^{56}Mn, ^{59}Fe, ^{56}Co, ^{65}Zn, ^{76}As, ^{144}Ce, and ^{156}Eu, were also reported in some radiological surveys. However, because the once-through reactor designs ceased operations in 1990 at the SCC and in 1992 at the MCC (Bradley, 1997), the release of these short-lived radionuclides (all with half-lives of less than one year) has decreased significantly. Only releases from open-loop cooling of the control rods of the dual-purpose reactors result in continued release of these short-lived radionuclides.

Based on available data concerning plutonium production at the SCC and the MCC and on data from similar reactors at the Hanford site in the United States, Bradley (1997) suggests that 75–80% of the decay-adjusted radioactivity released to the environment may result from ^{63}Ni (half-life = 100 years). This radionuclide, a weak beta emitter, has not been reported in the environment at either site, which is no indication that it is not present. However, assuming the relative releases of

radionuclides provided by Bradley and using the exposure scenarios discussed in Section 3.4, the contribution of the dose from ^{63}Ni is approximately 15% of that provided by ^{90}Sr, indicating a relatively low dose contribution even if the radionuclide is present in large amounts.

Data related to levels and locations of specific radionuclides were based on site reports and analysis of data in the literature. For the Yenisei River, the primary sources of information on existing contamination were site data provided for this study, summaries of radiological surveys of the river made in 1990–1991 (Khizhnyak, 1995; Kosmakov, 1996), and a 1995 river sampling expedition by a joint US/Russian team of investigators (Phillips *et al.*, 1997). Selected results of the 1990–1991 expedition have been published by Bradley (1997) and Robinson and Volosov (1996), so that combining the data from those reports with data provided by the site gives the most complete picture to date, outside Russia, of the existing contamination in the river valley. The data of the joint US/Russian expedition are considered a limited independent verification of Russian data in the few areas of overlap.

For the Tom River below the SCC, the primary sources of data were the monitoring activities of the SCC (Andreev *et al*., 1994) and the research activities of off-site organizations such as Roskomgidromet (1991), Goskomecologia of the Tomsk Oblast (1996), and Tomsk Spravka (1994). Other contamination data were provided by Rikhvanov (1997), Lyaschenko *et al*. (1993), Zubkov (1997), Arkhangelskii *et al*. (1996), and Rikhvanov (1994). Summaries of some of these references were provided by the site contacts, and some references were summarized by Bradley (1997). According to the available data, surprisingly low levels of radioactivity were reported in the Tom River relative to the Yenisei; possible reasons for this situation are discussed in Chapter 5.

The primary measure for reporting contamination data for river bottom sediments and floodplain soil samples was surface contamination density (in curies per square kilometer, Ci/km^2). Less frequently, the data were reported in terms of concentrations [e.g., microcuries per kilogram (μCi/kg) dry weight of sediment or soil]. Typical contamination profiles by depth were reported for the Yenisei River but not for the Tom River.

Results of aerogamma surveys of the Yenisei and Tom Rivers were used to estimate the length of contamination along the river channel. Widths of contaminated plots were estimated for the Yenisei using statistical contamination data from a 13-km reach of that river. For the Tom, assumptions about the widths of contamination were made using expert judgement based on the topography of the floodplains. The contamination data for the radionuclides of interest were converted to soil mass concentration values by assuming a mixing depth of 20 centimeters (cm) and a bulk soil density of 1,800 kilograms per cubic meter (kg/m^3).

3.3 Modeling Radionuclide Transport by River Sediment

For Scenarios 2 and 3, redistribution of radionuclides was estimated using HEC-RAS to calculate river hydraulic parameters and a post-processing routine developed by the RAD staff to estimate radionuclide transport with sediment. Modeling redistribution of contaminated sediment proved challenging, as few models are capable of modeling contaminated sediment transport in rivers and deposition on floodplains. For this reason, an original post-processing model was developed. The development of original models is, of course, fraught with uncertainty, and the lack of validation means considerable caution is necessary when interpreting the results of such models. In this case, the RAD staff developed the model for sediment transport based on widely accepted theory and used the results of the computations as a guide for insight into the significance of different processes. Although it is likely that this model will prove to be of limited use in rigorous predictive modeling, it is expected to provide sufficiently reliable qualitative results to allow conservative scoping analyses.

3.3.1 Evaluation and selection of models

The hydraulic model used, HEC-RAS, was designed to perform one-dimensional hydraulic calculations for a full network of natural and constructed channels. Steady-flow water surface profile calculations are currently supported; unsteady-flow simulations and sediment transport/movable boundary computations are currently being added to the code.

The steady-flow component of the code is used for calculating water surface profiles for steady and gradually varying flow. The system can handle a full network of channels, a dendritic system, or a single river reach. It is capable of modeling subcritical, supercritical, and mixed-flow regime water surface profiles. The basic computational procedure is based on the solution of the one-dimensional energy equation. Energy losses are evaluated by friction (Manning's equation) and contraction/expansion (coefficient multiplied by the change in velocity head). The momentum equation is used in situations where the water surface profile varies rapidly. These situations include mixed-flow regime calculations (i.e., hydraulic jumps), hydraulics of bridges, and river confluences (stream junctions). The steady-flow system is designed for application in floodplain management and flood insurance studies to evaluate floodway encroachments. Capabilities are also available for assessing the change in water surface profiles due to channel improvements and levees.

Given the lack of existing contaminated sediment transport models, a post-processing routine developed by the RAD staff was used to evaluate contaminated sediment transport based on the sediment transport theory and using the output from

HEC-RAS. This routine was developed after extensive evaluation of the HEC-6 computer code (USACE, 1993), which was designed to evaluate sediment scour and deposition in rivers. Deposition of contaminated sediment in the floodplains was of primary interest in this study, and the use of HEC-6 was abandoned after extensive evaluation due to limitations concerning evaluating flow and deposition conditions in the floodplain regions. HEC-RAS, which relies on the same body of theory and uses essentially the same computational methods, has considerably more data output options. Because HEC-RAS is capable of providing output on hydraulic conditions in the floodplains where deposition was expected to occur, the decision was made to use the output from HEC-RAS as input to the post-processing routine, rather than the channel-floodplain aggregate hydraulic data available from HEC-6.

Although both the Tom and Yenisei Rivers have predominantly sand and gravel bottoms, it was hypothesized that the radionuclides were mainly associated with fine particles (i.e., silt and clay), and only these particle size classes were evaluated. This assumption was based on the limited data available indicating the distribution of contamination by particle size and the fact that sorption is generally proportional to surface area, with small particles having relatively larger surface area per unit mass. A mass of fine particles will thus have a greater capacity for sorbing contamination than an equivalent mass of coarse particles. The underlying theory of fine sediment transport is quite limited in terms of predictive capability; it is governed by empirical relations based on deposition velocities as a function of particle size and critical shear stresses for deposition and scour. The theory used in HEC-6 for fine particle scour and deposition was used in the post-processing routine summarized below. Although limited, this theory is expected to be satisfactory for the scoping-level analyses provided here.

3.3.2 Cohesive sediment and radionuclide transport model

The river was divided into reaches, denoted by the index i, and channel and overbank sections, denoted by the index k (***Figure 3.1***). HEC-RAS was run with a symmetric channel composed of three lateral sections: the right overbank, the left overbank, and the main channel. Water elevations were calibrated to available discharge curves along the river reach of interest by adjusting the Manning's numbers. The outputs of HEC-RAS were the surface areas, flow rates, and computed bed shear stresses for the channel and overbank sections.

The sediment scour rate in the post-processing routine was calculated as

$$^{SED}\dot{M}_{i,k} = ER \cdot \left(\tau_{i,k} - {}^{SCR}\tau_{CRIT}\right) \cdot SA, \tag{3.1}$$

where $\dot{M}$ is the erosion rate in kilograms per hour, ***ER*** is the slope of the erosion rate curve, τ is the bed shear stress in the segment, $^{SCR}\tau_{CRIT}$ is the critical shear

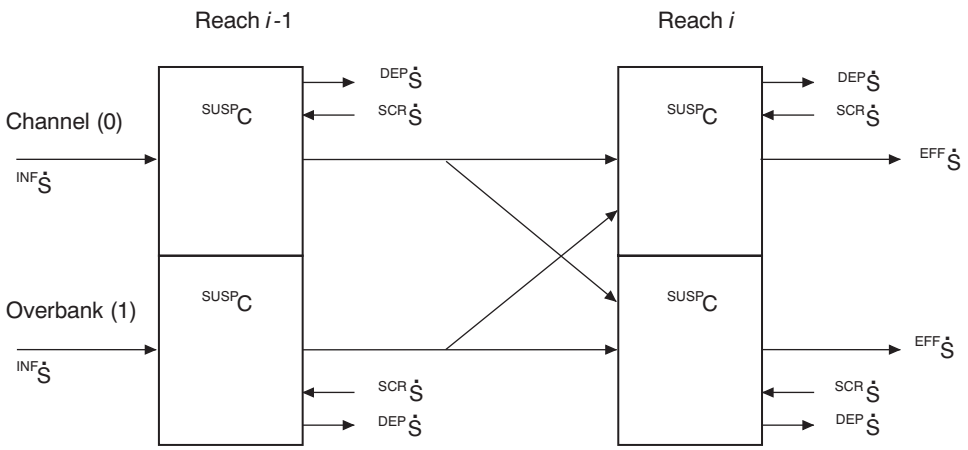

Figure 3.1. Conceptual model for sediment transport.

stress for scour, and *SA* is the surface area of the section. The critical shear stresses for silt and clay were assumed to be 0.7 and 2.1 kg/m^2, respectively (A. Brenkert, Oak Ridge National Laboratory, and R. Waters, IIASA, personal communication, 31 July 1997). Due to the lack of site-specific data, the critical shear stresses for scour and deposition were set equal to each other. Therefore, scour was assumed to occur above these critical stresses and deposition was assumed to occur below them.

The conceptual model for activity transport (*Figure 3.1*) shows the transport of adsorbed contaminants into and out of individual sections in the suspended phase. Complete mixing is assumed within each box and conservation of mass in terms of water and radioactively contaminated sediment is preserved. The activity transport model was developed for equilibrium, steady-state calculations.

The concentration of the activity suspended in the water column is based on an equilibrium homogeneous compartment model given by

$$C = \frac{\dot{S}}{Q}, \tag{3.2}$$

where C is the concentration, S is the activity-input rate, and Q is the discharge in the compartment. Activity effluent rates from each section were determined as follows:

$$^{EFF}\dot{S}_{i,k} = C_{i,k} \cdot Q_{i,k}. \tag{3.3}$$

The influent input rate to a section in a reach is the activity input due to advection from the previous reach. This rate is the sum of two sources: influent

suspended sediment from the same section in the upstream reach and a cross term indicating input from the opposite section of the upstream reach. Therefore, input into a channel section of a particular reach may be composed of inputs from the channel in the upstream reach and the overbank (floodplain) section in the upstream reach:

$$^{INF}\dot{S}_{i,k} = f_{i-1,k} \cdot^{EFF} \dot{S}_{i-1,k} + (1 - f_{i-1,k}) \cdot^{EFF} \dot{S}_{i-1,k'}, \tag{3.4}$$

where

$$f_{i,k} = \min\left(1, \frac{Q_{i,k}}{Q_{i-1,k}}\right). \tag{3.5}$$

The fraction $f_{i,k}$ indicates the fraction of flow and activity into a given section from the same section in the previous reach; the difference in flows between the two reaches in a section is equalized by the flows in the opposite section of the previous reach. For example, if overbank water discharge in reach i is 1,000 m^3/sec and is 4,000 m^3/sec in reach $i-1$, then $f = 0.25$, indicating that 25% of the overbank activity of reach $i-1$ flows into the overbank of reach i; the remaining 75% of flow and activity is diverted to the channel of reach i.

The input rate of activity into a section by scouring, $^{SCR}S_{i,k}$, is obtained by multiplying the mass input rate due to scour in a reach, $^{SED}M_{i,k}$, by the activity concentration in the soil or sediment of that reach, $^{SED}C_{i,k}$. We assume that the radionuclides are homogeneously distributed within a reach and the activity concentration is constant within a section:

$$^{SCR}\dot{S}_{i,k} = {}^{SED}C_{i,k} \cdot^{SED} \dot{M}_{i,k}. \tag{3.6}$$

Releases from the site to the river (Scenario 3) were assumed to be discharged into the overbank or into the channel when no overbank is present. The mechanism for the release is not specified. Possible mechanisms for release include (1) floodwaters washing into the pond and suspending the contaminated pond sediments; (2) a pond failure causing overland flow of water and sediments to the river; or (3) heavy rains causing overtopping of the pond banks and subsequent overland flow.

The amount of activity released, ^{PND}S, can be adjusted by a release fraction f to account for less-than-total release of activity from the pond:

$$^{PND}\dot{S} = f \cdot^{PND} C \cdot^{PND} Q = f \cdot^{PND} C \cdot \frac{V_{Release}}{t_{Release}}, \tag{3.7}$$

where ^{PND}C is the concentration of radionuclides in the release, and $V_{Release}$ and $t_{Release}$ are the volume and duration of the release, respectively.

The suspended concentration in a reach section is determined as follows:

$$^{SUSP}C_{i,k} = \frac{^{SCR}\dot{S}_{i,k} + ^{INF}\dot{S}_{i,k}}{Q_{i,k}}. \tag{3.8}$$

The product of the deposition velocity, ν, and the concentration of suspended activity determines the areal deposition rate. This rate is adjusted by a factor P to account for the dependence of deposition on the bed shear stress. This factor is sometimes interpreted as the probability that a settling particle will remain on the bed:

$$^{DEP}\dot{S}_{i,k} = \nu \cdot ^{SUSP}C_{i,k} \cdot P_{i,k}, \tag{3.9}$$

$$P = 1 - \frac{\tau_{i,k}}{^{DEP}\tau_{CRIT}}, \tag{3.10}$$

where $^{DEP}\tau_{CRIT}$ is the critical shear stress for deposition.

The areal deposition rate is multiplied by the time step to obtain the total areal concentration, which is then converted to an activity density by dividing by a mixing depth d and a bulk soil density ρ:

$$^{SED}C_{i,k} = \frac{^{DEP}\dot{S}_{i,k}}{d \cdot \rho} \cdot t. \tag{3.11}$$

In each reach, a check was performed to indicate the proportion of the activity deposited in a time step, and total activity in the reach was reduced accordingly to conserve total activity. At low flows (and consequently low bed shear stresses), 100% deposition in a section was possible, indicating that the activity was subsequently unavailable for further transport and deposition downstream. However, at higher flows, 100% deposition was generally not expected and the radioactivity was available for downstream transport. The deposition pattern is dependent on the assumed critical shear stress. Plots of the channel and floodplain shear stresses are provided in Chapters 4 and 5. The qualitative pattern of deposition at low flows and scour at high flows was expected because the potential range of critical stresses was within the range of predicted shear stresses at both sites.

3.4 Exposure: Dose Analysis

A unit-exposure approach was used in this study. Estimated doses from unit soil concentrations were scaled to the soil concentrations calculated for each scenario to estimate doses resulting from the scenarios. Lack of data on variability in lifestyles of inhabitants along both river valleys precluded more detailed assessment.

3.4.1 Evaluation and selection of dose assessment model

Evaluation of the doses to individuals from contaminated sediments and floodplain soils was performed independently using two computer codes: the American code RESRAD (Yu *et al.,* 1993) and the Russian code SAMAD (Georgievskii, 1994). Both codes were developed for use on a microcomputer and have some complementary features. RESRAD is a dose assessment methodology recommended for deriving site-specific soil guidelines for use in implementing the US Department of Energy's residual radioactive material guidelines. The radiation dose calculated by RESRAD is the effective dose equivalent (EDE) from the external radiation plus the committed EDE from internal radiation (ICRP, 1984, Section 2.1).

The exposure pathways considered by RESRAD include the following:

- Direct exposure to external radiation from the contaminated soil material.
- Internal dose from inhalation of airborne radionuclides, including radon progeny.
- Internal doses from ingestion of:
  - Plant foods grown in the contaminated soil and irrigated with contaminated water.
  - Meat and milk from livestock fed with contaminated fodder and water.
  - Drinking water from a contaminated well or pond.
  - Fish from a contaminated pond.
  - Contaminated soil.

SAMAD was created for analyzing the dynamics of radioactive contamination through ecological and trophic chains; in particular, it permits dose assessment during vegetative periods. SAMAD was calibrated using data on radioactive contamination after the Chernobyl accident. The code is currently used as a basic code in the Ukrainian Ministry for Emergency Situations and in the Russian "State Uniform Automatic System for Radiation Monitoring."

SAMAD calculates the EDE due to external exposure and committed EDE from inhalation and ingestion. The concept of SAMAD is similar to the systems analysis method described in ICRP Publication 29 (ICRP, 1978). It also includes additional compartment "eggs" and identifies transfer parameters for 18 major dose-inducing radionuclides: ^{89}Sr, ^{90}Sr, ^{95}Zr, ^{95}Nb, ^{103}Ru, ^{106}Ru, ^{131}I, ^{132}Te, ^{133}I, ^{134}Cs, ^{136}Cs, ^{137}Cs, ^{140}Ba, ^{141}Ce, ^{144}Ce, ^{239}Pu, ^{240}Pu, ^{241}Am. Specific transfer rates between compartments were determined for these nuclides, taking into account special features of agriculture in the former Soviet Union. In some cases these transfer rates differ significantly from those used in Western codes. For instance, doses due to unit contamination of some compartments by ^{90}Sr and ^{137}Cs might differ by twofold.

SAMAD can also be used to evaluate the doses from short-lived radionuclides such as ^{24}Na, ^{32}P, and ^{51}Cr. This feature was applied in this study for calculating doses from consumption of contaminated fish. SAMAD can model stochastic processes of nuclide transfer through ecological and trophic pathways, thus giving dose assessments in stochastic terms while describing soil contamination deterministically.

Despite these differences, the average characteristics (annual doses, integral contamination of agriculture products, etc.) calculated by RESRAD and SAMAD coincided. Therefore, only the results from RESRAD are presented and discussed. Models for estimating doses from soil contamination are simplified representations of complex processes. It is not feasible to obtain sufficient data to fully or accurately characterize transport and exposure processes. Similarly, it is not possible to predict future conditions with certainty. Consequently, there will always be uncertainties in the results. The models and input parameters incorporated into RESRAD have been chosen so as to be realistic but reasonably conservative, and the calculated doses are expected to be reasonably conservative estimates (overestimates) of the actual doses (Yu *et al.*, 1993).

3.4.2 General exposure assumptions

The primary assumptions associated with exposure and dose calculations are:

- The amount of time spent on contaminated land.
- The amount of shielding provided by the house while indoors.
- The diet consumed by the exposed individuals.
- The fraction of the diet grown on contaminated land.

The lifestyle of the inhabitants along the Yenisei and Tom Rivers is generally sustenance farming; almost all their time is spent on their land and little time is spent away from the village. Because the houses are primarily made of wood, shielding while in the house is expected to be relatively low.

Potable water is drawn from artesian wells rather than from the rivers. Few sampling data are available for these wells and we assume that they are not contaminated. Site contacts report that water in the Tom River is so contaminated by chemicals introduced upstream from Tomsk that it cannot be used for drinking water.

The factors used in RESRAD to compute doses resulting from unit exposures are given in *Table 3.2*. The values used in this study were based on the recommended values from “The Project of Program for Stabilization and Development Industry of the Krasnoyarsk Region by 1996–2000” (KRA, 1995). Ilyin (1995) provides an estimate of the doses received by residents of Georgievka from the

Table 3.2. Factors used in RESRAD unit-exposure dose calculations and comparative values.

Factor	Value used	Value in Ilyin (1995)	Default RESRAD value	Reference for value used
Shielding factor for inhalation	0.4	–	0.4	Default value
Shielding factor for external gamma	0.7	–	0.7	Default value
Fraction of day spent indoors	0.5	0.4	0.5	Default value
Fraction of day spent outdoors on contaminated land	0.5	0.6	0.25	KRA, 1995
Fruit, vegetable, and grain consumption (kg/yr)	140	610	160	KRA, 1995
Leafy vegetable consumption (kg/yr)	14	–[a]	14	KRA, 1995
Milk consumption (L/yr)	278	740	92	KRA, 1995
Meat and poultry consumption (kg/yr)	52	60	63	KRA, 1995
Fish consumption (kg/yr)	17	–	54	KRA, 1995
Soil ingestion rate (g/yr)	36.5	–	36.5	Default value

[a]Reported consumption of potatoes (440 kg/yr) and vegetables (170 kg/yr) was grouped into the fruits, vegetables, and grains category.

Table 3.3. Pathway dose conversion factors from RESRAD (μSv/yr)/(Bq/g).

Radionuclide	Soil	Inhalation	Plants	Meat	Milk	Soil	All pathways
^{60}Co	3,200	0.07	89	40	18	0.26	3,500
^{90}Sr	5.4	0.41	1900	320	350	1.5	2,600
^{137}Cs	730	0.01	84	62	76	0.49	950
^{106}Ru	270	0.15	32	1.6	0.01	0.27	320
^{152}Eu	1,500	0.07	0.68	0.12	0.0062	0.065	1,500
^{154}Eu	6.0	0.00033	0.0037	0.00064	0.000033	0.00035	6.0
^{232}Th	0.12	510	110	2.2	0.57	27	650
^{238}U	30	38	27	0.84	7.6	2.6	100
^{239}Pu	0.068	140	150	2.7	0.14	35	320

1993 accident at Tomsk. The value used for fraction of time spent outdoors on contaminated land is twice the RESRAD default value but is similar to the value used by Ilyin, which reflects the large amount of time spent outdoors.

The consumption values used are similar in magnitude to the default RESRAD values, except for milk consumption, which is three times higher. Ilyin assumed much higher values for milk and vegetable consumption. Velichkin *et al*., (1996) report a value of 1.3 liters per day (475 liters per year) for milk and milk-product consumption in the Tomsk Region.

A distribution of fish consumption was reported by Il'inskhikh (1996) for the village of Samus on the Tom River (*Figure 3.2*). Assuming consumption of

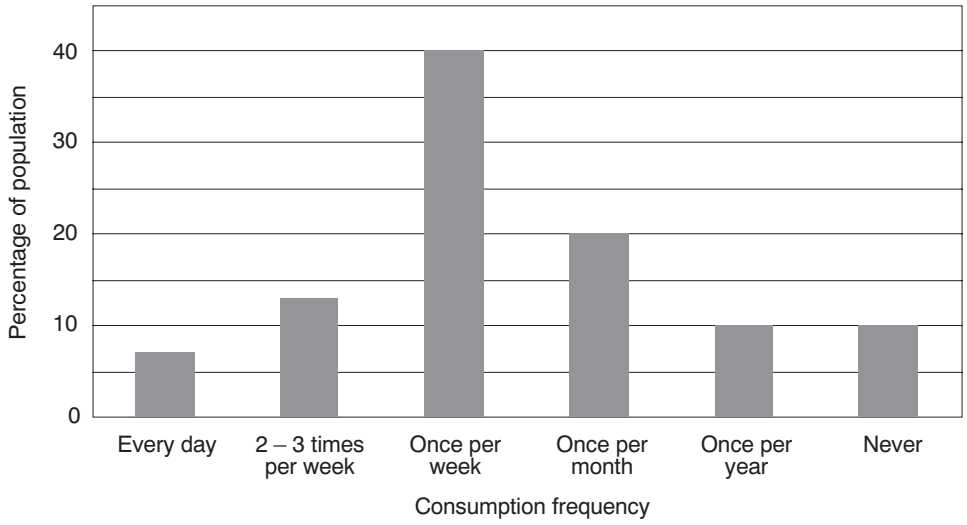

Figure 3.2. Distribution of fish consumption for the residents of Samus.

300 grams of fish per week (the most frequent consumption rate), the average annual consumption is 16 kg, which is very close to the value used in the analysis.

The unit pathway dose conversion factors from RESRAD are given in *Table 3.3* for each evaluated radionuclide. These factors were applied to the calculated radionuclide concentrations for the three scenarios at each site to estimate doses from occupying contaminated land.

For the gamma-emitting radionuclides (^{60}Co, ^{137}Cs, ^{106}Ru, ^{152}Eu, and ^{154}Eu), the primary exposure pathway is direct external exposure to contaminated ground; the primary pathway for the beta emitter (^{90}Sr) is food consumption. The alpha emitters (^{238}U and ^{239}Pu) contribute to the dose via several exposure pathways.

4

The Mining and Chemical Combine and the Yenisei River

An overview of the environmental conditions, sources of contamination, and releases of contaminants from the Mining and Chemical Combine (MCC) to the Yenisei River is given in Chapter 2. This chapter provides the site-specific scenarios, data, and results of radioactive contamination of the Yenisei River valley.

4.1 Site-specific Scenarios

The first scenario, MCC-1, is identical to the generic baseline scenario described in Section 3.1.1. The approximately 240 km of river between the release point and the confluence of the Yenisei and Angara Rivers is the study reach. The contamination levels and locations for this reach are described in Section 4.2.

The second scenario, MCC-2, is based on a redistribution of radionuclides in the river sediments and floodplain soils due to floods of various magnitudes. Because in the region of interest the Yenisei is controlled by the hydroelectric dam and large reservoir upstream from Krasnoyarsk, the magnitude of the most severe flooding has been reduced by a factor of two relative to pre-dam conditions (see *Figure 2.2*). A discharge equal to the maximum design discharge of the dam has occurred twice since the dam was constructed and filled in the late 1960s, most likely in response to rapidly rising reservoir levels. Except for the case of dam failure, any flood downstream from the dam will be influenced by anthropogenic activities and will likely be of short (a few days) duration. Proper planning of reservoir levels should minimize the frequency of maximum releases.

The third scenario, MCC-3, is based on a release of radionuclides in suspension from the sediments of holding pond 365 due to a hypothetical failure of the engineered systems surrounding the pond. Pond 365 is located 100 m from the right bank of the Yenisei River approximately 0.5 km upstream from Atamanovo on the first super floodplain terrace. The redistribution of radionuclides released from the pond is calculated for various river discharges using the same approach as in scenario MCC-2. The engineers at the MCC provided the radionuclide inventory of pond 365 (Shishlov *et al*., 1997). Because over 99% of the contaminants were associated with the pond's bottom sediments (see Section 4.2), the release was assumed to enter the river as contaminated sediments via overland flow.

4.2 Data and Data Analysis

The site-specific data used in the analysis of the three scenarios are contained in this section. Many of these data required further processing and analysis before they were used. Results of these data analyses are also contained in this section.

4.2.1 River hydrology and sediment transport

River Geometry. The geometry of the Yenisei River in the study area is characterized by a broad floodplain from Atamanovo to Predivinsk (1–100 km downstream from the discharge point), followed by a narrowing of the river valley between Predivinsk and Kazachinskoe (100–180 km downstream), and a subsequent opening into floodplains from Kazachinskoe to Strelka (180–245 km downstream). The river is dotted with islands throughout the study area. Some of the larger islands are Atamanovskii near Atamanovo, Zaboka and Zolotoi near Yuksevo, and Momotovo and Kazachii near Kazachinskoe.

Radiological surveys have indicated that the upstream and downstream ends of islands tend to function as traps for the released radioactive contamination. This contamination is likely the result of low-flow zones due to island wake effects, resulting in increased sediment deposition. The modeling used in this analysis cannot predict deposition based on these processes.

Simplified representations of river channel profiles were provided by technical contacts (Lapschin, 1997). These symmetric profiles were developed for a river flow of 2,500 cubic meters per second (m^3/sec). The simplified representation of the river channel profile was consistent with the one-dimensional hydraulic modeling provided by HEC-RAS. We compared the cross-sectional areas of these simplified channel profiles with those resulting from analysis of a navigation chart of the Yenisei River (Lopatin *et al*., 1988) and found them to be similar.

The slopes of the water surface between each given cross-sectional profile were used to calculate the relative and absolute elevations of the river reaches. These elevations were checked against known gauge elevations and found to be in reasonable agreement. The resultant longitudinal river profile is shown in *Figure 4.1*.

Floodplain geometry was developed from topographic maps by measuring the width of the nearest contour line at each selected cross section. The width of the floodplain overbank was defined as the distance from the shore to the nearest topographic contour on a 1:500,000-scale 1995 map of the Krasnoyarsk Krai. The resultant river geometry (*Figure 4.2*) is both linear and symmetrical. For simplification, the linear river geometry was used instead of the more meandering geometry because losses due to curvatures were expected to be low (USACE, 1997). The symmetrical geometry is consistent with the level of sophistication of the transport analysis. Water elevations were calibrated by adjusting the Manning's number. The

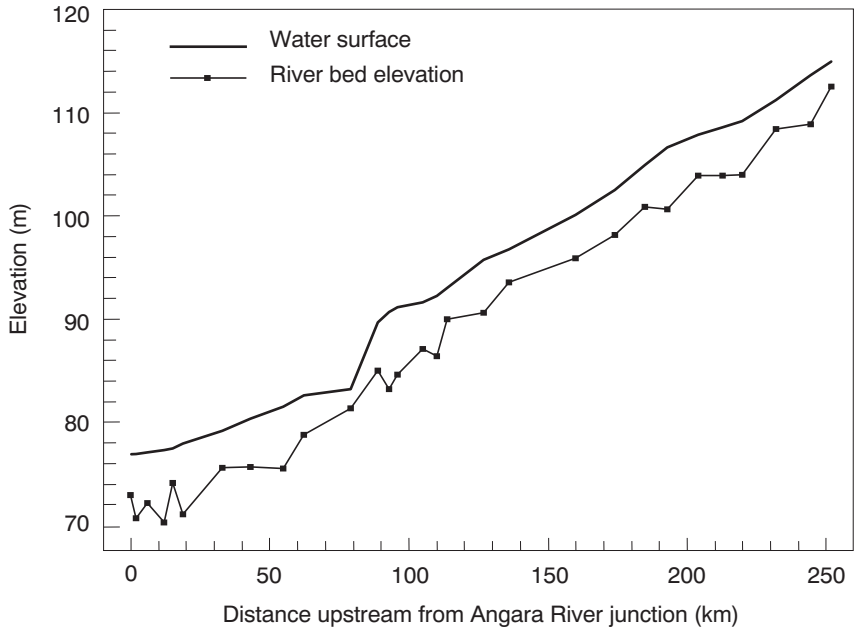

Figure 4.1. Longitudinal profile of the Yenisei River.

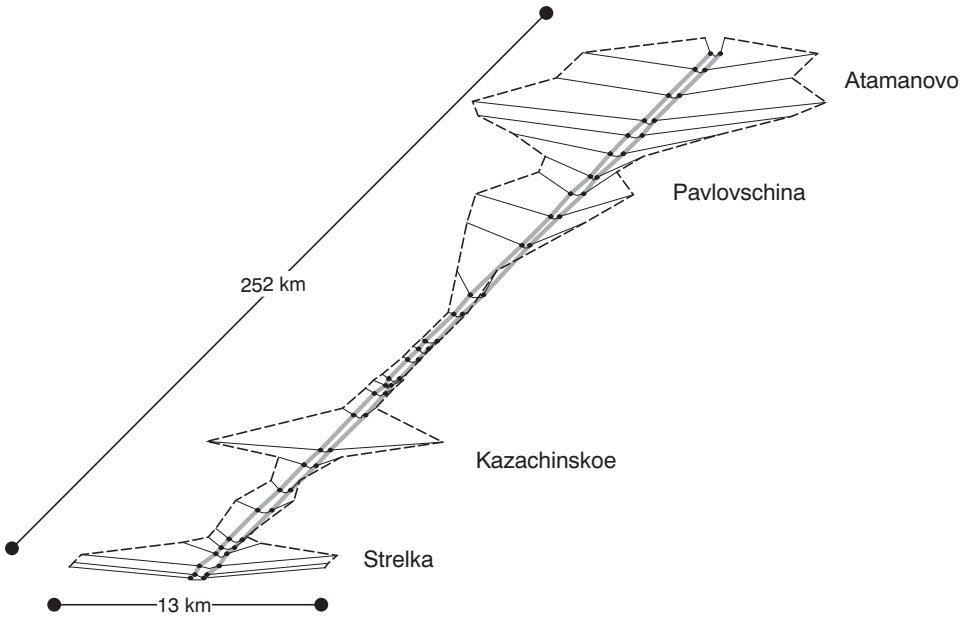

Figure 4.2. Schematic representation of the Yenisei River for HEC-RAS.

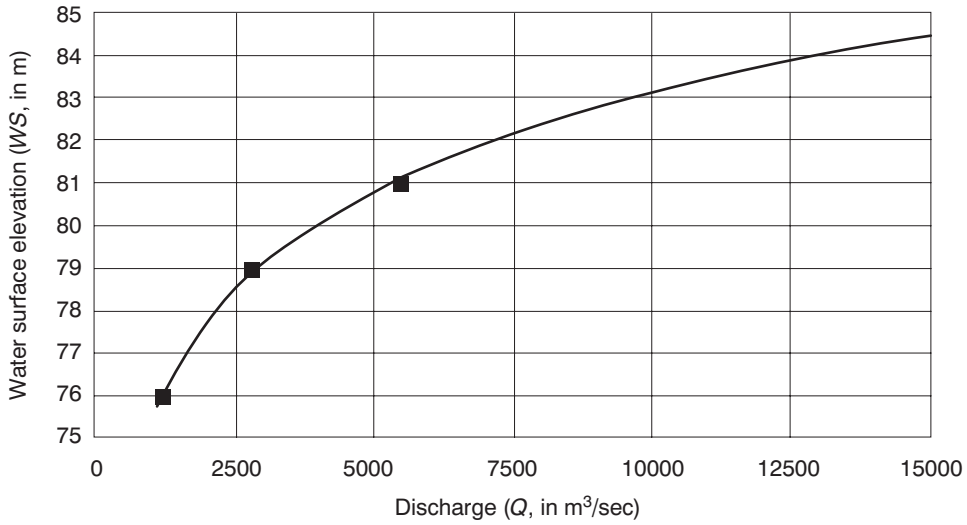

Figure 4.3. Constructed stage-discharge curves for the Yenisei River at Strelka (km).

most important parameters for calibrating water levels are the cross-sectional area and the wetted perimeter. Values for these parameters were similar to actual values.

River Hydraulic Data. HEC-RAS requires a downstream stage-discharge curve to perform the hydraulic computations. Therefore, a rating curve was developed for this location, referred to by the name of the nearby settlement Strelka. Because data were not available to directly input a rating curve at this location, an estimate of the rating curve was developed by correlating the minimum, average, and maximum water levels (from 1987–1989 data) with their associated minimum, average, and maximum discharges (Kosmakov, 1996). These data were fitted to a power series to determine a functional relationship for water level dependence on discharge, resulting in the following equation:

$$WS = 57.546Q^{0.0399}, \tag{4.1}$$

where Q is discharge (m^3/sec) and *WS* is the absolute water level elevation (m) above the Baltic Sea reference level. Although the water level of the Angara River at Strelka is likely to have a significant influence on this rating curve, the rating curves for upstream locations using this curve were found to be consistent with observed water surface elevations. The constructed stage-discharge curve (*Figure 4.3*) was used as input for HEC-RAS.

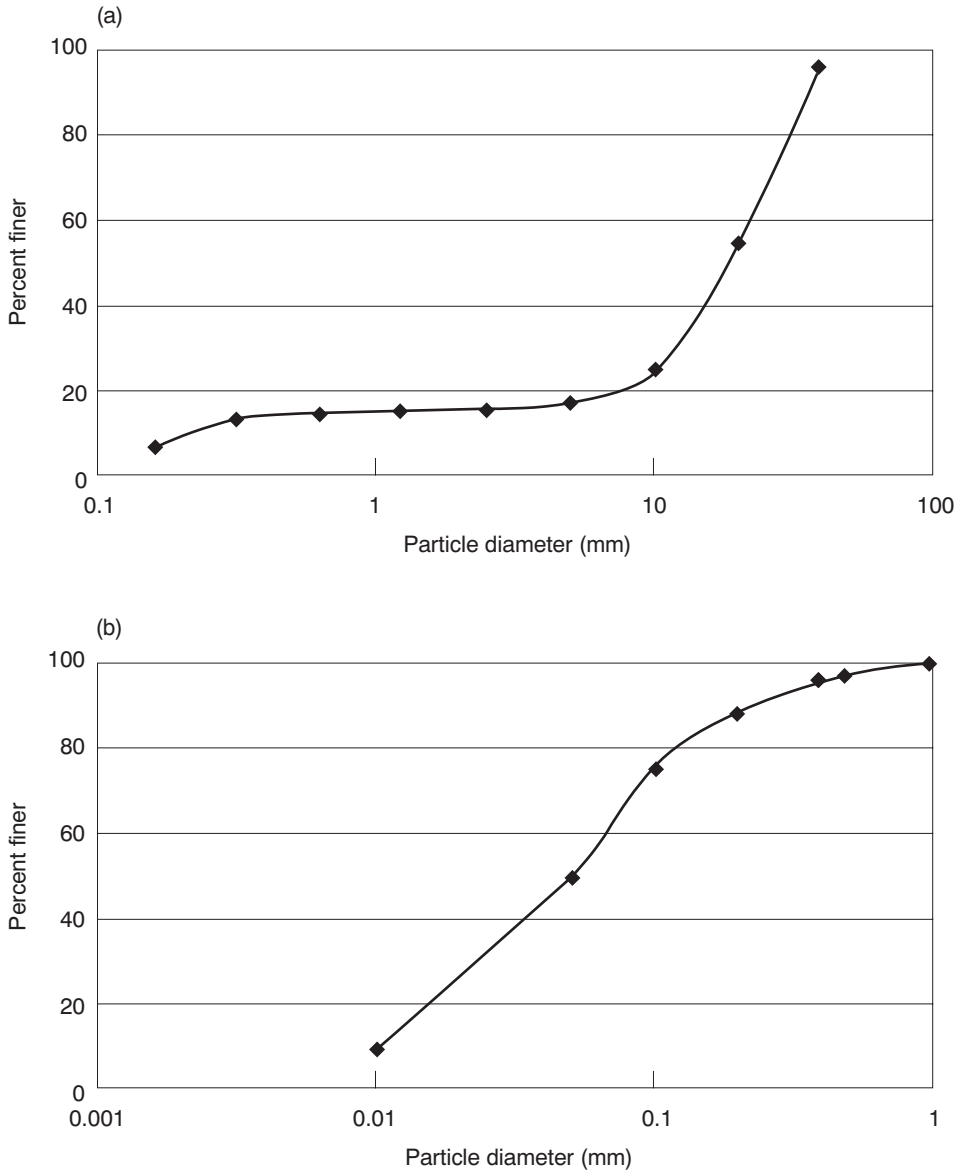

Figure 4.4. Typical material gradation in the (a) bed sediments and (b) suspended sediments of the Yenisei River.

Sediment Transport. The bed of the Yenisei River is composed primarily of gravel and cobbles (*Figure 4.4a*). Although the bed comprises mostly coarse sediments, the radionuclides are expected to be sorbed primarily to the finer particles of silt and clay (Kosmakov, 1996).

The suspended load in the Yenisei River is also relatively coarse (*Figure 4.4b*; Kosmakov, 1996), which is likely due to trapping of large amounts of finer sediments behind the hydroelectric dam upstream from the city of Krasnoyarsk. The suspended load in the study reach may be more indicative of floodplain material than channel bed material.

4.2.2 Existing contamination in the river valley

The existing contamination profile in the Yenisei River valley (see Appendix I), used in scenarios MCC-1 and MCC-2, was based on an analysis of six data sources. The data sources were prioritized in the following order:

1. Radionuclide-specific concentration or surface contamination data in order of priority (more recent survey data had higher priority): Shishlov *et al*. (1997); Velichkin *et al*. (1996); Phillips *et al*. (1996); Bradley (1997); Robinson and Volosov (1996).
2. Total surface contamination data. The geographically nearest radionuclide-specific data set was used to calculate radionuclide-specific concentrations: Ashanin and Nosov (1991), Karimulina and Klimenko (1991), and Nesterenko (1992), summarized in Khizhnyak (1995).
3. Gamma exposure dose rate (EDR) data. The geographically nearest radionuclide-specific data set was scaled to the reported EDR values in areas of overlap to estimate radionuclide-specific concentrations where data were otherwise unavailable: Khizhnyak (1995).

Results of the radiological survey performed in 1990–1991 provided average gamma counts for locations along the left and right banks and on islands in the Yenisei River (Kosmakov, 1996). These data were used to estimate the extent of radionuclide-specific contamination assuming that the radionuclide concentrations associated with the gamma count regions were equal to the sample point data located within the gamma count region. Surface contamination sometimes exceeded 1 million becquerels per square meter (Bq/m^2), or approximately 100 curies per square kilometer (Ci/km^2), during the 1990–1991 time frame.

The most recently collected data, from Shishlov *et al*. (1997) and Velichkin *et al*. (1996), are summaries of samples collected in 1996. The data provided by Bradley (1997) and Robinson and Volosov (1996), and contained in the Khizhnyak summary were incomplete summaries of the 1990–1991 radiological expedition.

The only data collected independently of the MCC are those of Phillips *et al*. (1996). These data summarize results from a joint US/Russian radiological expedition along the Yenisei River in spring and summer 1995. The expedition sampled as far south on the Yenisei as Kurbatovo (59 km upstream from the confluence with

the Angara River and 187 km downstream from the discharge point). For the three data points on the Yenisei provided by this expedition, the contamination values were lower than the MCC data but within the same order of magnitude as those of the nearby samples reported by others. While this certainly does not provide a validation of the nearby data, it does provide a degree of comfort about otherwise unverifiable data.

Widths of contamination on floodplains and islands were estimated from sampling data contained in Robinson and Volosov (1996, Table 5.4) for a 13-km reach between the Bolshoi Tel and Kan Rivers. The 217 contaminated plots in this reach were catalogued into 11 dose rate ranges, 12 surface area ranges, and 12 length ranges. We estimated an average width of contamination from the length and surface area data within each dose rate range and developed a normal distribution of width with a mean of 30.4 m and standard deviation of 13.8 m. To estimate widths of contamination for the Yenisei River, we assumed the maximum and minimum widths of contamination were ± 2 standard deviations from the mean and that they were correlated to the width of the water surface calculated by HEC-RAS for a discharge of 13,500 m^3/sec. The radionuclide concentration given in Appendix I was developed by assuming that the maximum reported concentration in each 1-km stretch of the river is representative of the stretch, whether located on the banks, on an island, or in the sediments. This assumption tends to give very conservative overestimates of the concentration, as the maximum values are often several times larger than the average values when both are given.

All the data are decayed from the time of measurement to 1997 to provide a consistent picture of the inventory. In some areas, particularly those with significant amounts of shorter-lived radioactivity such as ^{60}Co, ^{152}Eu, or ^{154}Eu, this results in a significant reduction of the initial activity.

Depth profiles of several gamma-emitting radionuclides in soils of islands in the Yenisei are given in *Figure 4.5*. The data, provided by Shishlov *et al*. (1997), were collected in 1996.

The total calculated radioactivity of long-lived radionuclides in the floodplains of the Yenisei River valley (*Table 4.1*) was based on the available data sources and on estimates of widths, as summarized in Appendix I. Almost no contamination data were available for ^{90}Sr, probably because it is a beta emitter and almost all measurements were for gamma emitters. Because ^{90}Sr is usually an important radionuclide in most environmental analyses, and because we have few measurements of its concentrations in the floodplain soil, we have assumed that its concentration in floodplain soils is equal to that of ^{137}Cs. The rationale for this assumption is as follows:

- ^{90}Sr and ^{137}Cs are typically produced in a reactor in relatively equal proportions.

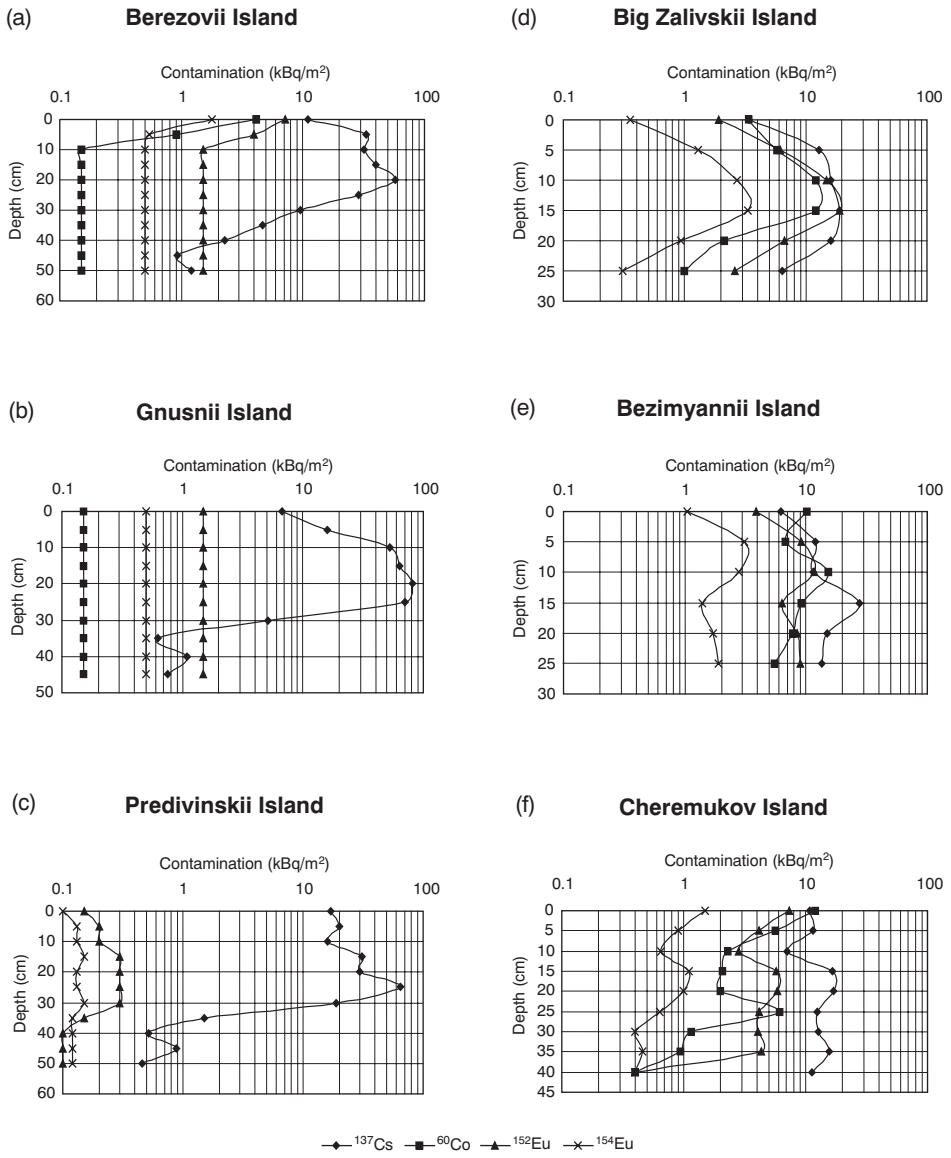

Figure 4.5. Profiles of concentration versus depth in soil of islands in the Yenisei.

- Prior to discharge to the river, the ^{137}Cs and ^{90}Sr were retained in holding ponds. During this period, it is likely that these nuclides were sorbed to suspended sediments, so that these nuclides are transported as suspended sediment. The degree of sorption of cesium is usually significantly greater than that of strontium.

Table 4.1. Estimate of total radioactivity (GBq) in Yenisei River floodplains from MCC release point to confluence with Angara River.

Radionuclide	Total radioactivity
^{60}Co	170
^{90}Sr	310
^{137}Cs	310
^{152}Eu	290
^{154}Eu	90
Total	1,170

Patterns of ^{137}Cs contamination in the Yenisei floodplains are likely the result of redistribution of contaminated sediment. Although ^{90}Sr does not sorb to sediments as strongly as ^{137}Cs, it sorbs relatively strongly so that its redistribution by flooding is also determined by sediment redistribution. By using the same values, the results can be scaled to better estimates of the contamination should they become available. We note that at Mayak, ^{137}Cs and ^{90}Sr were separated during reprocessing and stored separately for commercial purposes. Such separation would invalidate the assumption of equal proportions; however, there is no available information to determine if this separation was also performed at the MCC.

4.2.3 Estimation of inventory released from surface pond 365

Flow Rate and Duration from Failed Pond. Pond 365 was designed for reception and interim storage of the reactor emergency waters and off-grade, non-process wastewater of the radiochemical plant. The water in this pond is sent for further cleaning to nearby pond 366 prior to its disposition. The pond bottom and sides are lined with two layers of asphalt and one layer of clay. Bottom and bank drainage systems are designed to intercept and collect any leaks from the pond.

The data from Shishlov *et al*. (1997) and results of interim calculations are summarized in *Table 4.2*.

Based on the volume and surface area of the pond and assuming that the shape is generally triangular to represent a stream channel dammed at the lower end, the height of the resulting dam was estimated to be 8 m. The maximum flow rate from this pond was calculated using the broad-crested weir flow equation in the National Weather Service simplified dam break code, or SMPDBK (Wetmore and Fread, 1983), where $Q_{\max}$ (ft^3/sec) is given by

$$Q_{\max} = 3.1 B_r \left(\frac{C}{\frac{t_f}{60} + \frac{C}{\sqrt{H}}} \right)^3 , \tag{4.2}$$

Table 4.2. Data for pond 365 at the MCC.

Parameter	Value
Water	
Volume (m^3)	204,000
Surface area (m^2)	53,000
Average depth (m)	3.8
Radionuclide content (GBq)	
^{60}Co	13
^{137}Cs	310
^{154}Eu	3
Total β-activity	7,800
Sediments	
Total volume: solids, slurry, fluidized (m^3)	3,400
Average thickness (m)	0.064
Average porosity	0.4
Radionuclide content (GBq)	
^{60}Co	1,700
^{103}Ru + ^{106}Ru	5,800
^{137}Cs	42,000
^{154}Eu	520
^{238}U	11
^{239}Pu	2,000
Total β-activity	25,000–50,000

where

$$C = 23.4\frac{A_S}{B_r}, \tag{4.3}$$

and A_S is surface area of the reservoir (acres), H is the depth of the breach cut (ft), t_f is time for breach formation (min), and B_r is final width of breach (ft). Wetmore and Fread (1983) provide default values for breach geometry and time to develop full breach as

$$\begin{aligned} H &= H_d \\ B_r &= 3H \\ t_f &= H/3, \end{aligned} \tag{4.4}$$

where H_d is height of the dam (ft).

Using default parameters for earthen dams for B_r, H, and t_f, the maximum rate of discharge is 525 m^3/sec. The duration of discharge at this rate is approximately six minutes, which is considerably less than the one-day time step used in the river transport model. Therefore, a one-day pulse release rate is used in the calculations.

Estimate of Radionuclide Inventory in Pond Water and Sediments. Estimates of radionuclide inventories in the water and sediments in the pond are shown in *Table 4.2*. For the radionuclides reported in both media, over 99% of the total activity is contained in the sediments. Therefore, during transport after a release from the pond, the pond water can be considered a relatively clean carrier of contaminated sediments. The particle size distribution for the pond sediments is unknown. Therefore, we assume that half of the radionuclides are sorbed to silt and half to clay. This assumption balances the deposition and washout between the silt and clay fractions.

4.2.4 Population of villages along the Yenisei River

Census data are typically considered sensitive in the Russian Federation, and no official population data were available for the villages along the Yenisei River. The population of towns and villages along the Yenisei between the release point and the confluence with the Angara River given in *Table 4.3* were estimated from data (population range as indicated by size and font of place name) on the 1:500,000-scale 1995 map of the Krasnoyarsk Krai. Based on these data, the estimated total population along this river reach may range from 12,000 to over 33,000. Although collective dose estimates were not performed, these population estimates provide information on areas where population centers are located.

4.3 Results

4.3.1 Scenario MCC-1: Existing contamination levels and locations

This scenario is used to evaluate doses due to existing contamination in the Yenisei floodplain. The available data about existing contamination are summarized in Appendix I, and the maximum concentrations of radionuclides are shown for each river kilometer in *Figure 4.6*.

The doses resulting from this distribution are shown in *Figure 4.7a*, in which the results of two methods of dose averaging are shown. For comparison purposes, *Figure 4.7b* shows the maximum EDR values recorded during the 1990 aerogamma survey. The individual points in *Figure 4.7a* represent the sum of the maximum soil contamination values multiplied by the pathway dose conversion factors for each nuclide, and hence represent an absolute maximum of potential individual doses. Because no data were available for ^{90}Sr contamination, for dose estimation purposes we assumed that its concentration was equal to that of ^{137}Cs (see Section 4.2.2).

To account for the lower probability of extended occupancy in the narrow bands of contamination, the first dose averaging method assumes that the doses can be

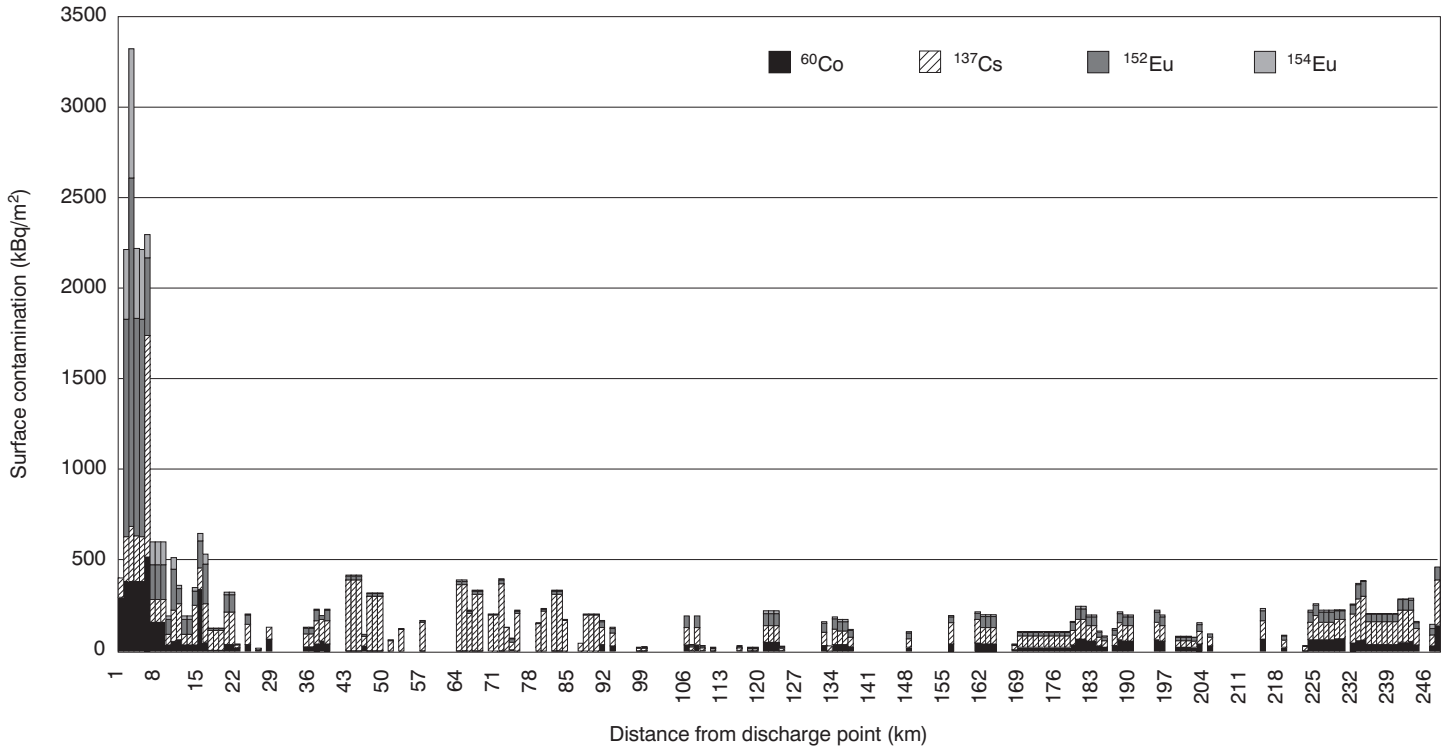

Figure 4.6. Maximum reported radionuclide concentrations in the Yenisei River floodplains.

Table 4.3. Population of villages along the Yenisei River from release point to confluence with Angara River.

Village, left bank	Village, right bank	Distance downstream of discharge point (km)	Population
Atamanovo		2–8	1,000–2,000
Bolshoi Balchug		11–13	$<$ 500
Khloptunovo		13	$<$500
Kononovo		18–20	1,000–2,000
	Ust-Kan	23–24	$<$500
Pavlovschina		54–55	1,000–2,000
Bereg Taskino		63–65	$<$500
Yuksevo		71–73	500–1,000
	Predivinsk	99–100	2,000–10,000
	Posolinaya	110	$<$500
Lugovskoa		130–131	$<$500
	Yazovka	132–133	1,000–2,000
Porog		150	$<$500
	Piskunovka	161–163	1,000–2,000
Galaneno		170–173	1,000–2,000
	Momotovo	171–172	1,000–2,000
	Kazachinskoe	178–182	1,000–2,000
Kurbatovo		185–187	$<$500
	Zharovka	191–193	1,000–2,000
	Strelka	244–246	$>$2000

scaled by the ratio of the estimated width of the contaminated zone (see Appendix I) to the maximum width (58 m). The second dose averaging method, reach averaging, assumes that although certain population groups may spend a great deal of time in contaminated zones immediately adjacent to the river, they move up and down the river. This is reflected in the plot of reach-averaged total doses, in which doses at each location were averaged over a distance of 3 km upstream and 3 km downstream from the specified location.

The average maximum dose along the entire length of the river (245 km) is 1.3 millisieverts (mSv), with a standard deviation of 2.35 mSv. If we exclude the peaks located within the first 10 km along the river, the average along the rest of the river is 0.94 mSv, with a standard deviation of 1.12 mSv. Although this technique of simple scaling results in maximum potential doses above the 1 mSv limit along much of the river, many of these points are either isolated spots along the river or are very narrow strips only a few meters wide, and it is therefore unlikely that the population would fulfill the assumptions of 100% occupancy used in deriving the pathway dose conversion factors. Dose averaging may therefore represent a more

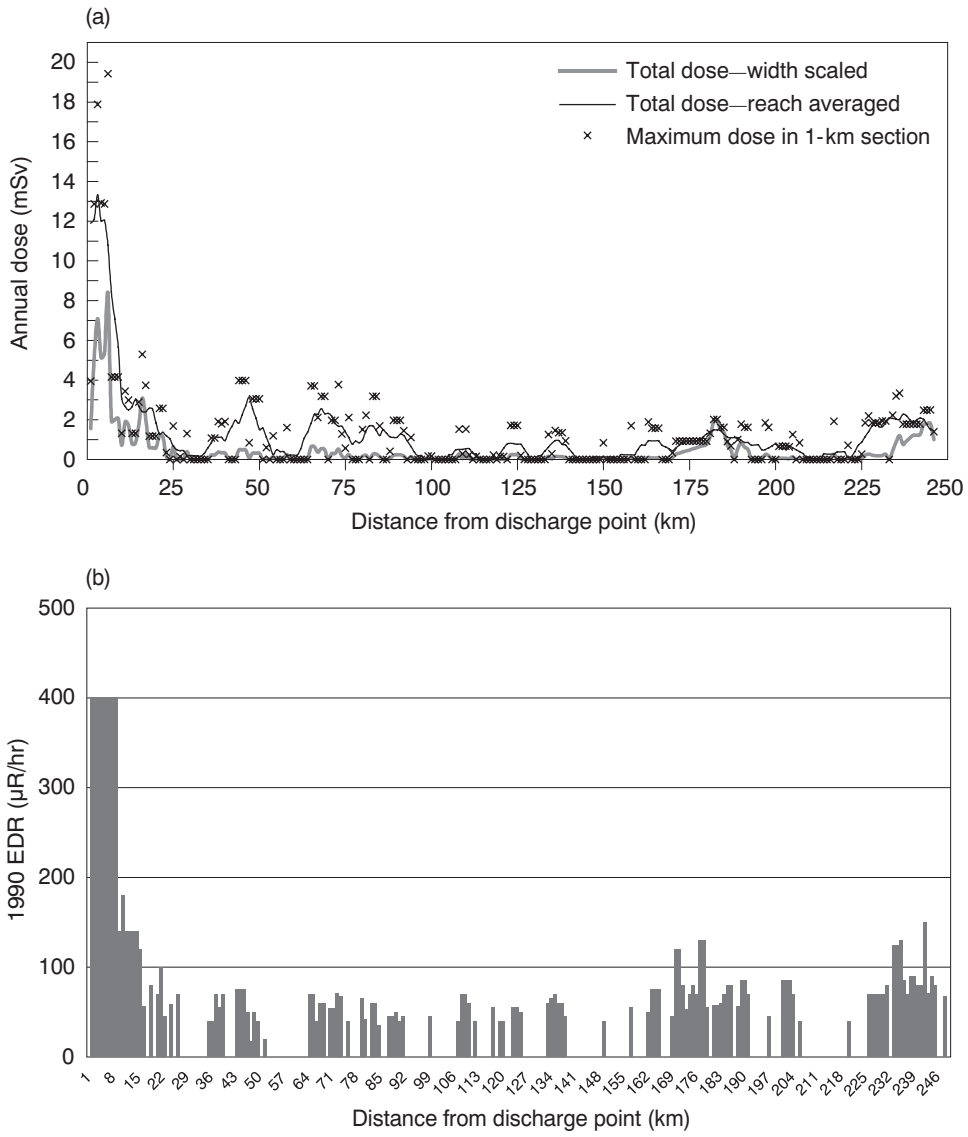

Figure 4.7. (a) Maximum and averaged annual doses from existing contamination of Yenisei River floodplains. (b) Maximum exposure dose rate (EDR) values recorded in 1990 aerogamma survey.

realistic picture of the potential doses along the river; the results are shown in the plot and discussed below.

The two averaging methods imply two different exposure patterns. Width scaling assumes that the exposed population stays in one location along the river, but

spends their time within a 58 m distance of the river. Doses are reduced because it is assumed that their time is spent equally within a 1-km-long, 58-m-wide stretch, and areas with narrower contaminated stretches are likely to result in smaller doses. For most locations along the river, the weighted dose is below Russia's 1 mSv per year (100 millirem per year) permissible dose to the population. The weighted annual dose exceeds the permissible annual limit at locations 1–25 km, 180–186 km, and 235–250 km downstream from the release point. At the first downstream location, individual nuclides sometimes exceed the annual dose limit two- to threefold. At the other points, only the total dose exceeds the dose limit.

The other averaging method, longitudinal averaging, assumes that the exposed population spends its time along the contaminated riverbanks but moves up and down the banks. Thus the doses are reduced because not all of their time is spent in regions of local contamination maxima. The general picture is quite similar to that of width scaling, except that additional peak exposures above the 1 mSv limit also occur 37–94 km downstream from the discharge point.

Interpretation of these dose plots, particularly the values for maximum individual doses, must be made with circumspection. Use of maximum rather than average values for surface contamination yields a dose which can be several times higher than that due to average values. In many areas, estimates of surface contamination were based solely on EDR values because of the lack of sampling data. The conservative assumptions used in deriving the pathway dose conversion factors (i.e., 24-hour occupation of the contaminated lands and all food grown on contaminated lands) may be unlikely to be valid for the observed pattern of contamination, in which maximum values are generally found in areas of limited areal extent (generally no more than 5–50 m wide). Finally, the assumption of a 1:1 ratio between ^{90}Sr and ^{137}Cs results in a high estimate of the dose, as ^{90}Sr has a higher pathway dose conversion factor than does ^{137}Cs. In addition, *Figure 4.7b* represents EDR values measured while the single-pass reactors were in operation, and thus a portion of the exposure rate may be due to short-lived induced activity discharged from the reactors during that time.

Nonetheless, the estimated annual doses from individual nuclides in the first 25 km downstream from the release point indicate that this location should be evaluated and possibly controlled more closely. In addition, as the total doses at the locations approximately 183 and 240 km downstream exceed annual dose limits under both averaging methods, they too are likely candidates for closer evaluation. The actual doses received are a function of the length and degree of exposure, and are likely to be significantly lower than the conservative values presented here. The potential exposure rates are such that the 1 mSv annual dose limit is only likely to be exceeded if there is extended occupation. Groups that may spend extended periods of time along the riverbanks, such as fishermen, are likely to be at the highest

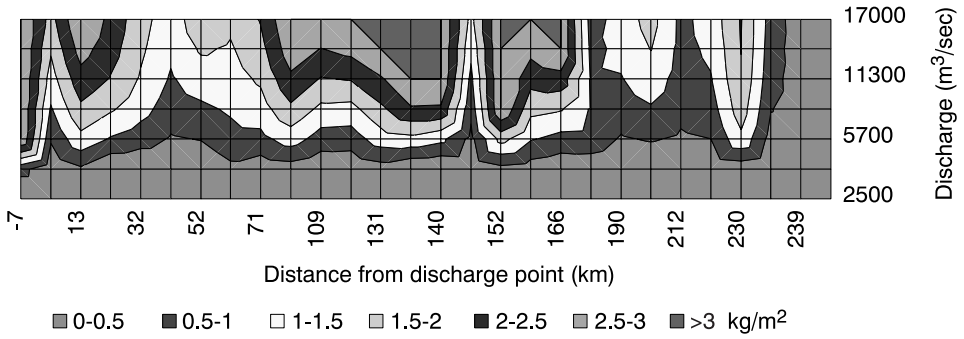

Figure 4.8. Shear stress (kg/m^2) in the overbank of the Yenisei River for various discharges.

risk of receiving unacceptably high doses. Periodic radiological surveys can be used to monitor the conditions within contaminated areas, and remedial or isolation activities such as erecting fences or posting warning signs in selected areas may be a reasonable technical solution. Therefore, limiting access to these sites may be sufficient to prevent unacceptable exposures. If social or political pressures dictate some form of physical remediation, the relatively few locations registering the highest concentrations of contamination over the largest areas are logical candidates for remediation. The limited areal extent of these contamination anomalies should facilitate remediation.

4.3.2 Scenario MCC-2: Redistribution of existing contamination by flooding

This scenario presents an evaluation of doses due to redistribution of existing radioactive contamination by high flows in the Yenisei River. The hydraulic properties of the river channel and overbanks are estimated using HEC-RAS. These properties, along with the existing levels and locations of radionuclides in the floodplains, are used as input to the contamination redistribution routine developed by the RAD staff. One of the primary calculated hydraulic properties provided by HEC-RAS is the pattern of shear stress in the overbank (*Figure 4.8*). The depth and velocity of water flowing in the different segments of the river primarily determine the shear stress pattern.

Figure 4.8 is a contour plot of shear stress on the floodplains at various locations for the range of flows observed in the Yenisei River after construction of the hydroelectric dam upstream from the city of Krasnoyarsk. It shows that shear stresses increase with increasing discharges for a given location. The critical shear stress

is the stress that determines whether the given conditions result in scour or deposition. The values for the critical shear stresses used in this analysis are 0.7 kg/m^2 for silt and 2 kg/m^2 for clay. At shear stresses above these values, scour is calculated to occur; below these discharges, deposition is calculated to occur. At a given location along the river, the discharges corresponding to the critical shear stresses can be estimated (e.g., 5,700 and 14,200 m^3/sec for clay and silt, respectively, at a location 32 km from the discharge point).

As discussed in Section 4.2, the appropriate values for critical shear stresses depend on many site-specific factors. *Figure 4.8* can be used to estimate the effects of selecting alternative values for the critical shear stresses. Note that for normal discharge conditions when the river is generally within its banks (below 2,850 m^3/sec) the shear stresses are below 0.7 kg/m^2 for the overbanks along the entire river reach, indicating deposition conditions for both silt and clay along the narrow strips of potentially flooded overbank.

The shear stresses indicated in *Figure 4.8* are average values over the areas of the individual cross sections. The individual cross sections were assumed to be constant for distances ranging between 3 km (149–152 km and 230–233 km from the discharge point) and 24 km (85–109 km from the discharge point). Because of the homogenization over these rather large areas, only average results can be provided. We expect that redistribution of radionuclides by flooding will result in localized areas of higher concentrations due to ponding in localized depressions along the riverbanks. However, the level of modeling used in this analysis, and the general level of the underlying theory, are not sufficient to make predictions at this level of detail. The past pattern of deposition gives an indication as to the most significant of these localized deposition zones. The primary concern in this analysis is the potential for widespread contamination of the floodplain, which could lead to high collective doses.

Estimates of trap efficiency for silt and clay of the river channel (*Figure 4.9*) and of the overbank (*Figure 4.10*) were based on the shear stress plot for the Yenisei, the assumed critical shear stresses, and the fall velocities for the silt and clay particles. Except at the lower range of discharges, almost all silt and clay in the channel remain in the wash load, with subsequent deposition either within the river system farther downstream from the study area or in the Kara Sea and Arctic Ocean.

At high discharges, the overbank of the Yenisei also has a relatively low trap efficiency for silt (40% or less for discharges over 8,500 m^3/sec; see *Figure 4.10*). According to the calculations, most of the clay in the overbank is deposited at 15–40 km, 170–180 km, and 240 km downstream from the discharge point. The soil particles (and adsorbed radionuclides) washed out of the reach of interest are either subsequently deposited within the Yenisei River system farther downstream or discharged into the Kara Sea and Arctic Ocean.

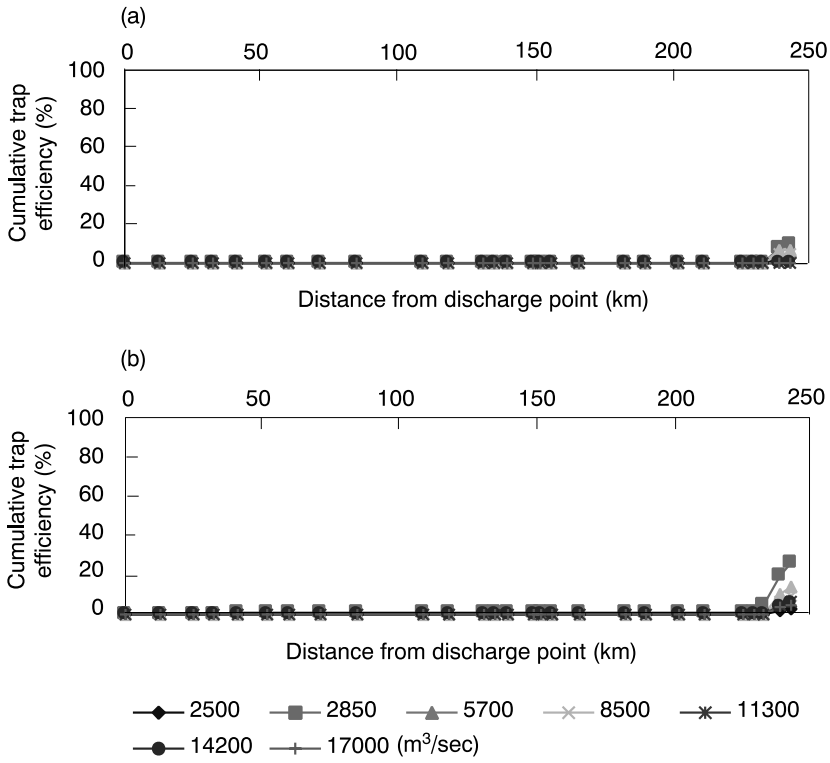

Figure 4.9. Trap efficiency for (a) silt and (b) clay for the Yenisei River channel for various flows (m^3/sec).

Soil concentrations of ^{137}Cs due to redistribution of existing contamination are shown in *Figure 4.11a*. These concentrations are calculated by assuming that the radionuclides are redistributed over a four-day flood. Because the Yenisei is a controlled river, the duration of high discharges cannot be determined from historical data, and this arbitrary value is based on historical operations data collected since the construction of the dam. The process of bed armoring (the prevention of continued erosion of fine particles by an "armor" of coarser particles) is assumed to prevail after one or two days of flooding, thereby limiting the scour rate after that time. In several locations, the contamination appears symmetric and rectangular. This effect is due to the interpolation of values at discrete modes in the graphics package.

Discharges in the range of 5,700 m^3/sec provide the highest levels of deposition and greatest extent of deposition within the reach of interest. Because the initial geographical distributions for the other evaluated radionuclides are similar to that for

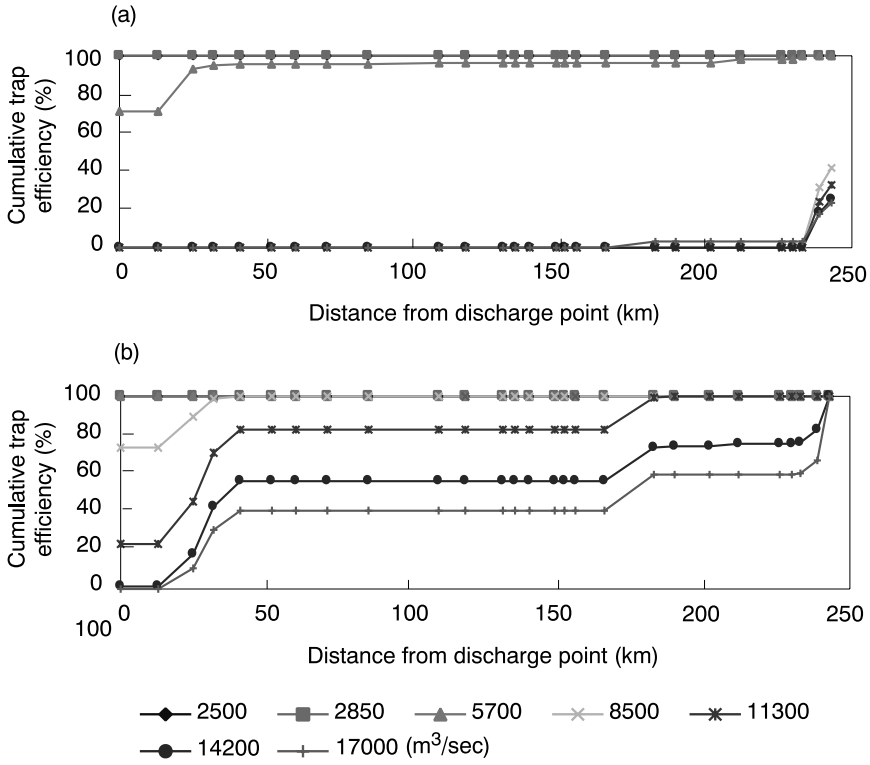

Figure 4.10. Trap efficiency for (a) silt and (b) clay for the Yenisei River overbank for various flows (m^3/sec).

^{137}Cs (see *Figure 4.6*), the redistribution of these radionuclides is likely to exhibit a pattern similar to that of ^{137}Cs.

The total additional dose resulting from the combination of all redistributed radionuclides and based on the exposure scenarios discussed in Section 3.4 is shown in *Figure 4.11b*. This plot shows the concentration of redeposited radioactive contamination along the river overbanks. The maximum average annual dose resulting from the redistribution of existing radionuclides is less than a few tens of microsieverts (μSv) per year at 42 km downstream from the release points. On average, the doses due to dilution, dispersion, and redistribution of existing radionuclides are below action levels based on Russian regulations. Of course, localized spots of higher levels of contamination will likely occur due to specific sediment-trapping characteristics of topography and biota.

Radiological surveys should be conducted periodically to monitor existing conditions and identify new localized spots of higher contamination. However, on average, the contamination levels are expected to be low enough that widespread

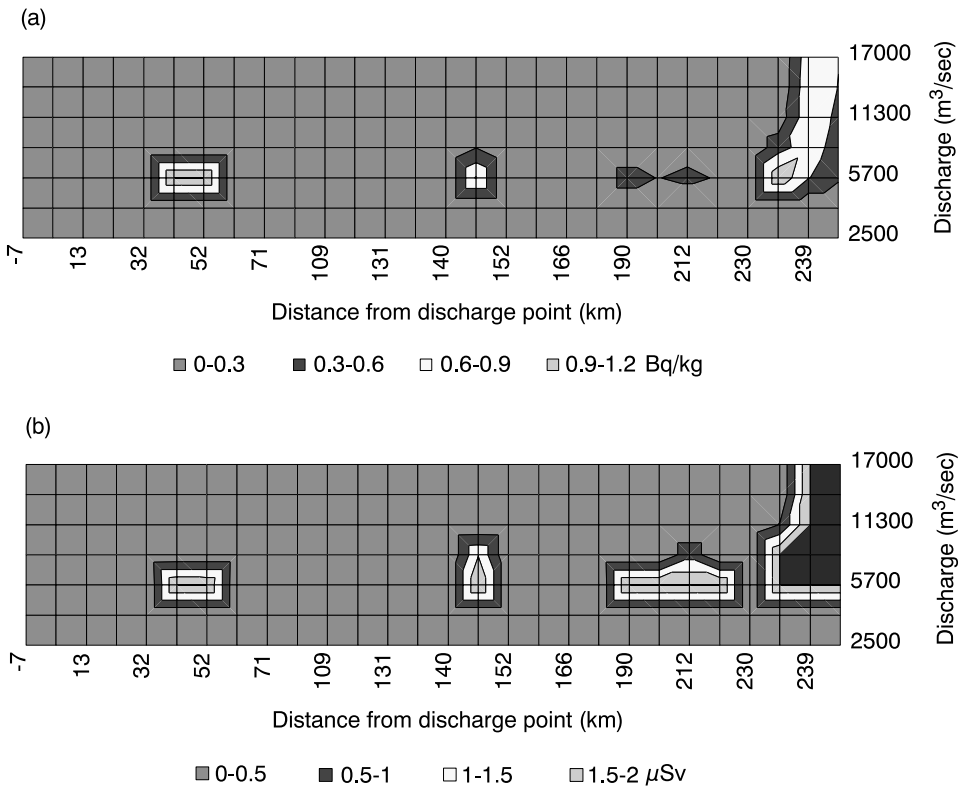

Figure 4.11. Results of (a) soil concentrations of ^{137}Cs (Bq/kg) and (b) total annual dose (μSv) from all radionuclides based on redistribution of existing contamination in the Yenisei River floodplains.

remediation measures do not appear to be warranted based on technical reasons alone. Should social or political pressures dictate the need for active remediation, approaches similar to those suggested for scenario MCC-1 (Section 4.3.1) may be appropriate. Measures that minimize or prevent access to localized spots will result in significant reductions in doses, because a significant fraction of the dose from localized spots of higher contamination will likely occur from gamma-emitting radionuclides via the external exposure route.

Trap efficiency calculations indicate that a significant fraction of radionuclides will likely be washed out of the river reach of interest along with the sediment wash load. Because significant population centers are located along the Yenisei River farther downstream from the reach of interest (e.g., Lesosibirsk, Yeniseisk, Igarka, and Dudinka), periodic radiological surveys can be used to monitor exposure conditions at critical locations along the river. Areas downstream that exhibit

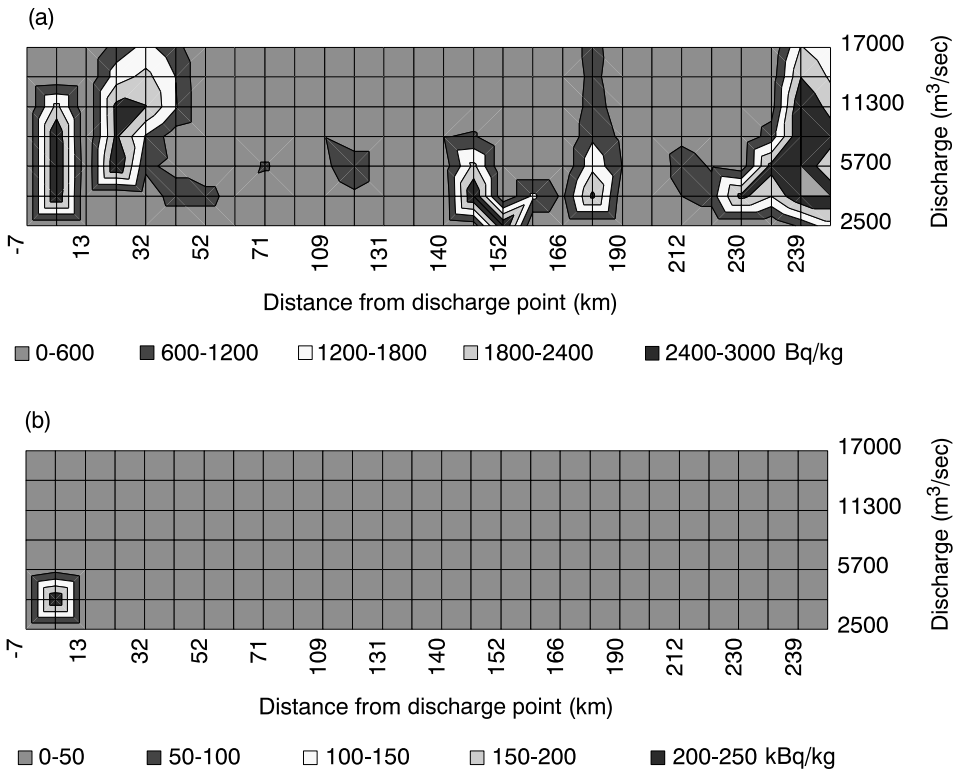

Figure 4.12. Soil contamination density resulting from a unit 37 TBq (1,000 Ci) release of radioactivity to the Yenisei River. (a) Fine-scale and (b) full-scale soil concentrations.

significant deposition, such as natural or artificial reservoirs downstream from the contaminated zone or islands/side channels that exhibit a tendency toward siltation, are particularly at risk and are logical candidates for increased monitoring.

4.3.3 Scenario MCC-3: Release of radionuclides from storage pond

This scenario is concerned with the dose effects of a hypothetical release of radionuclides from the MCC to the Yenisei River. The shear stress and trap efficiency profiles for the Yenisei River presented in Section 4.3.2 are also applicable to this scenario. Half the released radionuclides are assumed to be adsorbed to silt particles and half to clay particles.

The soil contamination density resulting from a unit release of 37 terabecquerels (TBq; 37 TBq = 1,000 Ci) from pond 365 to the Yenisei River is shown in *Figure 4.12*.

In *Figure 4.12a*, the upper level of contamination is limited to 3,000 Bq/kg so that the finer structure of the lower levels of contamination can be seen. Discharges around 3,000–10,000 m^3/sec provide the most significant redistribution of contamination downstream from the release point within the reach of interest. At these higher flow rates, much of the silt and clay is expected to be retained in the overbanks (see *Figure 4.10*). The highest levels of contamination are expected to occur at the lowest flows and at locations nearest the discharge point (*Figure 4.12b*). Contamination densities up to 40 Bq/g may be possible.

The plots presented in *Figure 4.12* can be converted directly to dose rate plots by multiplying soil contamination density by the activity released, dividing by the 37 TBq (1,000 Ci) release used to develop the plot, and multiplying by the pathway dose conversion factor for the radionuclide of interest (see *Table 3.3*). The total dose rate for all radionuclides is the sum of the individual dose rates. Using the inventory of pond 365 (*Table 4.2*), plots of total dose rate for the release of inventory into the Yenisei River are shown in *Figure 4.13*. At high flows, the radionuclides are washed downstream. Some deposition will occur at several places downstream in the reach, possibly resulting in dose rates over 10 mSv per year. At low flow rates, an annual dose up to 1 Sv may be expected near the release point. Such dose levels would be the result of essentially complete trapping of contaminated sediments on the floodplain before the release reaches the main channel of the river.

The highest doses resulting from large and sudden releases of radioactivity from the site into the river occur when the flows are lowest but still high enough for flow in the overbank. Low flows in the overbank result in significant deposition of contaminated sediments from the pond near the release point. There is thus a trade-off between the extent and the magnitude of the potential contamination. However, it is clear that any major release from surface ponds to the river could have severe consequences for distances on the order of tens of kilometers downstream and would exacerbate existing contamination problems even farther downstream.

Because the hydroelectric dam upstream from the city of Krasnoyarsk controls the river discharge, there is the potential for significant intervention capability should an accidental release occur. Various discharge control schemes should be evaluated to understand their effects on accidental releases prior to such an occurrence. For example, lowering the water level in the reservoir behind the dam by a few meters could provide significant water storage capacity in the reservoir so that discharges could be reduced or stopped to permit an emergency response to an accidental release. Conversely, the effects of high discharges, which reduce concentrations near the release and flush contamination downstream, should also be evaluated. How to control the discharges from the dam during and after an accidental release is a social and political decision. However, an informed decision can be made only if the range of possible actions has been evaluated. These contingency

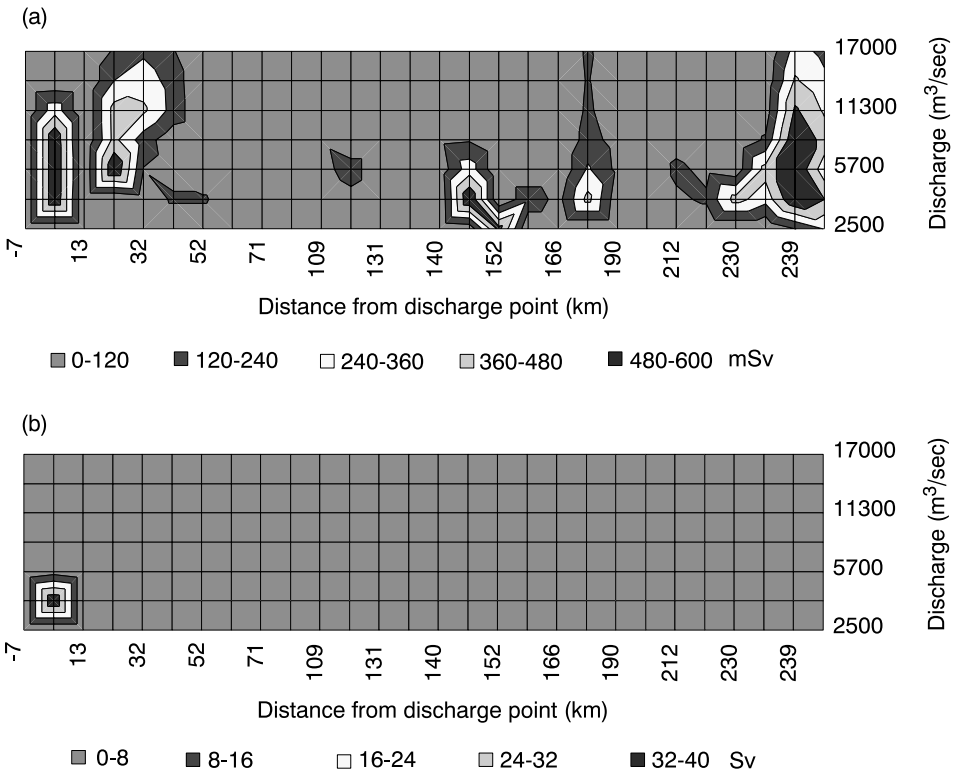

Figure 4.13. Total annual dose resulting from a release of pond 365 inventory to the Yenisei River. (a) Fine-scale and (b) full-scale annual dose.

planning activities indicate the need for site officials to coordinate with the organizations controlling the discharges from the hydroelectric dam, if such coordination has not already been established.

Perhaps the most important activities that can be conducted are those that focus on preventing large releases of radionuclides to the river. However, because there are currently few available data on the characteristics of storage ponds, tanks, and their appurtenances within the MCC, no specific evaluations can be conducted at this time. This consequence analysis indicates, however, that this is a problem worthy of further analysis.

5

The Siberian Chemical Combine and the Tom River

An overview of the environmental conditions, sources of contamination, and releases of contamination from the Siberian Chemical Combine (SCC) to the Tom River is given in Chapter 2. This chapter provides the site-specific scenarios, data, and results of analyses of radioactive contamination of the Tom River valley.

5.1 Site-specific Scenarios

Site-specific aspects of the generic scenarios are identified in this section for the SCC. The first scenario, SCC-1, is identical to the generic baseline scenario described in Section 3.1.1. The contamination levels and locations are described in Section 5.2. The second scenario, SCC-2, is based on a redistribution of radionuclides in the river sediments and floodplain soils due to floods of various magnitudes. The Tom River is uncontrolled and has discharges ranging between 150 cubic meters per second (m^3/sec), the monthly average in winter, and 8,500 m^3/sec, the annual maximum during the spring snowmelt. The ratio of maximum to minimum discharge is over 50 (Novosibirsk, 1985, 1986, 1987). This large range of discharges may result in significant scouring of the river channel, as is discussed in Section 5.3. The third scenario, SCC-3, is based on a release of radionuclides from the SCC due to a nonspecific hypothetical failure of one or more of the engineered containment systems on the site. The redistribution of radionuclides released from the site was calculated for various river discharges using the same approach as in scenario SCC-2. Insufficient radionuclide inventories were made available for this analysis, so unit releases of 37 terabecquerels (TBq), or 1,000 Curie (Ci), of ^{90}Sr and ^{137}Cs were used. The release was assumed to enter the river primarily as contaminated soils and sediments via overland flow and through the Ramashka River, which is used by the site to discharge process water.

A significant difference between the Tom and Yenisei Rivers is the general absence of a large floodplain on the Tom. The river lies in a fairly narrow gorge with bluffs rising steeply to the east of the river and to a lesser extent on the western bank. The primary potential for floodplain-type deposition is on the islands in the Tom River. Due to the relative lack of a floodplain and the fact that much of the

river channel is exposed during low flows, an overbank section was not modeled for the Tom River. The channel is assumed to be the contaminated region of interest.

5.2 Data and Data Analysis

The site-specific data used in the analysis of the three scenarios are described in this section. Many of these data required further processing and analysis before they were used. Results of these data analyses are also presented in this section.

5.2.1 River hydrology and sediment transport

River Geometry

The Tom River between Seversk and the confluence with the Ob is heavily braided with numerous islands and channels. Among the larger islands are Chernilschikovskii, Vemoyanii, Suzovskii, Elovii, Labzain, and Pushkarevckii. A steep bank profile and bluffs on the right side of the river and lower banks on the left side characterize the river reach. While no significant floodplains exist, there are several marshy areas, particularly on the right bank below Orlovka, that would provide good traps for radionuclides if water levels were to spill over the natural levees separating them from the river. Such backwater areas would result in deposition of the suspended activity in these areas as the floodwaters receded. These marshy areas were not included in this analysis due to a lack of data on contamination and specific topography of these areas. They could be of concern under adverse circumstances and may warrant further analysis.

As at Krasnoyarsk, the upstream and downstream ends of islands probably function as traps for radioactive contamination. This contamination is likely the result of low-flow zones due to island wake effects, resulting in increased sediment deposition. The modeling technique used in this analysis does not predict deposition based on these processes. Based on fundamentals of fluid mechanics, it is noted that upstream and downstream ends of islands are potential deposition areas for which site-specific surveys may be appropriate.

Simplified representations of river channel profiles were developed from the 1960 navigation chart for the Tom (Noskov *et al*., 1960), from more recent data on depths of the thalweg provided by the site contacts (Inishev, 1997; State Hydrological Institute, 1990), and from topographic maps of the Tomsk Oblast. Mining of the sand and gravel from the bed of the Tom River has occurred since 1960. This additional deepening of the thalweg may provide sediment-trapping mechanisms in the river due to reduced water velocity in these areas. Excavation of the channel may have also removed contamination previously deposited in these areas. In that

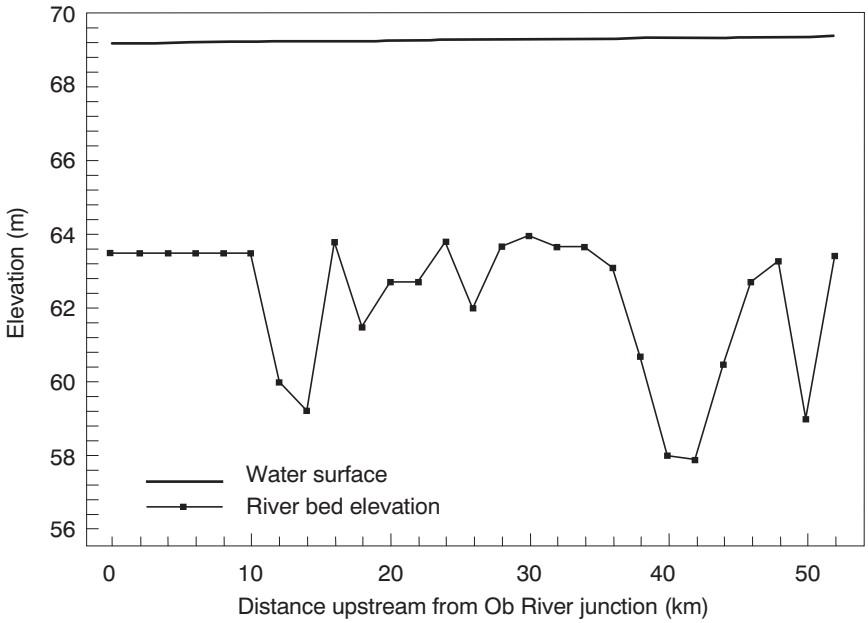

Figure 5.1. Longitudinal profile of the Tom River.

case, the impact of these contaminated sediments should be evaluated. Of particular importance would be the potential for increased contamination of fish as a result of feeding and residence in these deepened areas. These deeper areas may represent ice-free havens for fish during the months in which the river is frozen. Therefore, consumption of such fish could contribute a disproportionate share of the dose.

The modeled channel geometry was simplified near islands by using a single channel with the same cross-sectional area as the actual channel. As with the Yenisei River, the simplified representation of the river channel profile was consistent with the one-dimensional hydraulic modeling provided by HEC-RAS (see Section 3.3).

The relative and absolute elevations of the river reaches were used to calculate the slopes of the water surface between each given cross-sectional profile. These elevations were checked against known gauge zeros with reasonable agreement. The resulting longitudinal river profile is shown in *Figure 5.1*. The zero-km point corresponds to the confluence with the Ob River.

Floodplain geometry was developed from topographic maps by measuring the width to the nearest contour line at each selected cross section. The resulting model river geometry (*Figure 5.2*) is both linear and symmetrical. The linear river geometry was used instead of the more meandering geometry because losses due to

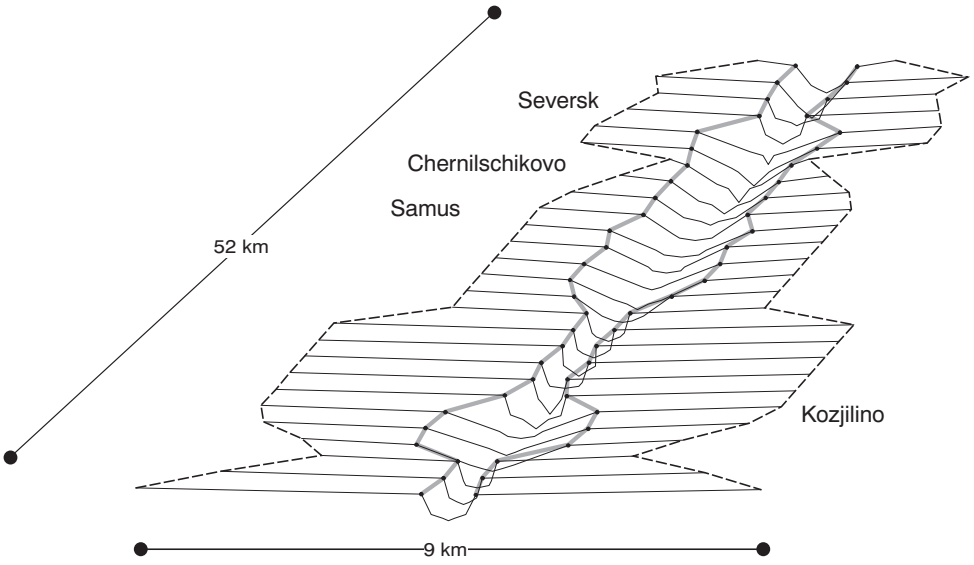

Figure 5.2. Schematic representation of the Tom River for HEC-RAS.

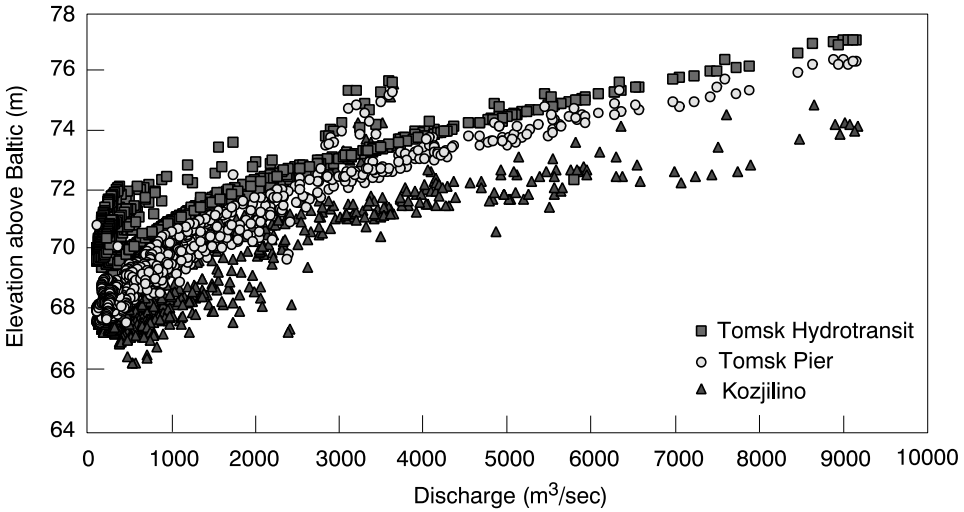

Figure 5.3. Observed stage-discharge curves for the Tom River.

curvatures were expected to be low (USACE, 1997). The simplified geometry was consistent with the limitations of the simple transport analysis. Water elevations were calibrated by adjusting channel roughness using the Manning's numbers. The most important parameters for calibrating water levels are the cross-sectional area and the wetted perimeter. Values for these parameters were similar to actual values.

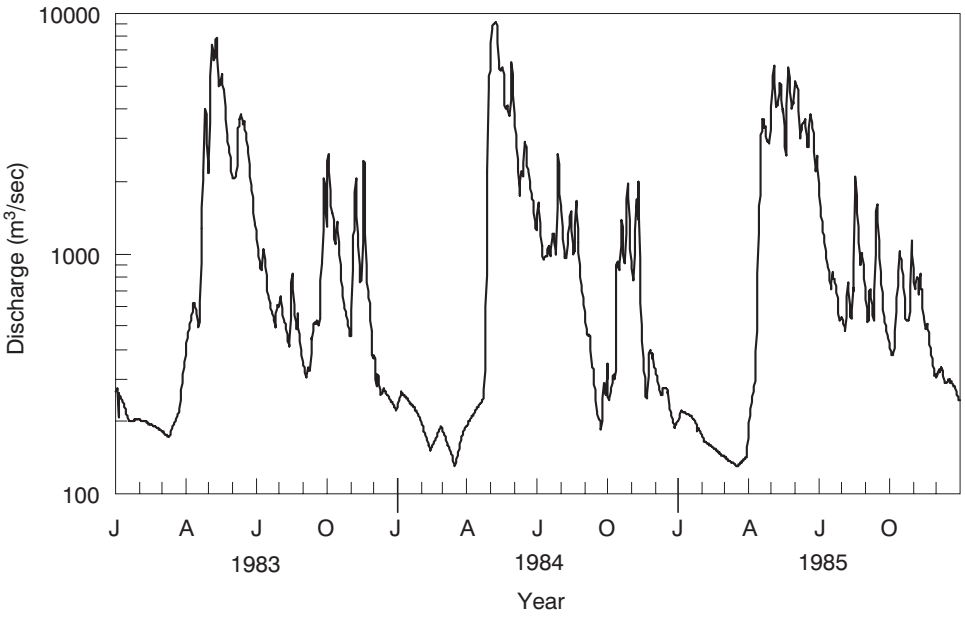

Figure 5.4. Daily discharge in the Tom River, 1983–1985.

River Hydraulic Data

HEC-RAS requires a downstream stage-discharge curve to perform the hydraulic computations. Data on three continuous years of daily discharge and on elevation (Novosibirsk, 1985, 1986, 1987) were used to develop stage-discharge curves for the Tom (*Figure 5.3*). Two of the locations were in the city of Tomsk, upstream from the site. The other was at Kozjilino, near the confluence with the Ob River. At lower discharges, there are significant variations in water surface elevations for given discharges at all three locations. The source of this variability is unknown but may be due to measurement reading or recording errors, or to problems with the measuring devices during winter, when ice covers much of the river.

A wide range of discharges occurs in the Tom River throughout the year (*Figure 5.4*), with the highest discharges occurring during the spring snowmelt and the lowest occurring in winter. The highest discharges in this three-year period are 70 times higher than the lowest discharges.

Sediment Transport

The bed of the Tom River is composed primarily of gravel and cobbles (*Figure 5.5a*), which are currently being excavated for use as building material. Although the channel bed consists predominantly of coarse sediments (State

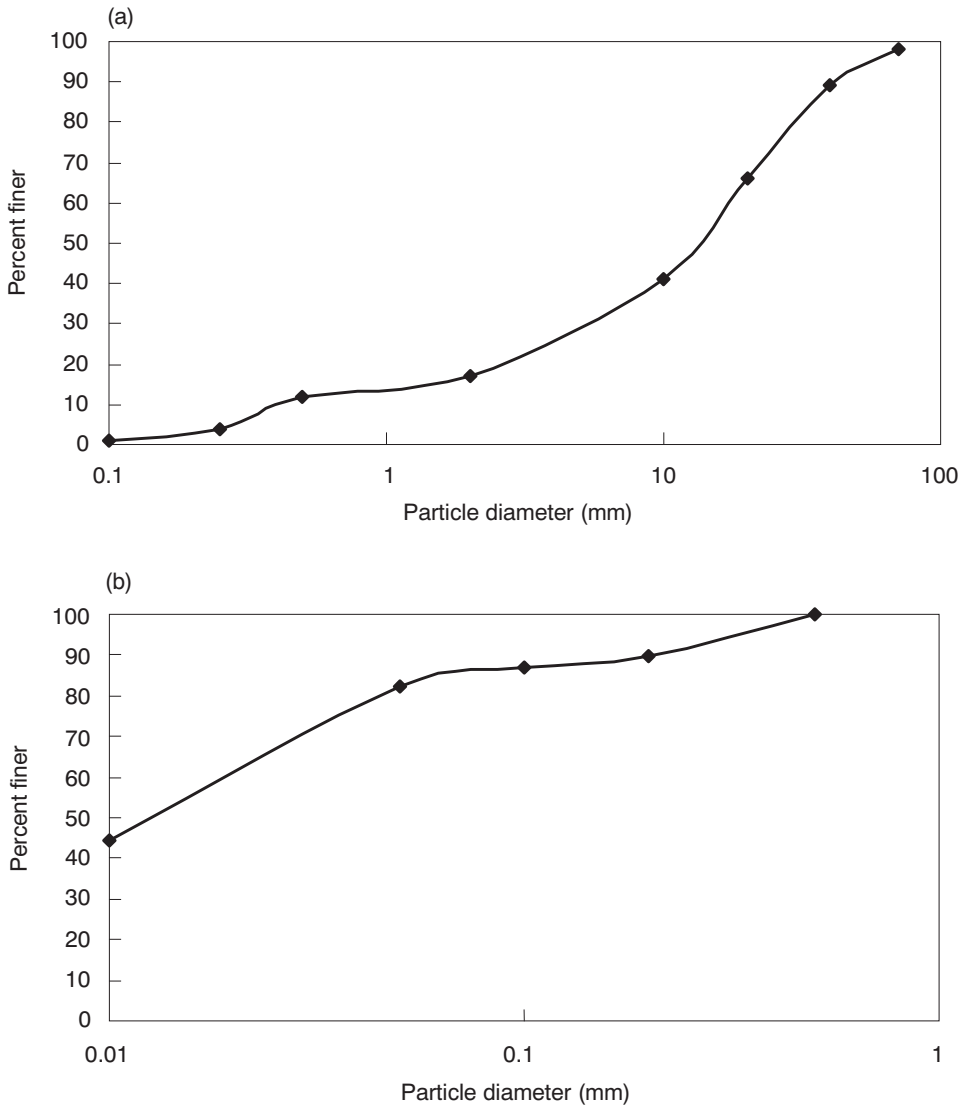

Figure 5.5. Typical material gradation in the (a) bed sediments and (b) suspended sediments of the Tom River.

Hydrological Institute, 1985; Hydrometizdat, 1984), the radionuclides are expected to be sorbed to the small fraction of silt and clay, as discussed previously. The suspended load in the Tom River is much finer than the bed sediments (*Figure 5.5b*), indicating a significant washload, typical of an uncontrolled river.

Table 5.1. Estimate of total radioactivity in the Tom River valley from the Tomsk-7 release point to the confluence with the Ob River (GBq).

Radionuclide	Total radioactivity
^{60}Co	26
^{90}Sr	52
^{137}Cs	110
^{152}Eu	7
^{232}Th	4
^{238}U	4
^{239,240,241}Pu	22
Total	230

5.2.2 Existing contamination in the river valley

The existing contamination profile of the floodplain soils and bed sediments of the Tom River valley (Appendix II), used in scenarios SCC-1 and SCC-2, was based on an analysis of summaries of five data sources. Several of the data sources appear to report sampling and analysis conducted independently of the SCC (Rikhvanov, 1997; Arkhangelskii *et al*., 1996; Tomsk Spravka, 1994). The data in other sources appear to have been collected and analyzed either by or for the SCC.

The concentrations of radionuclides reported in Appendix II for the Tom River valley are generally one order of magnitude lower than the levels reported in the Yenisei River valley (see Appendix I). This trend is evident in the data collected by and for the SCC and in data from sources independent of the SCC. This result is particularly surprising because similar production operations were conducted at the two sites and the average discharge in the Tom River is much lower than that in the Yenisei River. A possible explanation of these low contamination values is the flushing of contaminants provided by the river during the high discharges caused by the spring snowmelts.

No data were available for widths of contamination on the riverbanks and islands. A width of 100 m was assumed for each bank and for all islands within the reach of interest. Because of the relatively low values for radionuclide concentrations, this relatively wide width of contamination does not result in appreciable radionuclide inventories. No data were given to produce depth profiles of radionuclide concentrations. A mixing depth of 20 cm was assumed based on values observed in the Yenisei River valley. The total radioactivity of long-lived radionuclides in the Tom River valley based on the available data sources and on estimates of widths is summarized in *Table 5.1*.

Table 5.2. Radionuclide concentration of fish in the Tom River (Bq/kg).

Location	Samuski			Market				Popad
Sample	1	2	3	1	2	3	4	
Date	(5/1997)	(5/1997)	(5/1997)	(9/1996)	(9/1996)	(5/1997)	(9/1996)	(6/1997)
^{24}Na	76.2	34.2		11,998	18,310	18,074	19,375	
^{40}K	170	113	15	96	157	15	309	15
^{42}K					2,889	3,946		
^{46}Sc				103	41.4		42	
^{51}Cr				3,911	1,544	112	1,611	
^{59}Fe				29.6				
^{60}Co		1.5	2.4	108	51.5	18.8	51	
^{65}Zn	213	194	603	1,897	2,609	2,071	2,694	104.7
^{76}As				359	148			
^{82}Br						33.6		
^{103}Ru				7.3				
^{131}I				17				
^{134}Cs							9	
^{137}Cs				50.9	16.1		18	
^{140}Ba				38	18.1			
^{141}Ce				14.7				
^{152}Eu				65.2				
^{226}Ra	1.9		1.9					
^{232}Th	1.1							
^{239}Np		9.8	128	776	345		262	

Source: Rikhvanov (1997).

5.2.3 Short-lived radionuclide contamination of fish

The presence of short-lived activation products (e.g., ^{24}Na) and corrosion products (e.g., ^{51}Cr and ^{65}Zn) in fish from the Tom River has been reported as recently as 1997 (*Table 5.2*) and in muscular tissue of fish in 1995 and 1996 (*Table 5.3*). The concentrations of these short-lived radionuclides have decreased appreciably since the once-through production reactor was shut down and decommissioned in 1990, but they persist. The explanation for the persistence of short-lived radionuclides is that the remaining closed-loop dual-purpose reactors still in operation have open-loop cooling for the control rods. The water from this open-loop system is discharged directly into the Tom River without appreciable retention.

An analysis of the dose effects from these short-lived radionuclides is presented in Section 5.3.1.

Table 5.3. Radionuclide concentration in muscular tissue of fish in the Tom River (Bq/kg).

	Year	^{137}Cs	^{90}Sr	^{65}Zn	^{32}P
Release point	1996	24.1	1.96	146	3446
	1995	4.96	0.961	165	4753
Chernilschikovo	1996	11.1	14.8	396	753
	1995	414	2.44	80.7	380
Samus	1996	12.4	0.37	14.4	443
	1995	95.8	3.99	43.5	349
Orlovka	1996	12.9	0.57	13.8	625
	1995	35.5	1.07	12.5	474
Kozjilino	1996	1.95	0.35	10.8	395
	1995	1.15	0.2	14.8	42.2
Iglovsk	1996	5.18	2.22	11.8	3.07
	1995	21.8	0.022	1.22	
Krasnii Yar	1996	92.5	2.59	14.4	16.3
	1995	28.9	1.39	10.7	121
Tugulino	1996	81.4		11.5	8.51
	1995	0.15	0.15	3.7	

Source: Masluck *et al.* (1996).

5.2.4 Hypothetical release of inventory from the site

Although some data were provided relevant to hypothetical releases (Rikhvanov, 1996), they were insufficient for analysis. Therefore, a unit release of 37 TBq (1,000 Ci) of ^{137}Cs and 37 TBq (1,000 Ci) of ^{90}Sr was assumed. This magnitude of release is similar to the release postulated by engineers at the Mining and Chemical Combine (MCC) for evaluation of consequences to the Yenisei River, although it is significantly smaller than the total inventory of the surface ponds at the SCC. However, there are significant uncertainties regarding these ponds. The use of a unit release thus allows both the potential for scaling the release and a determination of the magnitude of release to the river system that is required for significant contamination of the river. These unit releases can be scaled to actual values, should such values be obtained in the future.

Similar to the analysis of the MCC, half the radionuclides were assumed to be associated with silty sediments and half with clay sediments. Doses from ^{137}Cs and ^{90}Sr were analyzed separately because there is no information as to whether these radionuclides were chemically separated and stored separately for industrial purposes, as they were at the Mayak site.

Table 5.4. Population of villages along the Tom River from release point to confluence with the Ob River.

Village, left bank	Village, right bank	Distance downstream from discharge point (km)	Population	
			Site data	Map data
	Chernilschikovo	2–8	15	<100
Moryakovskii zaton		11–13	5000	>1,000
	Samus	13	6000	>2,000
	Kizhirovo	18–20	10	<100
Nagornii Ishtar		23–24	8	<100
	Orlovka	54–55	300	500–1,000
Kozjilino		63–65	100	<100

5.2.5 Populations of villages along the Tom River

Census data are typically considered sensitive in the Russian Federation, and no official population data were available for the villages along the Tom River. However, some data for populations of villages on the Tom River were provided during a site visit (*Table 5.4*). In addition, the populations in towns and villages along the Tom between the release point and the confluence with the Ob River were estimated from data (population range as indicated by size and font of place name) on a 1:200,000-scale 1995 map of the Tomsk Oblast. The agreement between the two data sources appears reasonable. Based on site data, the total population along this river reach is approximately 12,000. Because individual dose estimates were made, these population estimates provide qualitative value to the study.

5.3 Results

5.3.1 Scenario SCC-1: Existing contamination levels and locations

Soil and Sediment Contamination

This scenario presents an evaluation of doses due to existing contamination in the Tom River channel and floodplain. The available data about existing contamination are summarized in Appendix II; the maximum concentrations of radionuclides are shown in *Figure 5.6*. The methodology for constructing the table in Appendix II is the same as that used to generate the table in Appendix I for the Yenisei River, and the same caveats apply here.

The highest concentrations are located within the first 7 km downstream from the Ramashka River discharge point. The primary contributors are ^{137}Cs, ^{90}Sr, and plutonium (calculated as ^{239}Pu). For most other locations, the concentrations of radionuclides are an order of magnitude lower. The annual dose plot (*Figure 5.7*) is calculated by multiplying the existing radionuclide concentrations by the pathway dose conversion factors (*Table 3.3*).

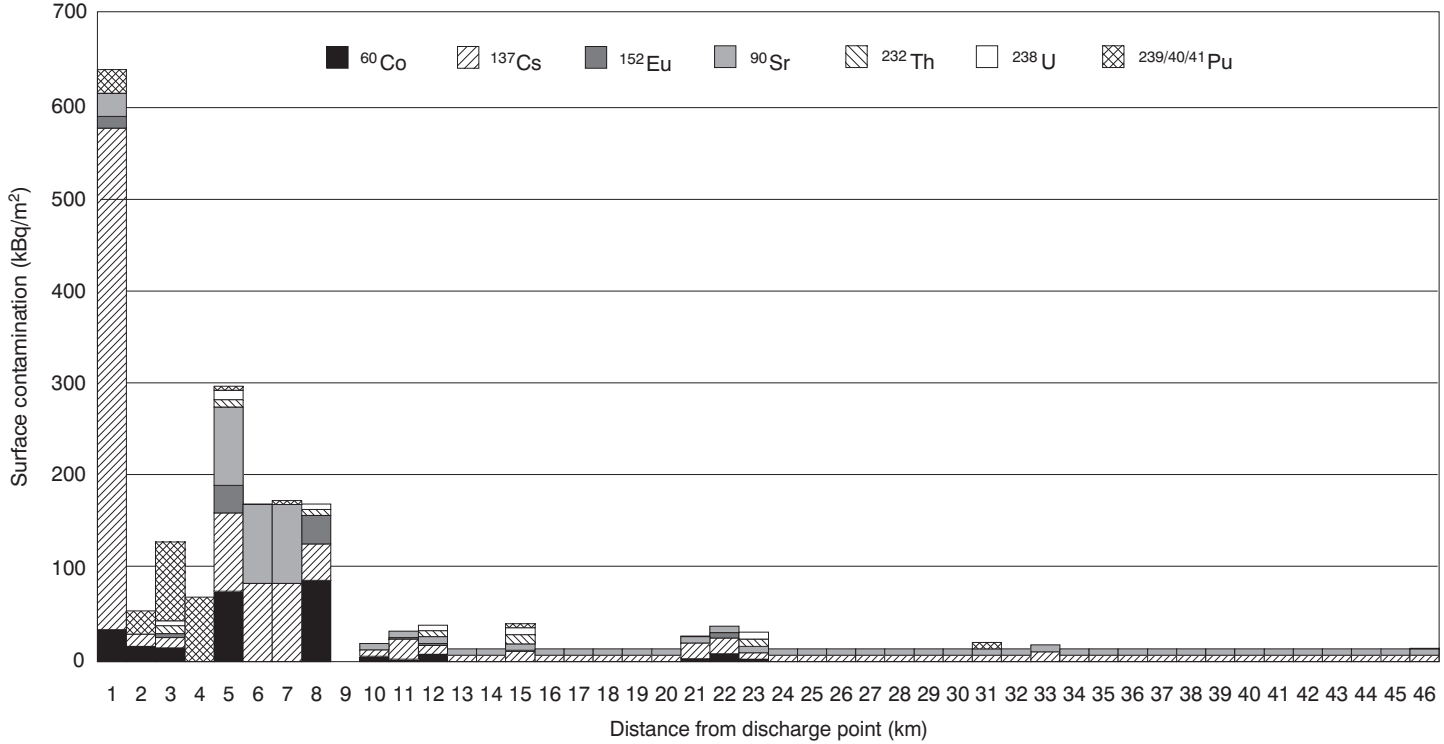

Figure 5.6. Maximum radionuclide concentrations (kBq/m^2) in each kilometer of the Tom River floodplains (decayed to 1997).

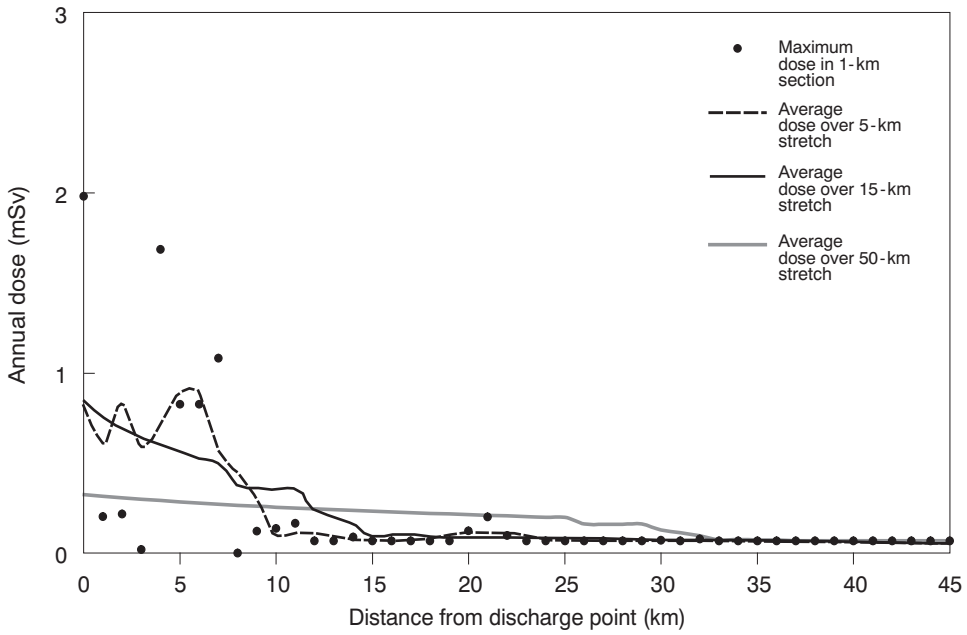

Figure 5.7. Maximum and averaged annual doses from existing contamination of the Tom River floodplains.

An averaging procedure similar to the longitudinal averaging procedure used for the Yenisei River dose estimation was used. Several different longitudinal intervals were used (5 km, 15 km, and 50 km). Width scaling was not used, since data were insufficient to estimate contamination widths; a uniform 100 m width was assumed. It can be seen that there are only a few locations, all within the first 7 km of the discharge point, where doses could potentially exceed the 1 millisievert (mSv) limit. If reach averaged doses are used, the entire river is below the 1 mSv dose limit. The majority of the river exhibits maximum potential doses of no more than 0.1 mSv regardless of the method used to estimate exposure. Doses due to transuranic nuclides contribute only a very small fraction of the total dose; most of the doses are due to external exposure from gamma-emitting nuclides.

Periodic radiological surveys could be used to monitor the conditions within contaminated areas, and remedial or isolation activities such as erecting fences or posting warning signs in selected areas may be an adequate solution from a dose-limiting perspective. However, the experience gained at Mayak raises doubts that all of the population will observe these restrictions. Of course, social and political forces may require that remediation be performed. If social or political pressures dictate some form of physical remediation, the relatively few areas registering the

highest concentrations of contamination are logical candidates. The limited areal extent of these contamination anomalies should facilitate remediation.

The levels of contamination reported were surprisingly low relative to those at the MCC. These low levels of contamination may result from incomplete available data, although sample coverage along the river was sufficiently extensive to provide confidence that extensive contamination would have been detected (see Appendix II). Another possible explanation, scouring of contamination during high discharges, is discussed in the Section 5.3.2.

Contaminated Fish

Doses from eating fish contaminated with both short- and long-lived radionuclides at the levels shown in *Tables 5.2* and *5.3* (Section 5.2.3) are shown in *Tables 5.5* and *5.6*, respectively. Estimated doses based on a consumption rate of 17 kg/yr range between 0.4 and 350 microsieverts (μSv) per year depending on the radionuclides contained in the sampled fish, the fish type, and their location; it is assumed that the fish are consumed soon after they are caught (before short-lived radionuclides decay). The majority of this dose is from ^{65}Zn and ^{24}Na. The dose is reduced by half after several days due to decay of ^{24}Na (15-hour half-life). When short-lived radionuclides have decayed, a large fraction of the remaining dose comes from naturally occurring radionuclides.

In an attempt to fill gaps in the sampled data, Russian health physicists calculate doses using the assumption that each sample contains all reported radionuclides. The procedure they use is illustrated here:

1. Concentrations of all radionuclides in *Table 5.2* are divided by the ^{65}Zn concentration, and these ratios are averaged.
2. The dose from this mixture is calculated as the product of the fish consumption rate (17 kg/yr), an effective dose conversion factor (EDCF1), and the ^{65}Zn concentration of the sample.
3. EDCF1 is calculated as the sum of the dose conversion factors for each radionuclide multiplied by the average concentration ratio for that radionuclide as calculated in step (1) above (Mixture 1).
4. The procedure is repeated for concentration data in *Table 5.3* using an EDCF2 representing the radionuclides contained in that table (Mixture 2).
5. The radionuclide concentrations from the two separate data sources (*Tables 5.2* and *5.3*) are then combined using the rationale that ^{65}Zn is a common denominator for both data sets. The EDCF3 of this combined data set represents the averaged concentration ratios of all radionuclides (Mixture 3). (Note that only ^{65}Zn and ^{137}Cs are common to both data sets, and that Russian health physicists use the larger ratio for ^{137}Cs.)

Table 5.5. Estimated doses (μSv per year) from consuming fish from the Tom River based on radionuclide concentration in fish from *Table 5.2*.

Radio-			Samus			Market				
nuclide	Half-life	DCF[a]	1	2	3	1	2	3	4	Popad
^{24}Na	15 hrs	1.5E-06	0.5	0.2		82.6	126.0	124.0	133.0	
^{40}K	1.28×10^{9}yrs	1.9E-05	14.8	9.8	1.3	8.4	13.7	1.3	27.0	1.3
^{42}K	12.3 hrs	1.5E-06					22.2	27.2		
^{46}Sc	84 days	7.5E-06				3.5	1.4		1.5	
^{51}Cr	28 days	1.5E-07				2.7	1.1	0.1	1.1	
^{59}Fe	45 days	7.5E-06				1.0				
^{60}Co	5.3 yrs	2.6E-05		0.2	0.3	12.9	6.1	2.3	6.1	
^{65}Zn	244 days	1.4E-05	13.7	12.4	38.8	122.0	168.0	133.0	173.0	6.8
^{76}As	26 hrs	5.0E-06				8.2	3.4			
^{82}Br	1.5 days	1.8E-06						0.3		
^{103}Ru	39 days	3.0E-06				0.1				
^{131}I	8 days	5.0E-05				3.9				
^{134}Cs	2 yrs	7.4E-05							3.1	
^{137}Cs	30.2 yrs	5.0E-05				11.7	3.7		4.1	
^{140}Ba	13 days	7.5E-06				1.3	0.6			
^{141}Ce	285 days	3.0E-06				0.2				
^{152}Eu	13.5 yrs	6.0E-06				1.8				
^{226}Ra	1,600 yrs	1.1E-03	9.5		9.5					
^{232}Th	1.4×10^{10}yrs	2.8E-03	14.3							
^{239}Np	2.4 days	3.0E-06		0.1	1.8	10.7	4.8		3.6	
Total dose:										
All nuclides			52.9	22.8	51.7	271.1	351.0	288.1	352.5	8.1
Long-lived nuclides			38.6	10.0	11.1	34.8	23.5	3.6	37.2	1.3
Naturally occurring nuclides			38.6	9.8	10.9	8.4	13.7	1.3	27.0	1.3

[a] DCF = Dose conversion factor (μSv/Bq).

The results of these calculations are shown in *Table 5.7*. The mixture procedure gives results similar to doses based on measured data for Mixtures 1 and 2, except for Chernilschikovo in 1996, where the dose is nearly an order of magnitude higher. Mixture 3 gives results similar to doses based on measured data except for Chernilschikovo in 1996 and the four Market samples, where they are nearly an order of magnitude higher. It is difficult to determine if the differences in these results are real effects or are due to the procedure the Russians used to fill possible gaps in the data to obtain an upper bound on the dose due to fish consumption. However, as these analyses indicate the potential for annual doses above the 1 mSv annual dose limit, fish consumption may be a significant radiological pathway in the Tom River and warrants further study.

Table 5.6. Estimated doses (μSv per year) from consuming fish from the Tom River based on radionuclide concentration in muscular tissue of fish from *Table 5.3*.

		Radionuclide				Total dose	
	Year	^{137}Cs	^{90}Sr	^{65}Zn	^{32}P	All nuclides	Long-lived nuclides
Release point	1996	55	13	94	1,200	1,400	68
	1995	11	6	110	1,600	1,800	18
Chernilschikovo	1996	26	95	250	260	640	120
	1995	950	16	52	130	1,100	970
Samus	1996	28	2	9	150	190	31
	1995	220	26	28	120	390	250
Orlovka	1996	30	4	9	220	260	33
	1995	81	7	8	160	260	88
Kozjilino	1996	4	2	7	140	150	7
	1995	3	1	10	15	28	4
Iglovsk	1996	12	14	8	1	35	26

Note: For ^{137}Cs, half-life (t_h) = 30.2 yrs and dose conversion factor, or DCF (in μSv/Bq) = 5.00E-05; for ^{90}Sr, t_h = 29.1 yrs, DCF = 1.40E-04; for ^{65}Zn, t_h = 244 days, DCF = 1.40E-05; for ^{32}P, t_h = 14.2 days, DCF = 7.50E-06.

5.3.2 Scenario SCC-2: Redistribution of existing contamination by flooding

This scenario is concerned with redistribution of existing radioactive contamination by high levels of water flow in the Tom River. The hydraulic properties of the river channel and overbanks were estimated using HEC-RAS. Because of the limited floodplains, the properties of the channel were used to calculate scour and deposition. The primary calculated hydraulic property provided by HEC-RAS was the pattern of shear stress in the channel portion of the river (*Figure 5.8*). The velocity of water flowing in the river primarily determines this shear stress pattern. These properties were used, along with the existing levels and locations of radionuclides in the floodplains, as input to the contamination redistribution routine developed by the RAD staff.

Figure 5.8 is a contour plot of shear stresses in the channel at various locations for the range of discharges observed in the Tom River. It shows that shear stresses increase with increasing discharges. The critical shear stress is the stress that determines whether the given conditions result in scour or deposition. As with the analysis of the Yenisei, the values for the critical shear stresses used in this analysis were 0.7 kg/m^2 for silt and 2 kg/m^2 for clay. At a given location along the river, the discharges corresponding to the critical shear stresses can be estimated (e.g., 2,000 and 4,000 m^3/sec for silt and clay, respectively, at 26 km). At discharges above

Table 5.7. Doses from fish consumption (mSv per year) resulting from the Russian procedure for filling gaps in sampled data.

		Based on			
Location	Date	Measured data	Mixture 1	Mixture 2	Mixture 3
Samus 1	5/97	0.05	0.03		0.3
Samus 2	5/97	0.02	0.03		0.2
Samus 3	5/97	0.05	0.1		0.7
Market 1	9/96	0.3	0.3		2
Market 2	9/96	0.4	0.4		3
Market 3	5/97	0.3	0.3		3
Market 4	9/96	0.4	0.4		3
Popad	6/97	0.01	0.02		0.1
Release point	1996	0.1		0.2	0.2
	1995	0.2		0.2	0.2
Chernilschikovo	1996	0.06		0.4	0.5
	1995	0.1		0.09	0.1
Samus	1996	0.02		0.02	0.02
	1995	0.04		0.05	0.05
Orlovka	1996	0.03		0.01	0.02
	1995	0.03		0.01	0.02
Kozjilino	1996	0.01		0.01	0.01
	1995	0.003		0.02	0.02
Iglovsk	1996	0.003		0.01	0.01
Krasnii Yar	1996	0.02		0.02	0.02
	1995	0.01		0.01	0.01
Tugulino	1996	0.02		0.01	0.01
	1995	0.0004		0.004	0.005

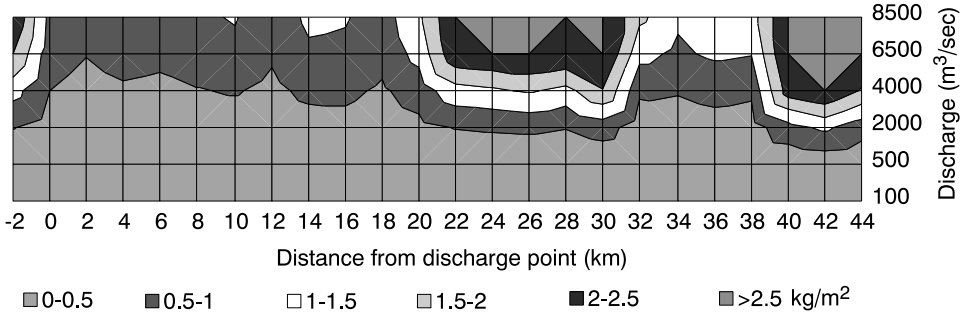

Figure 5.8. Shear stresses (kg/m^2) in the channel of the Tom River for various discharges.

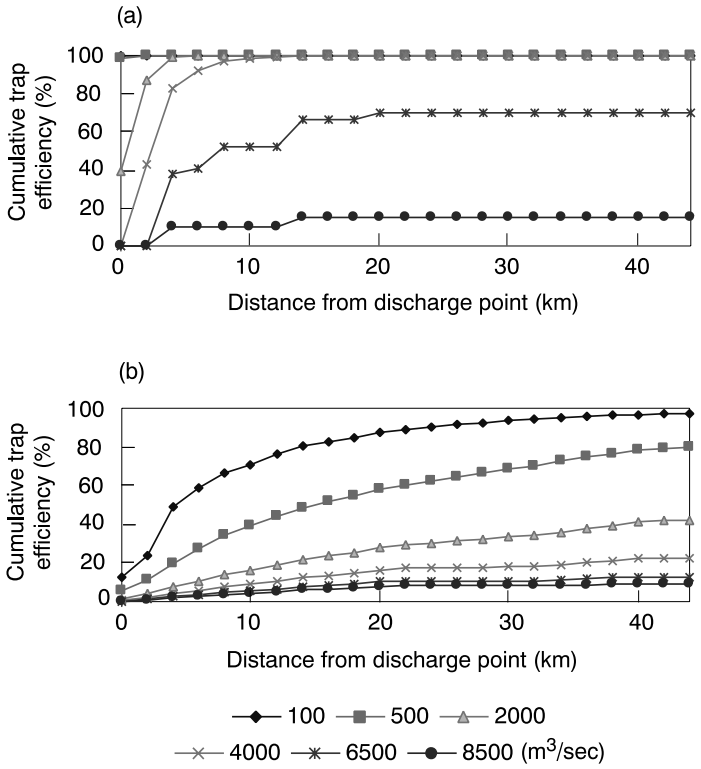

Figure 5.9. Trap efficiency for (a) silt and (b) clay for the Tom River channel.

these values, scour is calculated to occur at this location; below these discharges, deposition is calculated to occur.

As discussed in Section 3.2, the appropriate values for critical shear stresses depend on many site-specific factors. *Figure 5.8* can be used to estimate the effects of selecting alternative values for the critical shear stresses. Note that for normal discharge conditions when the river is within its banks (below 500 m^3/sec), the shear stresses are below 0.7 kg/m^2 for the entire river reach, indicating deposition conditions for both silt and clay for the selected critical shear stresses.

The shear stresses indicated in *Figure 5.8* are average values over the length and width of the individual cross sections. The length of cross sections used in this analysis is 2 km. Because shear stresses are averaged over these areas, only average results can be provided. Localized areas of higher concentrations may be expected; however, the detail of modeling used in this analysis and the sufficiency of the underlying theory are not enough to make predictions at this level of detail.

Trap efficiency estimates for individual cross sections in the reach of interest for silt and clay for various discharges (*Figure 5.9*) were based on the shear stress plot

for the Tom, the assumed critical shear stresses, and the fall velocities for the silt and clay particles. At discharges of less than 4,000 m^3/sec, the river traps nearly 100% of the suspended silt particles; at discharges of 8,500 m^3/sec (the annual maximum discharge), approximately 85% of the silt particles are carried away in the wash load. Only at the lowest discharge values are clay particles trapped in the reach. The soil particles (and adsorbed radionuclides) washed out of the reach are either subsequently deposited within the Ob River system farther downstream or discharged into the Kara Sea. For this reason, sampling of potential deposition areas farther downstream along the Ob River system may be warranted.

Soil concentrations of ^{137}Cs due to redistribution of existing contamination are shown in *Figure 5.10a*. These concentrations are calculated by assuming that the radionuclides are redistributed due to typical spring flooding lasting 20 days. Bed armoring – prevention of continued erosion of fine particles due to an "armor" of coarser particles – is assumed to prevail after one or two days of flooding, thereafter limiting the scour rate of silt and clay. Discharges in the range of 4,000 m^3/sec provide the only levels of deposition within the reach of interest, and the concentration values are low compared with those of the Yenisei River. Because the initial geographical distribution of the other evaluated radionuclides is similar to that of ^{137}Cs (see *Figure 5.6*), the redistribution of these radionuclides is also similar. The lack of significant concentrations of radionuclides due to deposition of existing radionuclides is primarily due to the lack of significant levels of radionuclides in the river valley to act as a contaminant source. This analysis did not include ongoing discharges from the plant. They may represent the main potential source of future contamination. However, assuming that the river regime remains similar to what it has been, the spatial pattern of deposition is likely to remain similar to that currently observed. Remedial measures based on existing contamination profiles are therefore likely to be sufficient for providing protection against the effects of flood-borne redistributed contaminated sediments.

The total dose resulting from the combination of all redistributed radionuclides and based on the exposure scenarios discussed in Section 2.4 is shown in *Figure 5.10b*. The maximum dose resulting from the redistribution of existing radionuclides is less than 0.03 μSv per year, indicating that on average the doses due to dilution, dispersion, and redistribution of existing radionuclides would be lower than the already low existing contamination. Of course, localized spots of higher levels of contamination would likely occur due to specific sediment-trapping characteristics of topography and plants, grasses, and trees.

Radiological surveys should be conducted periodically to monitor existing conditions and identify new localized spots of higher contamination. However, on average, the contamination levels are expected to be low enough that widespread remediation measures do not appear to be warranted for technical reasons alone.

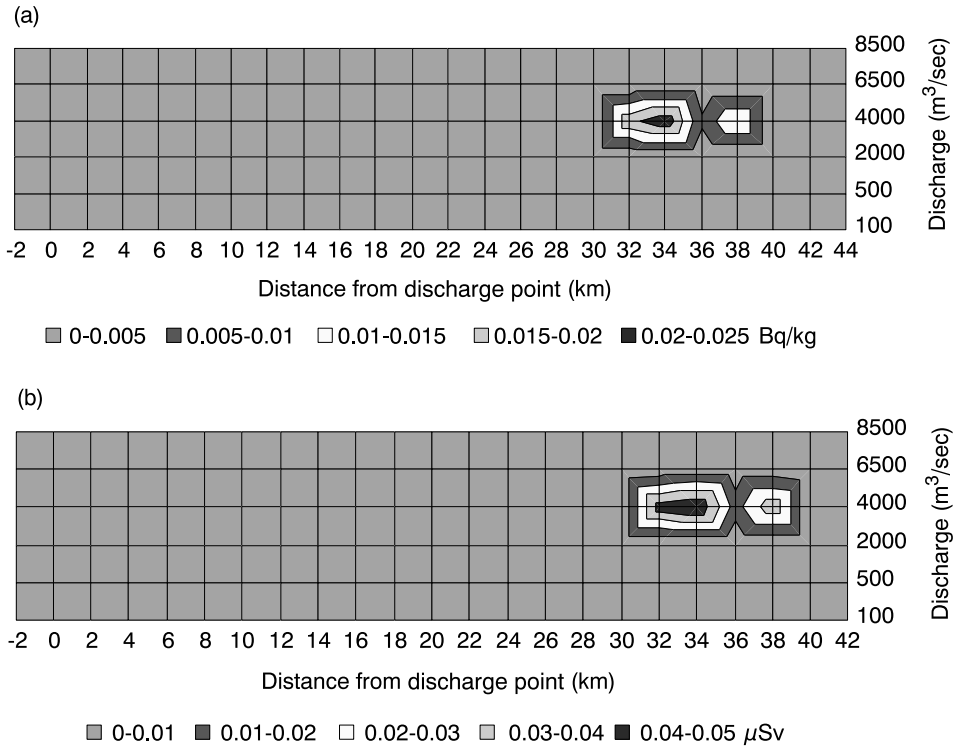

Figure 5.10. Estimates of (a) soil concentrations of ^{137}Cs (Bq/kg) and (b) total annual dose (μSv/yr) from all radionuclides due to redistribution of existing contamination in the Tom River valley.

Of course, social and political forces may require that remediation be performed. Trap efficiency calculations indicate that a significant fraction of radionuclides will likely be washed out of the river reach along with the sediment wash load. Because several population centers are located along the Ob River farther below the confluence with the Tom (e.g., Krasnii Yar, Krivoshenino, Molchanovo, and Kolpashevo within the first 200 km), periodic radiological surveys may be important to monitor exposure conditions at critical locations along the river.

The high shear stresses and low trap efficiency associated with high discharges may explain the relatively low contamination levels in the Tom River valley downstream from the SCC. Our modeling indicates that, with annual high discharges due to spring snowmelt, shear stresses in the channel bed are high enough that significant scour and transport could be expected on an annual basis (see *Figure 5.8*). Once suspended, over 80% of the finer particles, expected to contain most of the sorbed radionuclides, will be washed out of the system (see *Figure 5.10*). Although

this hypothesis cannot be verified with the available data, it supports the general picture of the existing low levels of radiological contamination in the Tom River valley. Alternatively, it is possible that the sparse available sampling data simply did not locate the significant contamination that is present in the reach. For example, we have no sampling data for the swampy areas below Orlovka, which could become inundated during high discharges. This area appears to be a logical location for sampling because radionuclides on suspended particles that become trapped by receding floodwater will likely be retained in this relatively closed system.

5.3.3 Scenario SCC-3: Release of radionuclides from the site

This scenario is concerned with the dose effects of a hypothetical release of radionuclides from the SCC to the Tom River. The shear stress and trap efficiency profiles for the Tom River presented in Section 5.3.2 are also applicable to this scenario. The released radioactivity is assumed to be partitioned equally between silt and clay particles.

Because a specific inventory of radionuclides was not provided for analysis, a unit release of 37 TBq (1,000 Ci) of radioactivity was assumed. The soil contamination density for this release is shown in *Figure 5.11*.

In *Figure 5.11a* the upper level of contamination is limited to 3,700 Bq/kg so that the finer structure of the lower levels of contamination can be seen. Discharges around 4,000 m^3/sec provide the most significant redistribution of contamination downstream from the release point within the reach of interest. At this rate of discharge, approximately 70% of the silt is expected to be retained in the reach (see *Figure 5.9a*).

The highest levels of contamination are expected to occur at the lowest discharges and at locations nearest the discharge point (*Figure 5.11b*). Contamination densities of over 400 Bq/g may be possible.

The plots presented in *Figure 5.11* can be converted directly to dose plots by multiplying the soil contamination density by the activity released, dividing by the 37 TBq (1,000 Ci) release used to develop the plot, and multiplying by the pathway dose conversion factor for the radionuclide of interest (see *Table 3.3*). For a 37 TBq (1,000 Ci) release of ^{137}Cs, the dose resulting from the contamination at the location 18 km downstream from the release point (*Figure 5.11a*) is approximately 100 μSv per year. At the highest concentrations near the release point, the dose may be over 100 mSv per year. Similarly, for a 37 TBq (1,000 Ci) release of ^{90}Sr, the dose resulting from the contamination at the location 18 km downstream from the release point (*Figure 5.11a*) is approximately 300 μSv per year. At the highest concentrations near the release point, the dose may be over 300 mSv per year.

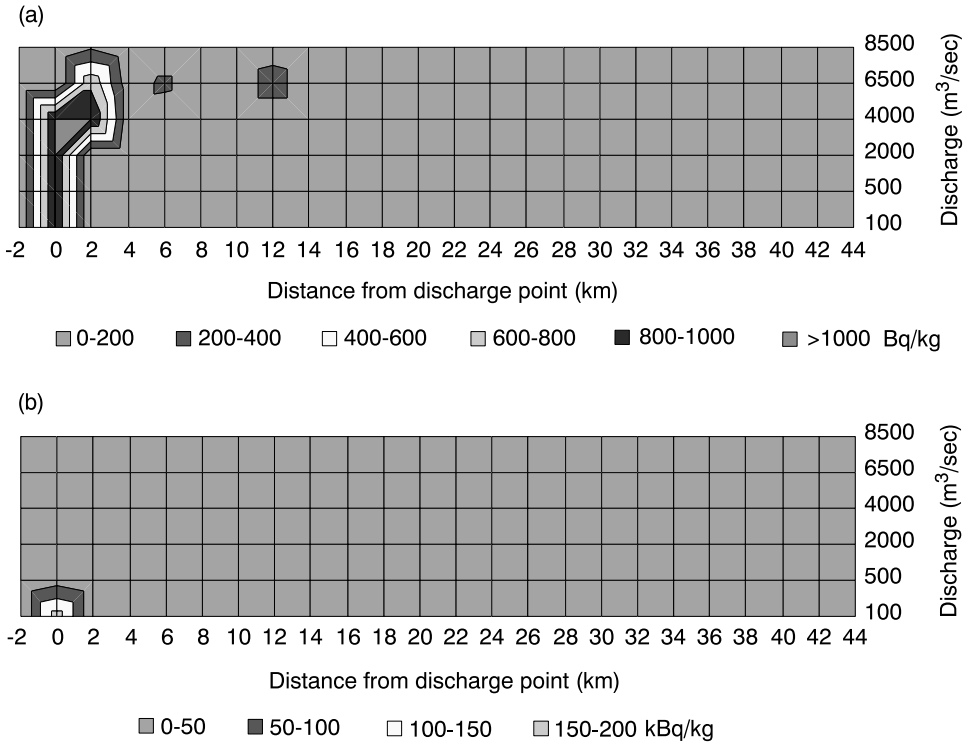

Figure 5.11. Soil contamination density resulting from a 37 TBq (1,000 Ci) release of radioactivity to the Tom River. (a) Fine-scale and (b) full-scale soil concentrations.

The highest doses resulting from a large and sudden release of radioactivity from the site into the river occur when the discharges are lowest, which is typically in the winter months. However, significant redistribution of contaminants would likely occur during high discharge conditions resulting from the spring snowmelt (see *Figure 5.4*), when the trap efficiency of the reach for both silt and clay is low. Because spring flooding would result in a significant redistribution of radionuclides released to the Tom, a relatively fast response may be necessary to remediate or contain a release prior to this flooding. This potential need for a relatively quick response indicates that there may be value in contingency planning prior to such a release.

The results of this unit analysis indicate that the release of even a small fraction of the inventory known to exist in the surface basins could result in locally severe contamination. Larger releases, of course, would result in an increase of both the magnitude and extent of contamination. The most important remedial activities

that can be conducted in response to this scenario are likely to be those that focus on preventing large releases of radionuclides to the river. Contingency planning should be carried out to establish measures to prevent the spread of contamination from the Romashka to the Tom River system should such an event occur. However, because there are few available data on the characteristics of storage ponds, tanks, and their appurtenances within the SCC, no specific evaluations can be conducted at this time. Studies of the potential radiological impact of these surface basins, from this pathway and others, may yield a more accurate picture of potential risks posed by operations at the SCC.

6
Conclusions

The work to date has provided one of the most comprehensive pictures of the extent and significance of contamination in the Yenisei and Tom River valleys due to releases from the weapons facilities at Krasnoyarsk-26 and Tomsk-7. In addition, the nature of the problem has dictated the development of original models for estimating the significance of contaminated sediment transport. As with all original work, much remains to be done on model development and validation. However, by basing the development on theoretical principles, these models can assist in scoping the problems posed by contaminated sediment transport in river systems. The work synthesizes all known data relevant to contamination of these river systems. As the modeling has been done on a unit basis for each radionuclide of interest, it will be possible to linearly scale the results of sediment transport modeling from the results reported here should new data become available.

The two sites, Tomsk-7 (the Siberian Chemical Combine, or SCC) and Krasnoyarsk-26 (the Mining and Chemical Combine, or MCC), have discharged millions of curies of radioactivity directly to the rivers. Despite the release of these sizable amounts of radioactive materials and the high hazard associated with such materials, the environs seem remarkably clean. The concentrations in the sediments of the Yenisei and Tom Rivers, decayed to 1997 values, range between less than one to thousands of kilobecquerels per square meter (kBq/m^2) and less than tenths to hundreds of kBq/m^2. The concentrations of radionuclides in the river water have decreased markedly since the shutdown of the once-through water-cooled reactors. These studies have tried to determine the impact of these discharges to the accessible environment (outside Combine boundaries) in the Tom and Yenisei Rivers and their floodplains. The impacts from the other releases (e.g., atmospheric, global fallout, accidents, etc.) have not been evaluated, nor has a dose reconstruction of the impact of river water contamination prior to the shutdown of the single-pass reactors been conducted.

Evidence of the discharges from the two sites can be traced all the way to the Arctic Ocean. There are clearly many places along the riverbanks and islands where discharges from the sites have resulted in contamination levels well above natural background levels. However, when the doses to inhabitants near the Combines are calculated, in many places they turn out to be less than 1 millisievert (mSv) per year in the Yenisei River valley and below tenths of millisieverts per year in the Tom River valley. In areas within the first 25 km below Krasnoyarsk-26 on the

right bank the calculated dose is greater than 5 mSv per year. This dose is based on assumptions of a relatively high degree of occupancy and all the population's food being grown on contaminated lands. At discrete locations downstream, the doses can exceed 1 mSv per year under conservative exposure assumptions. For the Tom River, contamination at the confluence of the Romashka River and on Chernilschikovskii Island might produce doses of millisieverts per year to fishermen under the same conservative assumptions. Although there are areas in these river valleys that exhibit significant contamination, it appears that these areas are known to regional authorities and in most places are relatively small or are inaccessible for extended occupation. Future studies focused specifically on the potential exposure of nearby populations in these areas may prove valuable. In the meantime, access controls are likely to prevent significant doses to the population.

Consumption of contaminated fish may also contribute to these doses. Since the shutdown at Tomsk-7 and Krasnoyarsk-26 of those production reactors with once-through cooling, the release of short-lived radionuclides (e.g., ^{24}Na, ^{32}P, and ^{65}Zn) into the river system has been mainly due to discharges of cooling waters from the control rod system of the dual-purpose reactors still in operation. It is likely that these releases are responsible for reported fish contamination in the Tom River. The calculation shows that contaminated fish consumption near Tomsk might result in maximum individual doses in the range of millisieverts per year (based on Russian techniques for combining concentrations from various sources), with most of this dose due to short-lived radionuclides. If the fish are stored for several days prior to consumption, the dose is reduced by half, primarily due to decay of ^{24}Na. It may be worthwhile to consider technical options to reduce the releases of induced activity or to increase their retention time. It should be noted that fish in this region are also biologically and chemically contaminated, and therefore radioactive contamination is not the only public health concern arising from fish consumption. No fish contamination data were received from Krasnoyarsk.

When flooding redistributes the existing contamination, the resulting increases in annual doses are less than tens of microsieverts per year in the Yenisei valley and less than tenths of microsieverts per year in the Tom River. These incremental doses are much less than those due to background radiation. While most of the data on contamination come from the two Combines, there are enough independent studies to indicate that the Combines' assessments of present conditions are reasonably accurate. Possible reasons for the low reported levels of contamination in the Tom River include incomplete reporting of the sediment content in the river and the floodplains or, as hypothesized in Chapter 4, annual washout of accumulated sediments and accompanying radionuclides. The occurrence of high flows during spring snowmelt and the sandy river bottom create conditions conducive to an annual washout of sediments.

For the "extreme events" agreed upon by engineers at the two Combines, regional authorities, and the RAD staff, the results are more ambiguous. For the Yenisei River all sediments from pond 365 – approximately 52 terabecquerels (TBq), or about 1,400 curies (Ci) of gamma emitters, of which approximately 83% is ^{137}Cs, and 41 TBq (1,100 Ci) of beta emitters – were assumed to enter the river due to a hypothetical failure of the berm caused by flooding. The computed doses for inhabitants of the floodplains of the Yenisei River could exceed 10 mSv per year. As there are two ponds on that terrace at the MCC, it seems likely that if the contents of one of the ponds were washed into the river then the contents of the other would also be washed into the river.

The fact that the hydroelectric dam above Krasnoyarsk controls the Yenisei River at and below Krasnoyarsk-26 should not be overlooked. The dam has dampened maximum discharges to half pre-dam maximums and has significantly dampened variations in flows. Because the dam provides such an important control of the river discharge, contingency measures for its use in the event of an accidental release should be evaluated. For example, by lowering the operating level of the reservoir behind the dam, additional storage capacity can be added, which would allow reduced discharges for extended times to allow emergency responses to a release. Conversely, the effects of high discharges, which lower concentrations near the release and flush contamination downstream, should also be evaluated.

For the Tom River, insufficient information was received from the SCC to establish a feasible "extreme event." Therefore, a generic release of 37 TBq (1,000 Ci) of ^{137}Cs and 37 TBq (1,000 Ci) of ^{90}Sr, a release similar in scale to that evaluated at Krasnoyarsk-26, was used. The calculated dose was also in the tens of millisieverts per year.

Based on the results of hypothetical pond releases, it appears that the consequences of a major release could be locally severe. Although available data were insufficient to characterize such events, the consequences of such a release may warrant further studies into the details of such a release with a view to minimizing the probability of such events. Also, contingency plans to prevent the spread of contamination into the downstream reaches of the rivers should be developed.

The data on which this analysis is based are admittedly sparse, given that the areas under study extend for hundreds of square kilometers. In addition, significant questions remain regarding the quality of the data, and there is a significant lack of extensive independent verification of results reported by the two Combines. However, this is characteristic of initial investigations at contaminated sites, not only in the former Soviet Union but in the United States as well. The data that are available are sufficient to allow planning of interim responses and the development of more focused studies. This is not the final analysis on these sites, but hopefully it represents the beginning of detailed studies.

Based on the results of this analysis, the question remains, What should be done? This is a social, political, economic, and technical decision – what Alvin Weinberg calls "transcience," a public policy problem that has scientific underpinnings. Although there are benefits to minimizing the doses, the cost, exposure to workers, absolute reduction in risk to the general public, and disruption to the community must also be taken into account. The decision made could be different in each country (or even within different parts of the same country) depending on the economic situation, competing needs, mores, etc. For example, in the Clinch River below the nuclear complex in Oak Ridge, Tennessee, there is radioactive contamination in the floodplain. There is also substantial contamination of the sediments in the river by both hazardous chemicals (primarily mercury) and radioactive material (primarily ^{137}Cs). The major contaminants are a result of releases from two different facilities during the same time frame, 1957–1959. These contaminated sediments are now overlain by less contaminated sediments. The local population and the regulatory authorities together have decided to leave the sediments undisturbed because their remediation would pose even greater risks than leaving them in place. Of course, monitoring of the situation will continue. In part, this decision was possible because the local community is technically knowledgeable.

In summary, it appears that despite large releases into the Tom and Yenisei Rivers over the past several decades, extensive contamination is not present and is unlikely to occur unless major releases from liquid-waste storage facilities occur. This is partly due to the fact that much of the contamination released was short-lived and has now decayed to stable isotopes, and partly due to hydrological features of the river that allowed only a fraction of this activity to be retained in the rivers. The remainder was flushed downstream, deposited along the thousands of kilometers of these large river systems, and eventually discharged into the Kara Sea. The Tom River may have been particularly efficient at flushing contamination, and the high flows of the Yenisei may have provided dilution and suspension sufficient to prevent large depositions. Of course, contaminated areas exist, particularly in the Yenisei, and may require remediation. It does not appear that remediation of the contamination along the river would pose any intractable engineering problems. It is more likely that selection of a socially, politically, and financially acceptable management plan will pose greater difficulties for the local and regional decision makers.

Map of Tomsk Region. (See printed version or contact author.)

Map of Krasnoyarsk Krai – Part 1. (See printed version or contact author.)

Map of Krasnoyarsk Krai – Part 2. (See printed version or contact author.)

Appendix I:
Input Contamination Data for the Yenisei River

The following table shows the input concentrations (in kBq/m^2) used for analysis of the doses in Scenario MCC-1 and the potential for redistribution in Scenario MCC-2. These values represent an estimated value derived from the sources listed in Chapter 4. Isotopic concentrations, where available, were given first priority. If isotopic concentrations were unavailable, values were derived from exposure dose rate (EDR) values from the 1990 aerogamma survey and scaled to the nearest location where isotopic concentrations were available. Estimated widths of contamination were based on scaling the results of HEC-RAS to the distribution of contaminated lands given in Table 5.4 of Robinson and Volosov (1996). All values were decayed to 1997 values to allow comparison between sources for different years. The equivalent total concentration in 1990 is given to facilitate comparison with the values reported in Khizhnyak. The discharge point is located 85 km downstream from the dam and 246 km upstream from the junction of the Yenisei and Angara Rivers.

Kilometers from discharge point	Contamination width (m)	^{60}Co	^{137}Cs	^{152}Eu	^{154}Eu	1997 Total	1990 Total
1	23	296	107			403	866
2	23	385	248	1,199	385	2,216	3,647
3	23	385	303	1,924	710	3,323	5,322
4	23	385	252	1,199	385	2,220	3,651
5	24	385	248	1,199	385	2,216	3,647
6	25	521	1,220	431	126	2,297	3,574
7	27	159	126	192	126	603	1,041
8	28	159	126	192	126	603	1,041
9	29	159	126	192	126	603	1,041
10	31	33	59	81	19	192	302
11	32	52	174	226	63	514	768
12	33	63	200	81	19	363	541
13	35	33	59	81	19	192	302
14	36	33	59	81	19	192	302
15	35	33	218	81	19	352	489
16	34	340	118	148	44	651	1,280

Kilometers from discharge point	Contamination width (m)	^{60}Co	^{137}Cs	^{152}Eu	^{154}Eu	1997 Total	1990 Total
17	32	47	217	215	58	537	783
18	31	5	109	10	2	127	160
19	30	5	109	10	2	127	160
20	29	5	109	10	2	127	160
21	27	37	178	96	15	326	465
22	26	37	178	96	15	326	465
23	25	19	15	7		41	74
24	24						
25	22	37	111	52	4	204	304
26	21						
27	20	7	7			15	27
28	19						
29	18	67	67			133	245
30	17						
31	16						
32	16						
33	15						
34	14						
35	13						
36	12	23	73	33	3	132	195
37	12	23	73	33	3	132	195
38	11	40	128	57	6	230	342
39	11	56	118	22		196	310
40	10	40	128	57	6	230	342
41	10						
42	7						
43	7						
44	7	2	390	21	7	421	507
45	7	2	390	21	7	421	507
46	7	2	390	21	7	421	507
47	6	26	56	11		93	146
48	6	4	300	15	4	322	389
49	6	4	300	15	4	322	389
50	6	4	300	15	4	322	389
51	6						
52	6		59	4		63	75
53	5						
54	6		118	7		126	150
55	7						
56	8						
57	8						

Kilometers from discharge point	Contamination width (m)	^{60}Co	^{137}Cs	^{152}Eu	^{154}Eu	1997 Total	1990 Total
58	9	4	155	7	4	170	209
59	10						
60	11						
61	11						
62	11						
63	11						
64	11						
65	10	2	364	20	6	393	473
66	10	2	364	20	6	393	473
67	10	1	208	11	4	224	270
68	10	2	312	17	6	336	405
69	9	2	312	17	6	336	405
70	9						
71	9		200	4		204	240
72	9		200	4		204	240
73	8	2	369	20	7	398	480
74	8		130	4		133	158
75	8	7	40	21	3	72	101
76	7	1	208	11	4	224	270
77	7						
78	7						
79	6						
80	6		152	4		155	184
81	6	1	219	12	4	236	284
82	5						
83	5	2	312	17	6	336	405
84	5	2	312	17	6	336	405
85	5		170	4		174	205
86	6						
87	6						
88	6		42			42	50
89	6		200	4		204	240
90	7		200	4		204	240
91	7		200	4		204	240
92	7	37	93	33	7	170	262
93	7						
94	7	30	70	26	7	133	207
95	8						
96	8						
97	8						
98	8						

Kilometers from discharge point	Contamination width (m)	^{60}Co	^{137}Cs	^{152}Eu	^{154}Eu	1997 Total	1990 Total
99	9	4	11	7		22	33
100	9	4	11	8	1	23	35
101	9						
102	9						
103	10						
104	10						
105	10						
106	10						
107	11						
108	11	33	96	63		192	287
109	11	6	17	12	2	36	54
110	11	33	96	63		192	287
111	11	5	15	10	2	31	47
112	11						
113	10	3	10	7	1	21	31
114	10						
115	10						
116	9						
117	9						
118	8	4	14	9	1	29	43
119	8						
120	8	3	10	7	1	21	31
121	8	3	10	7	1	21	31
122	8						
123	8	48	93	67	15	222	350
124	8	48	93	67	15	222	350
125	8	48	93	67	15	222	350
126	7	4	12	8	1	26	39
127	7						
128	7						
129	7						
130	7						
131	7						
132	7						
133	7						
134	7	32	72	49	8	161	249
135	6		28			29	34
136	6	37	84	57	10	188	290
137	6	37	74	52	11	174	273
138	6	37	74	52	11	174	273
139	6	24	54	37	6	121	186

Kilometers from discharge point	Contamination width (m)	^{60}Co	^{137}Cs	^{152}Eu	^{154}Eu	1997 Total	1990 Total
140	5						
141	5						
142	6						
143	6						
144	6						
145	6						
146	7						
147	7						
148	7						
149	8						
150	8	21	48	33	5	107	166
151	7						
152	7						
153	6						
154	6						
155	5						
156	5						
157	4						
158	4	41	115	33	7	196	297
159	4						
160	4						
161	4						
162	4						
163	3	44	130	37	7	218	329
164	3	40	90	61	10	201	311
165	3	40	90	61	10	201	311
166	3	40	90	61	10	201	311
167	3						
168	6						
169	10						
170	13	8	24	7	1	39	59
171	17	22	63	19	4	107	162
172	20	22	63	19	4	107	162
173	24	22	63	19	4	107	162
174	27	22	63	19	4	107	162
175	30	22	63	19	4	107	162
176	34	22	63	19	4	107	162
177	37	22	63	19	4	107	162
178	41	22	63	19	4	107	162
179	44	22	63	19	4	107	162
180	48	22	63	19	4	107	162

Kilometers from discharge point	Contamination width (m)	^{60}Co	^{137}Cs	^{152}Eu	^{154}Eu	1997 Total	1990 Total
181	51	35	78	45	7	165	256
182	55	67	107	59	15	248	403
183	58	67	107	59	15	248	403
184	54	56	85	48	11	200	327
185	49	56	85	48	11	200	327
186	45	30	48	26	7	111	181
187	40	22	37	19	7	85	138
188	36						
189	31	32	55	30	7	124	200
190	27	63	93	52	11	218	360
191	22	56	85	48	11	200	327
192	18	56	85	48	11	200	327
193	14						
194	9						
195	9						
196	8						
197	8	63	96	56	11	226	369
198	7	56	85	48	11	200	327
199	7						
200	6						
201	6	22	37	19	4	81	132
202	6	22	37	19	4	81	132
203	5	22	37	19	4	81	132
204	5	22	33	19	4	78	128
205	6	39	69	38	9	155	250
206	6						
207	6	30	48	19		96	157
208	7						
209	7						
210	7						
211	8						
212	8						
213	8						
214	8						
215	8						
216	8						
217	8	67	100	56	15	237	389
218	8						
219	8						
220	8						
221	8	23	40	22	5	89	143

Kilometers from discharge point	Contamination width (m)	^{60}Co	^{137}Cs	^{152}Eu	^{154}Eu	1997 Total	1990 Total
222	7						
223	7						
224	7						
225	7	4	22	4		30	41
226	7	63	96	56	11	226	369
227	7	63	133	56	11	263	413
228	7	63	96	56	11	226	369
229	6	63	96	56	11	226	369
230	6	63	96	56	11	226	369
231	6	70	104	48	7	229	380
232	8	70	104	48	7	229	380
233	10						
234	11	44	159	52	4	259	379
235	16	59	230	76	7	373	541
236	21	62	241	80	7	391	568
237	25	37	126	41	4	207	305
238	30	37	126	41	4	207	305
239	35	37	126	41	4	207	305
240	40	37	126	41	4	207	305
241	40	37	126	41	4	207	305
242	41	37	126	41	4	207	305
243	41	48	178	59	4	289	421
244	42	48	178	59	4	289	421
245	42	52	174	56	11	292	433
246	42	34	92	31	6	163	249
247							
248							
249		28	62	34	24	148	234
250		144	249	73		465	757

Appendix II

Input Contamination Data for the Tom River

The following table shows the input concentrations (in kBq/m^2) used for analysis of the doses in Scenario SCC-1 and the potential for redistribution in Scenario SCC-2. These values represent an estimated value derived from the sources listed in Chapter 5. All values were decayed to 1997 values to allow comparison between sources for different years. The confluence of the Tom and Ob rivers is located 45 km downstream from the discharge point.

Kilometers from discharge point	^{60}Co	^{137}Cs	^{152}Eu	^{90}Sr	^{232}Th	^{238}U	$^{239/40/41}$Pu
0	34	536	13	25			25
1	16	13					25
2	15	11	4		8	6	84
3							69
4	75	84	29	84	8	10	4
5		84		84			0
6		84		84			4
7	87	39	31		6	6	
8							
9	6	7		7			
10	2	22	1	7			
11	8	9	3	7	7	6	
12		7		7			
13		7		7			
14		11	1	7	10	7	4
15		7		7			
16		7		7			
17		7		7			
18		7		7			
19		7		7			
20	3	17		7			0
21	8	17	6	7			
22	3	7		7	8	7	
23		7		7			
24		7		7			

Kilometers from discharge point	^{60}Co	^{137}Cs	^{152}Eu	^{90}Sr	^{232}Th	^{238}U	$^{239/40/41}$Pu
25		7		7			
26		7		7			
27		7		7			
28		7		7			
29		7		7			
30		7		7			7
31		7		7			
32		11		7			
33		7		7			
34		7		7			
35		7		7			
36		7		7			
37		7		7			
38		7		7			
39		7		7			
40		7		7			
41		7		7			
42		7		7			
43		7		7			
44		7		7			
45		7		7			1

References

Andreev, G.S., Belousov, G.P., and Bushuev, S.I., 1994, Unpublished data on plutonium sampling in 1993–1994 (measured at Radium Institute, St. Petersburg, Russia) and data from Rikhvanov, L. P. (Tomsk Polytechnic University) on americium sampling in October 1996 (measured at Moscow Engineering and Physics Institute, Moscow, Russia), Siberian Chemical Combine, Tomsk, Russia.

Arkhangelskii, V.V., Lyapunov, P.I., and Rikhvanov, L.P., 1996, Unpublished data on sampling conducted in October 1996, Tomsk Polytechnic University, Tomsk, Russia.

Ashanin, M.V., and Nosov, A.V., 1991, *Report on Scientific Investigation Works: Characteristic of River Yenisei Contamination*, Goskomgidromet USSR, Institute of Applied Geophysics, Moscow, Russia.

Bradley, D.J., 1997, *Behind the Nuclear Curtain: Radioactive Waste Management in the Former Soviet Union*, D.R. Payson, ed., Battelle Press, Columbus, OH, USA.

Bradley, D.J., and Jenquin, U.P., 1995, Radioactive inventories and sources for contamination of the Kara Sea, *International Conference on Radioactivity in the Arctic*, Norwegian Radiation Protection Authority, Oslo, Norway.

Cochran, T.B., Norris, R.S., and Bukharin, O.A., 1995, *Making the Russian Bomb: From Stalin to Yeltsin*, Westview Press, Boulder, CO, USA.

Egorov, N., Novikov, V.M., Parker, F.L., and Popov, V.K., *The Radiation Legacy of the Soviet Nuclear Complex*, Earthscan, forthcoming.

Georgievskii, V.B., 1994, Ecological and Dose Models for Radiation, Naukova Dumka, Kiev, Ukraine.

Goskomecologia of the Tomsk Oblast, 1996, Condition of Environment and Population Health in Zone of Impact of Siberian Chemical Combine, Analytical Review of the State Committee for Ecology and Natural Resources of the Tomsk Oblast, Tomsk, Russia.

Hydrometizdat, 1984, Data from Resources of Surface Waters in the USSR. Major Hydrological Characteristics, Volume 15, Number 1, Hydrometizdat, Leningrad, Russia.

Il'inskhikh, N., 1996, Unpublished data collected in 1996, Siberian Medical University, Tomsk, Russia.

Ilyin, L., 1995, *Incident at the Siberian Chemical Enterprises, (Tomsk-7), 1993: Course, Consequences and Countermeasures, Final Report*, State Research Center Institute of Biophysics of Ministry of Public Health and Medical Industry of Russian Federation, Moscow, Russia.

Inishev, N. G., 1997, Unpublished data from measurements taken in 1994 by Riverbed Exploring Crew #1, Tomsk Regional Water Department, Tomsk, Russia.

International Arctic Seas Assessment Project, 1997, Predicted Radionuclide Release from Marine Reactors Dumped in the Kara Sea, IAEA-TECDOC-938, International Atomic Energy Agency, Vienna, Austria.

International Commission on Radiological Protection (ICRP), 1978, Radionuclide Release into the Environment – Assessment of Doses to Man, ICRP Publication 29, Pergamon Press, New York, NY, USA.

International Commission on Radiological Protection (ICRP), 1984, A Compilation of the Major Concepts and Quantities in Use by ICRP, ICRP Publication 42, Pergamon Press, New York, NY, USA.

International Institute for Applied Systems Analysis (IIASA), 1996, Mayak Case Study, Final Draft Report, International Institute for Applied Systems Analysis, Laxenburg, Austria.

Karimulina, F.K., and Klimenko, V.L., 1991, Report of Noibin Expedition Results on Establishing of Contaminated Sections on Yenisei River, 1990–1991, PGO "Krasnoyarskgeologia," S-EGPE, Lesosibirsk, Russia.

Khizhnyak, V.G., 1995, About Radiation Conditions on the Floodplain of the River Yenisei (Review of Reports), Krasnoyarsk Regional Inspection for Radiation Safety, Krasnoyarsk, Russia.

Kosmakov, E.V., 1996, Determination of Possible Places of Radioactive Contamination of River Yenisei Valley between Villages of Atamanovo and Strelka (Based on Analysis of Hydrological Processes), Scientific and Research Enterprise on Natural Systems Ecology (EPRIS), Divnogorsk, Russia.

Krasnoyarsk Regional Administration (KRA), 1995, The Project of Program for Stabilization and Development Industry of the Krasnoyarsk Region by 1996–2000, Krasnoyarsk, Russia.

Lapschin, Yu., 1997, Written communication to IIASA staff, Ukranian State Committee on Chernobyl, Kiev, Ukraine.

Lopatin, V.P. *et al*., 1988, Navigation Charts of the Enisei River from the Krasnoyarsk Hydroelectric Power Plant to the Confluence with the Angara River, Edited by the Major Editorial Staff for Maps of In-Country Waterways. Geographical Crew of the Enisei Basin Department, Krasnoyarsk, Russia.

Lyaschenko, N.G. *et al*., 1993, Results of Aerogamma Survey in the Tomsk Region – Report of "Berozovgeolody," Tomsk, Russia.

Masluck, A.I. *et al*., 1996, Report of Gossanepidnadzor of Seversk, Seversk, Russia.

Nesterenko, A.E., 1992, Assessment of Radiation Conditions of the Banks and the Streams of the Yenisei River at the Section between Krasnoyarsk and Lesosibirsk in 1990–1992, GGP Krasnoyarskgeologia, Krasnoyarsk, Russia.

NRB-76/87, 1988, Normyy Radiatsionnoi Bezopasnosti-76/87 (Norms of Radiation Protection-76/87), issued 1976, revised 1987, Energoatomizdat, Moscow, Russia.

Noskov, A.I. *et al*., 1960, Navigation Charts of the Tom River from Tomsk to the Confluence with the Ob River, River Bed Exploring Crew #12, edited by M.M. Shumilova, Ob Basin Management Department, Tomsk, Russia.

Novosibirsk, 1985, State Water Cadastre: Annual Data on Regime and Resources of Surface Waters for 1983 – Basin of Ob (without Irtysh Basin), Nadim, Pura, Tasa, Volume 1, Number 10, Part I, Novosibirsk, Russia.

Novosibirsk, 1986, State Water Cadastre: Annual Data on Regime and Resources of Surface Waters for 1984 – Basin of Ob (without Irtysh Basin), Nadim, Pura, Tasa, Volume 1, Number 10, Part I, Novosibirsk, Russia.

Novosibirsk, 1987, State Water Cadastre: Annual Data on Regime and Resources of Surface Waters for 1985 – Basin of Ob (without Irtysh Basin), Nadim, Pura, Tasa, Volume 1, Number 10, Part I, Novosibirsk, Russia.

OSP-72/87, 1988, Osnovnie Sanitarnie Pravila-72/87 (Main Sanitary Rules-72/87), issued 1972, revised 1987, Energoatomizdat, Moscow, Russia.

Phillips, G.W., August, R.A., King, S.E., *et al*., 1996, *1993-94-95 Kara Sea Field Experiments and Analysis: 1995 Progress Report to ONR Arctic Nuclear Waste Assessment Program*, Office of Naval Research, Washington, DC, USA.

Rikhvanov, L.P., 1994, personal communication, data taken from unpublished report of the Special Committee of Security Council of the Russian Federation "Summary of Verification of Assurance of Radiation and Ecological Safety of the Siberian Chemical Combine (Tomsk-7) and Adjacent Territories," Moscow, Russia.

Rikhvanov, L.P., 1996, personal communication, data from Contingency Plans of the SCC, Seversk, Russia.

Rikhvanov, L.P., 1997, in *Ecological State, Natural Resources Use, Environment Protection in Tomsk Region for 1996*, Tomsk Regional Committee for Ecology, Tomsk, Russia.

Robinson, S., and Volosov, A., eds., 1996, Radioecology of the Southern Part of Krasnoyarsk Region in the Impact Zone of the Mining Chemical Combine, Green Cross Russia, Krasnoyarsk-Zheleznogorsk, Russia.

Roskomgidromet, 1991, Radiation survey for the territory of the Russian Federation and adjacent countries in 1991, *SPA "Typhoon*," Obninsk, Russia.

Shishlov, A.E., Saviskii, U.V., Sadriev, D.U., and Chervonii, A.I., 1997, Information on Radiation Conditions on the Flood Plain of the River Enisei, Registration No. 07-08/272 of 6 July 1997, Based on sampling and measurements of the Radioecological Monitoring Laboratory of the Mining and Chemical Combine in 1995–1996, Zheleznogorsk, Russia.

SPORO-85, 1985, Sanitarnie Pravila Obraschenia s Radioactivnimi Othodami-85 (Sanitary Rules of Radioactive Waste Handling-85), Energoatomizdat, Moscow, Russia.

State Hydrological Institute, 1985, Data from Investigation of Changes in Hydrological and Channel Regime of the Tom River, State Hydrological Institute, Leningrad, Russia.

State Hydrological Institute, 1990, Data from Estimation of the Possibility of Local Counterflows due to Sand and Gravel Excavation from the Tom River Bottom in the Reach between Tomsk and the Tom Estuary, State Hydrological Institute, Leningrad, Russia.

Tomsk Spravka, 1994, Report of Working Group of RF Security Council on Results of Verification of Assurance of Radiation and Ecological Safety of Siberian Chemical Combine (Tomsk-7) and Adjacent Territories, Tomsk Regional Administration, Tomsk, Russia.

United States Army Corps of Engineers (USACE) Hydraulic Engineering Center, 1993, HEC-6 Scour and Deposition in Rivers and Reservoirs: User's Manual, CPD-6, Davis, CA, USA.

United States Army Corps of Engineers (USACE) Hydraulic Engineering Center, 1997, HEC-RAS River Analysis System: Hydraulic Reference Manual, Version 2.0, CPD-69, Davis, CA, USA.

Yu, C., Zielen, A.J., Cheng, J.-J., Yuan, Y.C., Jones, L.G., LePoire, D.J., Wang, Y.Y., Loureiro, C.O., Gnanpragasam, E., Faillace, E., Wallo, A. III, Williams, W.A., and Peterson, H., 1993, Manual for Implementing Residual Radioactive Material Guidelines Using RESRAD, Version 5.0, Working Draft for Comment, ANL/EAD/LD-2, Environmental Assessment Division, Argonne National Laboratory, Argonne, IL, USA.

Velichkin, V., Georgievskii, V., Gorlinskii, Yu., Iskra, A., Smirnov, V., and Asadulin, E., 1996, Evaluation of Radiation Legacy of the Former USSR Analytical Research Draft Report on Task "Environmental Characteristics of the SCC (Tomsk-7) and MCC (Krasnoyarsk-26) Territories," Moscow, Russia.

Wetmore, J.N., and Fread, D.L., 1983, The NWS Simplified Dam Break Flood Forecasting Model for Desk-Top and Hand-Held Microcomputers, Hydrologic Research Laboratory, Office of Hydrology, National Weather Service, National Oceanic and Atmospheric Administration (NOAA), Silver Spring, MD, USA.

Zubkov, Yu.G. *et al*., 1997, Unpublished data from sampling conducted in 1996 and 1997, Tomsk Regional Committee for Ecology, Tomsk, Russia.